

POLITECNICO DI TORINO

Dipartimento di Ingegneria Meccanica e Aerospaziale

Corso di Laurea in Ingegneria Aerospaziale



**The Planetary Environmental
Simulation Chamber PESCha -
Development and operation of
experimental set-up for thermal
vacuum test**

CANDIDATO
DARIO SECHI

RELATORE
Prof. PAOLO MAGGIORE

RELATORE
AZIENDALE
LILITH GRASSI
ROBERTO DESTEFANIS

Abstract

The life cycle of a space mission can be divided into different phases, each related to different aspects of the mission project.

The first phases, following the model of the European Space Agency, are focused on the development of functional systems and technical requirements, as well as the identification of the activities and the necessary resources.

The intermediate phases focus on project development activities and the qualification of the product and services.

The last phases cover the activities carried out during the period of activity of the mission, and its disposal.

Phase D is focused on the qualification and validation of the product. It provides confirmation that the project design meets the mission requirements through a verification process.

The work of the PEPS laboratory (Planetary Environment and Protection solutions) is linked to this phase of the project. Through a thermo-vacuum chamber called PESCha (Planetary Environmental Simulation Chamber) it is possible to simulate the space vacuum and to perform tests in planetary representative environment: these simulations are useful to carry out functional tests on space components and to perform thermal cycles to verify the effect of temperature on the structures. Another important activity is to carry out the forced outgassing of materials, through a procedure called bake-out.

The purpose of this thesis is to analyse in detail the operational phases of the PESCha facility and implement potential improvements, in order to speed up the testing activities and qualification processes, and to be able to detail it with more information.

This thesis is divided into 4 chapters:

- The first chapter focuses on the characterization of the space environment and its simulation. In the first part, its peculiar characteristics are described, such as the type of radiation present and the effect of orbital debris and vacuum. In the second part of the chapter, the systems to reach the vacuum and the sensors of both pressure and temperature are described in order to monitor the state of the experiments.
- The second chapter describes the PESCha facility, analysing its components, from the largest to the smallest, with a final analysis related to software components.
- The third chapter focuses on the operation of PESCha facility, that is, the vacuum procedures, in order to simulate the thermal and vacuum environment planned during the mission project, and the bakeout procedure, needed to ensure the cleaning of space components.
- The final chapter describes the implementation of a system for thermal feedback control, aimed at improving the thermal performance of the chamber, and of an RGA (residual gas analyser) sensor useful for improving the bakeout process.

Table of contents

ABSTRACT	II
TABLE OF CONTENTS.....	III
LIST OF FIGURES.....	V
LIST OF FIGURES.....	VIII
REFERENCE DOCUMENTS	IX
1. CHAPTER 1 – SPACE ENVIRONMENT	1
1.1 SPACE ENVIRONMENT	1
1.1.1 Vacuum.....	2
1.1.2 Electrically neutral particles	4
1.1.3 Micrometeoroids and orbital debris	5
1.1.4 Radiation	6
1.1.5 Gravity	7
1.1.6 Dust.....	7
1.2 SPACE ENVIRONMENT SIMULATION.....	8
1.2.1 Thermo-vacuum chamber.....	9
1.2.2 Pumping system.....	10
1.3 PRESSURE SENSORS.....	18
1.3.1 Mechanical gauges	19
1.3.2 Gas property gauges.....	20
1.3.3 Ionization Gauges.....	23
1.4 TEMPERATURE SENSORS	25
1.4.1 Contact temperature sensor	25
1.4.2 Non-contact temperature sensors	30
1.5 RESIDUAL GAS ANALYSERS.....	31
2. CHAPTER 2 - PESCHA.....	32
2.1 PESCHA FACILITY	33
THE EQUIPMENT OF THE PESCHA FACILITY LOCATED INTO TWO SPACES, THE PEPS LABORATORY AND THE THERMAL CONTROL SYSTEM ROOM:	33
• IN THE LABORATORY ARE LOCATED THE MAJORITY OF THE PESCHA EQUIPMENT’S. IN PARTICULAR THE PESCHA VACUUM CHAMBER THAT IS COMPOSED BY TWO DIFFERENT CHAMBERS.	33
2.2 COMPONENTS.....	35
2.2.1 Main chamber.....	35
2.2.2 Baffle trap.....	36
2.2.3 PESCha pumps.....	38
2.2.4 PESCha pressure sensors	41
2.2.5 PESCha temperature sensors.....	43
2.2.6 PESCha mass flow controller	44
2.2.7 PESCha temperature control system.....	46
2.2.8 Water cooling circuit.....	49
2.2.9 PESCha venting valves.....	50
2.3 OTHER COMPONENTS.....	50
2.3.1 TQCM.....	50
2.3.2 RGA (VQM)	51
2.4 SOFTWARE	56
2.4.1 Control and data acquisition software.....	57
3. CHAPTER 3 – PESCHA FACILITY: APPLICATIONS ANALYSIS AND PROCEDURES.....	62
3.1 VACUUM PROCEDURE.....	62
3.2 BAKEOUT PROCEDURE	64

4. CHAPTER 4 – PESCHA FACILITY: SENSORS IMPLEMENTATION.....	70
4.1 THERMAL CONTROL	70
4.2 RESIDUAL GAS ANALYSIS.....	76
CONCLUSIONS	92
APPENDIX 1 – TQCM FITTING CODE.....	93
ACKNOWLEDGMENTS	99

List of figures

<i>Figure 1 - Space weather illustration adapted from NASA.</i> https://www.nationalgeographic.org/media/space-weather	1
<i>Figure 2 - Principal effects of space environment</i>	2
<i>Figure 3 - Atomic oxygen flux versus altitude for minimum, nominal and maximum solar conditions.</i> https://www.researchgate.net/publication/237393396_Low_Earth_Orbital_Atomic_Oxygen_Interactions_With_Materials/figures?lo=1	4
<i>Figure 4 - Orbital debris distribution.</i> https://www.nasa.gov/centers/wstf/site_tour/remote_hypervelocity_test_laboratory/micrometeoroid_and_orbital_debris.html	5
<i>Figure 5 - Radiation Types and effects on Humans.</i> https://www.physicscentral.com/explore/action/shields-up.cfm	6
<i>Figure 6 - A successful scoop of Martian regolith performed by NASA's Phoenix lander.</i> https://www.universetoday.com/20360/lunar-regolith/	7
<i>Figure 7 - Alan Bean takes a sample of lunar regolith during the Apollo 12 mission.</i> https://www.universetoday.com/20360/lunar-regolith/	8
<i>Figure 8 - Chamber A located in the Space Environment Simulation Laboratory at NASA's Johnson Space Center in Houston.</i>	9
<i>Figure 9 - Classification of vacuum pumps. Leybold - Fundamentals of Vacuum Technology</i>	10
<i>Figure 10 - Cross section of a diaphragm pump. Leybold - Fundamentals of Vacuum Technology</i>	11
<i>Figure 11 - Cross section of a rotary vane pump. Leybold - Fundamentals of Vacuum Technology</i>	12
<i>Figure 12 - Cross section of a root pump. Leybold - Fundamentals of Vacuum Technology</i>	13
<i>Figure 13 - Cross section of a diffusion pump. Leybold - Fundamentals of Vacuum Technology</i>	14
<i>Figure 14 - Cross section of a molecular pump. Leybold - Fundamentals of Vacuum Technology</i>	15
<i>Figure 15 - Cross section of a Sputter-ion pump. Leybold - Fundamentals of Vacuum Technology</i>	16
<i>Figure 16 - Cross section of a cryopump. Leybold - Fundamentals of Vacuum Technology</i>	17
<i>Figure 17 - Pressure Ranges of different Vacuum Gauges.</i> https://www.lesker.com/newweb/gauges/gauges_technicalnotes_1.cfm	18
<i>Figure 18 - Bourdon gauge.</i> http://www.marshallinstruments.com/faqs/detail.cfm?id=22	19
<i>Figure 19 - Typical quartz pressure sensor cross section.</i> http://www.pcb.com/Resources/Technical-Information/Tech_Pres	19
<i>Figure 20 - Typical capacitance manometer cross section.</i> https://www.lesker.com/newweb/gauges/gauges_technicalnotes_1.cfm	20
<i>Figure 21 - Pirani gauge electrical scheme.</i> http://instrumentationandcontrollers.blogspot.com/2012/03/pirani-gauge-thermal-conductivity-gauge.html	20
<i>Figure 22 - Pirani gauge: indicated pressure over actual pressure for different gas species - Thermal transfer function. Sergio Calatroni. Copper for particle accelerators: electron stimulated desorption and study of hydrogen content measurement by laser ablation</i>	21
<i>Figure 23 - Convection enhanced Pirani gauge scheme.</i> https://sens4.com/pirani-working-principle.html	22
<i>Figure 24 - Schematic of Hot Cathode Gauge.</i> https://www.supervacoils.com/vacuum-gauges-explained/ 23	23

<i>Figure 25 - Schematic of Cold Cathode Ionization Gauge.</i> http://www.instrumentationtoday.com/ionization-gauge-cold-cathode-type/2012/01/	24
<i>Figure 26 - Schematic of a thermocouple.</i> https://www.flukeprocessinstruments.com/en-us/service-and-support/knowledge-center/thermal-profiling-technology/thermocouple-theory	25
<i>Figure 27 - Thermocouple Temperature range</i>	26
<i>Figure 28 - Voltage function.</i> https://www.engineeringtoolbox.com/thermocouples-d_496.html	26
<i>Figure 29 - Resistance temperature detector scheme.</i> https://automationforum.co/resistance-temperature-detector-rtd/	27
<i>Figure 30 - Resistance function.</i> https://www.electrical4u.com/resistance-temperature-detector-or-rtd-construction-and-working-principle/	28
<i>Figure 31 - Type of thermistors</i>	28
<i>Figure 32 - Infrared thermometer</i>	30
<i>Figure 33 - The residual gas analyzer and the connection to the vessel. Ariel de Graaf. Deposition of CNH materials : plasma and film characterization</i>	31
<i>Figure 34 - PESCha overview</i>	32
<i>Figure 35 - PESCha main room functional diagram</i>	33
<i>Figure 36 - Water cooling functional diagram</i>	34
<i>Figure 37 - Main chamber</i>	35
<i>Figure 38 - Main chamber feedthroughs</i>	36
<i>Figure 39 - Baffle trap</i>	36
<i>Figure 40 - Baffle trap feedthroughs</i>	37
<i>Figure 41 - TRIVAC D40 BCS</i>	38
<i>Figure 42 - MAG 2000 CT</i>	39
<i>Figure 43 - Turbomolecular pumping speed</i>	40
<i>Figure 44 - COOLVAC iCL 2000</i>	41
<i>Figure 45 - PTR90N Pressure range</i>	42
<i>Figure 46 - PTR90N Output function</i>	42
<i>Figure 47 - Thermocouple Output. Wikipedia</i>	43
<i>Figure 48 - Mass flow controller functional scheme.</i> www.fcon-inc.jp	44
<i>Figure 49 - MKS 1179B</i>	45
<i>Figure 50 - LAUDA XT49W</i>	46
<i>Figure 51 - LAUDA functional scheme</i>	46
<i>Figure 52 - Lauda controlling Pad</i>	48
<i>Figure 53 - Lauda controlling Pad view</i>	48
<i>Figure 54 - Water cooling system functional scheme</i>	49
<i>Figure 55 - VARIAN AGILENT L6280</i>	50
<i>Figure 56 - MS Gauge</i>	52
<i>Figure 57 - Cross Section of MS Gauge and Electrostatic Trapping Potential Well</i>	52
<i>Figure 58 - VQM MS Gauge Ionizer</i>	53
<i>Figure 59 - VQM Viewer Tune screen</i>	54
<i>Figure 60 - VQM Viewer Summary screen</i>	55
<i>Figure 61 - VQM Viewer Settings screen</i>	55

<i>Figure 62 - PESCha facility controlling screens</i>	<i>56</i>
<i>Figure 63 - Test sample.....</i>	<i>63</i>
<i>Figure 64 - TQCM data output.....</i>	<i>66</i>
<i>Figure 65 - TQCM frequency function with interpolation.....</i>	<i>66</i>
<i>Figure 66 - Function included in the sum.....</i>	<i>67</i>
<i>Figure 67 - Frequency first derivative.....</i>	<i>67</i>
<i>Figure 68 - Frequency second derivative</i>	<i>68</i>
<i>Figure 69 - Relationship between first derivative and second derivative.....</i>	<i>68</i>
<i>Figure 70 - - Relationship between second derivative and first derivative</i>	<i>69</i>
<i>Figure 71 - Mster-Slave controler example. https://www.west-cs.com/news/how-does-cascade-control-work/</i>	<i>71</i>
<i>Figure 72 - Block scheme</i>	<i>73</i>
<i>Figure 73 - Temperature functions.....</i>	<i>73</i>
<i>Figure 74 - Lauda Control Parameters settings.....</i>	<i>75</i>
<i>Figure 75 - Empty chamber mass spectrum.....</i>	<i>80</i>
<i>Figure 76 - CO2 mass spectrum.....</i>	<i>81</i>
<i>Figure 77 - CO2 mass spectrum (1 minute delay)</i>	<i>81</i>
<i>Figure 78 - CO2 time function</i>	<i>82</i>
<i>Figure 79 - N2 mass spectrum</i>	<i>83</i>
<i>Figure 80 - N2 time function.....</i>	<i>83</i>
<i>Figure 81 - He mass spectrum.....</i>	<i>85</i>
<i>Figure 82 - He time function.....</i>	<i>85</i>
<i>Figure 83 - Kevlar experiment.....</i>	<i>87</i>
<i>Figure 84 - Scotch weld mass spectrum.....</i>	<i>88</i>
<i>Figure 85 - RGA bakeout - Heater and thermocouple</i>	<i>89</i>
<i>Figure 86 - RGA bakeout - Protection</i>	<i>90</i>
<i>Figure 87 - Bakeout mass spectrum</i>	<i>90</i>

List of figures

<i>Table 1 - PESCha components</i>	34
<i>Table 2 - Primary pump data sheet</i>	38
<i>Table 3 - Turbomolecular pump data sheet</i>	40
<i>Table 4 - Cryopump data sheet</i>	41
<i>Table 5 - MFC data sheet</i>	45
<i>Table 6 - Lauda data sheet</i>	47
<i>Table 7 - Equations parameters</i>	72

Reference documents

SPACE ENVIRONMENT

- [RD1] WordlessTech. *NASA's Space Environment Simulation Lab*
- [RD2] Wikimedia Foundation, *Wikipedia The Free Encyclopaedia*
- [RD3] Jose Meseguer, Isabel Perez-Grande, Angel Sanz-Andres. *Spacecraft thermal control-Woodhead Publishing*
- [RD4] Mateo-Martí. *Planetary Simulation Chambers bring Mars to laboratory studies*
- [RD5] Miria M. Finckenor, Kim K. de Groh. *Space Environmental Effects*
- [RD6] FAA. *The Space Environment*
- [RD7] IFLscience. *How Impacting Space Dust Is Damaging Satellites*
- [RD8] Universe Today. *What is Lunar Regolith?*
- [RD9] Walter Umrath (Leybold). *Fundamentals of Vacuum Technology*
- [RD10] C. Day. *Basics and applications of cryopumps*
- [RD11] University of Notre Dame. *Introduction_to_vacuum_gauges*
- [RD12] K. Jousten. *Ultrahigh vacuum gauges*
- [RD13] J. H. Leck. *Total and Partial Pressure Measurement in Vacuum Systems*
- [RD14] Pfeiffer. *Indirect, gas-dependent pressure measurement*
- [RD15] Leybold. *Vacuum Measurement*
- [RD16] IIT Kanpur. *Vacuum gauges*
- [RD17] National Aeronautics and Space Administration. *Specialized Environmental Chamber Test Complex*
- [RD18] National Aeronautics and Space Administration. *Space Environmental Testing*
- [RD19] National Aeronautics and Space Administration. *Space Environment Simulator*
- [RD20] Mateo-Martí. *Planetary Atmosphere and Surfaces Chamber (PASC): A Platform to Address Various Challenges in Astrobiology*
- [RD21] Larry B. Rainey. *Space Modelling and Simulation*
- [RD22] Robert H. Johnson, Lisa D. Montierth, JR Dennison James S. Dyer, and E. R. Lindstrom. *Small Scale Simulation Chamber for Space Environment Survivability*
- [RD23] Angstrom engineering. *Space & Environmental Simulation*
- [RD24] FDM Environment Makers. *How does an environmental chamber work?*
- [RD25] Inor. *Temperature transmitters*

- [RD26] STS Southeast Thermal systems. *RTF theory*
- [RD27] Pyromation. *Thermocouple theory*
- [RD28] R. M. Park. *Thermocouple fundamentals*
- [RD29] Kerlin, Thomas W. Johnson, Mitchell. *Practical Thermocouple Thermometry*

PESCha

- [RD30] Thales Alenia Space. *Formazione PESCha*
- [RD31] Thales Alenia Space. *PESCha facility user manual*
- [RD32] Alta. *Environmental Simulation Facility Manual*
- [RD33] Lauda. *Product Data Sheet: Integral XT 490 W*
- [RD34] Lauda. *Integral XT 490 W Operating manual*
- [RD35] Lauda. *Heat transfer Liquids*

PESCHA FACILITY: APPLICATIONS ANALYSIS AND PROCEDURES PESCHA

- [RD36] Thales Alenia Space. *PESCha Procedures*
- [RD37] Leybold. *PENNINGVAC Transmitter PTR 90 N Operating Manual*
- [RD38] G. Chiocchia, M. Germano, *Termofluidodinamica*
- [RD39] J. Grant. *How it works: Quartz crystal microbalance*
- [RD40] Gamry. *Basics of a Quartz Crystal Microbalance*
- [RD41] P. Danielson. *Contamination in Vacuum Systems: Sources and Remedies*
- [RD42] ASTM Internation. *Standard Practice for Spacecraft Hardware Thermal Vacuum Bakeout*
- [RD43] Crystaltek. *CrystalTek Model 66TR Controller Reference Manual*
- [RD44] R. Rampini, E. Ftaka, M. Van Eesbeek. *Dynamic outgassing testing: revisited mathematical approach*
- [RD45] Paul de Heij. *Analysis of bake-out monitoring data*
- [RD46] A. Rampini. *A procedure for bakeout and outgassing measurement in thermal vacuum chambers monitored by TQCM*
- [RD47] O. Manuel Uy, Russell P. Cain, Bliss G. Carkhuff, Richard T. Cusick. *Miniature Quartz crystal Microbalance for Spacecraft and Missile Applications*

FACILITY: SENSORS IMPLEMENTATION

- [RD48] Brooks. *Vacuum Quality Monitor Series 835 Instruction manual*
- [RD49] Brooks. *Micro-Ion ATM Series 390 Instruction manual*
- [RD50] J. A. Colony. *Mass Spectrometry of aerospace materials*
- [RD51] E. de Hoffmann, V. Stroobant. *Mass Spectrometry. Principles and Applications*

- [RD52] F. McLafferty. *Mass Spectral Correlations*
- [RD53] T. A. Lee. *A beginner's guide to mass spectral interpretation*
- [RD54] Leybold. *Fundamentals of leak detection*
- [RD55] Silverstein. *Spectrometric Identification of Organic Compounds*
- [RD56] Valter Maurino. *Analytical Chemistry in Material Sciences*
- [RD57] P. Turner, S. Taylor, E. Clarke, C. Harwood, K. Cooke, H. Frampton. *Calibration effects during natural gas analysis using a quadrupole mass spectrometer*
- [RD58] G. S. Anufriev, B. S. Boltenev, and A. I. Ryabinkov. *High-Resolution Mass Spectra of the Residual Gas in a Metallic Vacuum System*
- [RD59] Nagamitsu Yoshimura. *Vacuum Technology - Practice for Scientific Instruments*
- [RD60] G. F. Weston. *Ultrahigh Vacuum Practice*
- [RD61] J. M. Lafferty. *Foundations of vacuum science and technology*
- [RD62] Peter H. Dawson. *Quadrupole Mass Spectrometry and its Applications*
- [RD63] S. Shannon. *Fundamentals of RGA: a perspective of the development of an essential vacuum diagnostic tool*
- [RD64] Hidden Analytical. *Mass spectrometers for Residual Gas Analysis Applications*
- [RD65] Ors Technical Brief. *Interpretation of RGA Data*

1. CHAPTER 1 – SPACE ENVIRONMENT

1.1 Space environment

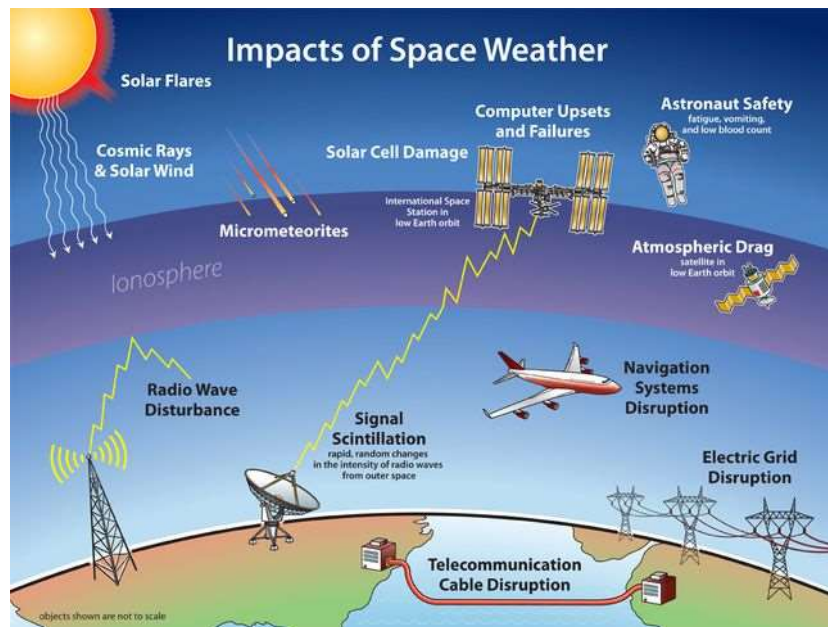


Figure 1 - Space weather illustration adapted from NASA.
<https://www.nationalgeographic.org/media/space-weather>

Space environment offers unique challenges to spacecraft designers.

It concerns all the environmental conditions affecting the development of a space mission, from the beginning of the design phase to the end of the life in orbit.

This thesis will focus mainly on the simulation of vacuum, dust and thermal environment conditions for testing purposes.

It is difficult to reproduce in controlled chamber all the variables that occurs during a space mission, not only the extreme environment that the spacecraft will face in outer space, but also the potential sources of damage the vehicle can encounter.

In general, the effect of space medium can be grouped in six categories:

- Vacuum
- Electrically neutral particles
- Plasma
- Radiation
- Micrometeoroids and orbital debris
- Gravity

CHAPTER 1 – SPACE ENVIRONMENT

Environment	Effect
Vacuum	<ul style="list-style-type: none">■ Pressure differentials■ Surface degradation due to solar ultraviolet radiation■ Contamination
Electrically neutral particles	<ul style="list-style-type: none">■ Mechanical effects (aerodynamic drag, physical sputtering)■ Chemical effects (atomic oxygen attack, spacecraft glow)
Plasma	<ul style="list-style-type: none">■ Spacecraft charging (shift in electrical potential)■ Electrostatic discharge and dielectric breakdown■ Enhanced sputtering■ Re-attraction of contamination
Radiation	<ul style="list-style-type: none">■ Total dose effects (electronic degradation, crew safety hazards)■ Single event effects (upsets, latch-up, burnout)
Micrometeoroids and orbital debris	<ul style="list-style-type: none">■ Surface damage due to hypervelocity impacts

Source: After Tribble (2003).

Figure 2 - Principal effects of space environment

These elements cause material and components degradation, potential failures and instruments perturbation, jeopardizing the mission accomplishment.

In addition, when a spacecraft is designed to land on the surface of a planetary body, the presence of soil dust must be considered, affecting the behaviour and performance of both a spacecraft and onboard equipment.

Facilities like PESCha are built to simulate the vacuum environment and the dust effect. In the next section there will be a description of all the effect.

1.1.1 Vacuum

Beyond the thin skin of Earth's atmosphere, we enter the vacuum space.

Vacuum is defined as the total absence of matter. The spacecraft will not face the perfect vacuum but a pressure between 10^{-6} to 10^{-12} mbar.

This vacuum environment creates four potential problems for spacecraft:

- Outgassing – release of gasses from spacecraft materials
- Cold welding – fusing together of metal component
- Heat transfer – limited to radiation
- Pressure differential

The release of trapped gasses in vacuum is called **out-gassing**. Some materials used in space construction, especially composites, can trap tiny bubbles of gas while under atmospheric pressure. When this pressure goes down, particles begin to escape. This flow can damage delicate sensors, such as lenses or cause electronic components to arc, damaging them. A material known to outgas should be thermal vacuum baked for a minimum of 24 hours at a temperature above that expected in orbit or, if that is not known, at 100 °C.

CHAPTER 1 – SPACE ENVIRONMENT

Cold welding occurs between mechanical parts that have very little separation between them. When moving parts are tested on Earth, a tiny air space may allow the parts to move freely. Without air that separates both parts, they weld together. This problem can be solve exposing one part to the Sun, so that differential heating causes the parts to expand and contract, allowing them to separate or using lubricants.

The vacuum in space removes two important components of thermic transfer occurring on Earth. Without conduction or convection, the only heat transfer mechanism for spacecraft is through **radiation**. Overheating is a critical issue for spacecraft systems, in particular electronic devices that release heat during their functioning or parts and surfaces hit by solar rays during daylight (IR waves). The satellite will need to dissipate heat when facing to the sun, and to be heated when exposed to the cold deep space, so a thermal control system must be developed.

The last problem is structural, the designer must design a spacecraft that is able to resist at high level of pressure difference.

1.1.2 Electrically neutral particles

The Earth’s atmosphere affects a spacecraft in low Earth orbit in two ways:

- Drag
- Atomic oxygen

Even a thin layer of atmosphere can work to drag a satellite back to Earth. Drag depends on the air’s density, the speed and the shape of the spacecraft. The Earth’s atmosphere does not just end abruptly but extends to higher altitudes up to 500 km and above. Acting over months or years, this cause spacecraft in these orbits to lose altitude until they enter the atmosphere to burn up.

Atomic oxygen is created by separation of oxygen molecules by radiation and charged particles. Its oxidation properties make the atomic oxygen far more dangerous than the O_2 because of the significant breakdown and rusting of surfaces.

On the good side, the combination of atomic oxygen with oxygen molecules form ozone, which acts like a window shade blocking harmful radiation.

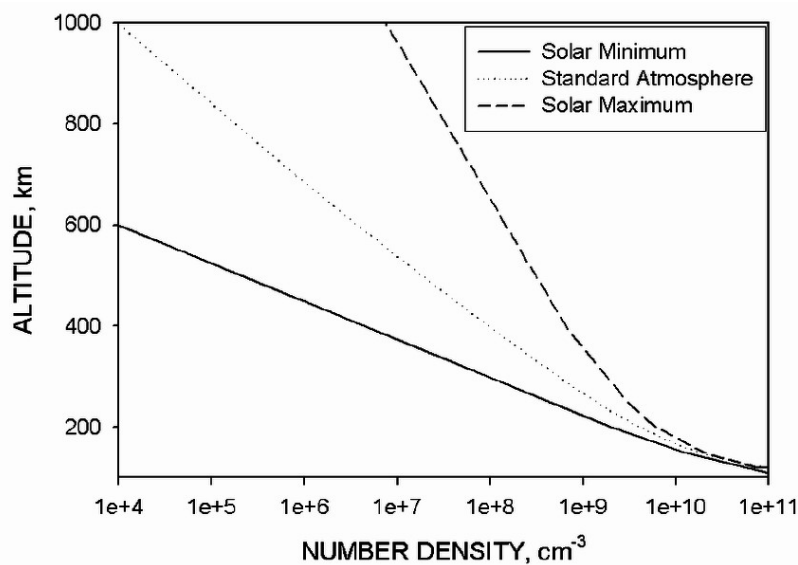


Figure 3 - Atomic oxygen flux versus altitude for minimum, nominal and maximum solar conditions.

https://www.researchgate.net/publication/237393396_Low_Earth_Orbital_Atomic_Oxygen_Interactions_With_Materials/figure/s?lo=1

1.1.3 Micrometeoroids and orbital debris



Figure 4 - Orbital debris distribution.

https://www.nasa.gov/centers/wstf/site_tour/remote_hypervelocity_test_laboratory/micrometeoroid_and_orbital_debris.html

Micrometeoroids and other space debris are critical elements of space environment. Space is full of both natural debris, like dust, meteoroids, chunk of asteroids, comets, and human debris, such as old satellites, remains of launchers' stages, equipment damaged or lost during missions.

Spacecraft may be impacted by micrometeoroids traveling as fast as 60 km/s or more. Surfaces facing the ram direction are more likely than those in the wake direction to be hit with space debris, traveling at an average velocity of 10 km/s in low Earth orbit.

Micrometeoroid or space debris impacts on an experiment may crater the material, spall off a coating or short out a solar cell.

This phenomenon is increasing in his importance because the environment near Earth is getting full of fragments of defunct spacecraft. A spacecraft in low orbit is now more likely to hit a piece of junk than a piece of natural material.

1.1.4 Radiation

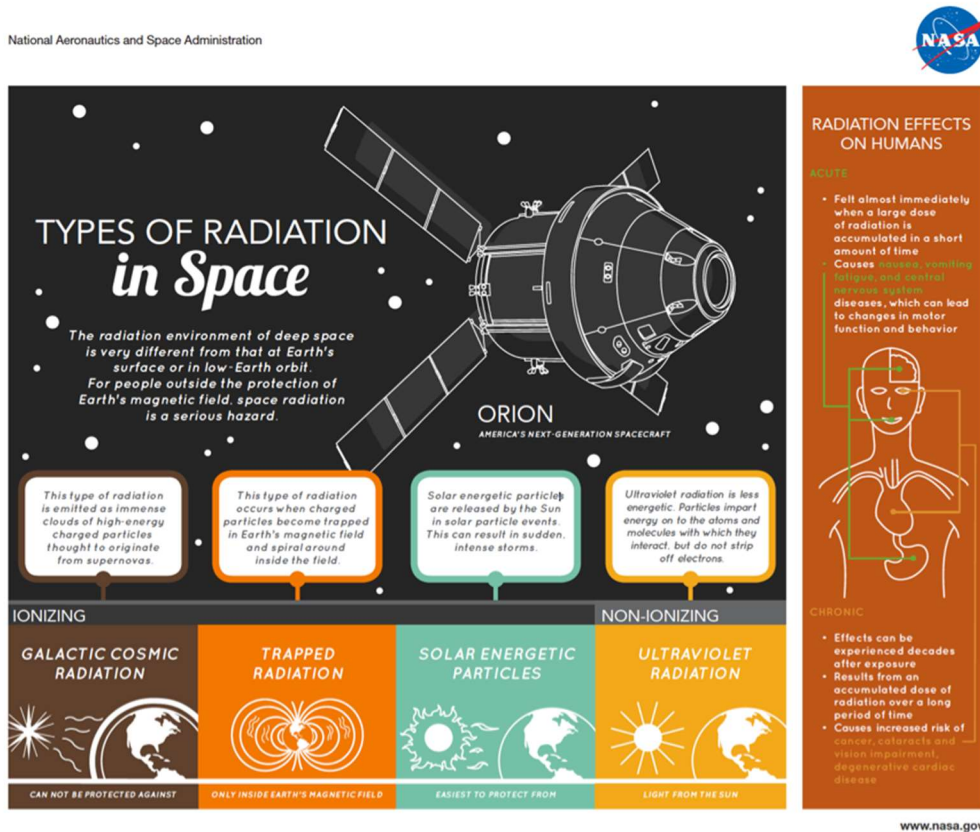


Figure 5 - Radiation Types and effects on Humans. <https://www.physicscentral.com/explore/action/shields-up.cfm>

Space outside Earth’s atmosphere is permeated by a lot of particles and radiation that can have great impact on spacecraft reliability.

The three main sources of charged particle radiation naturally occurring in space are galactic cosmic rays, solar proton events, and the trapped radiation belts. Spacecraft and astronauts are well above the atmosphere, so they bear the full brunt of the Sun’s output. The effect on a spacecraft depends on the wavelength of the radiation.

This can lead to several problems:

- Heating on exposed surfaces
- Degradation or damage to surfaces and electronic components
- Solar pressure

EM radiation, which is one of the main outputs of the Sun, can degrade spacecraft coating.

As to particle rations, they can harm spacecraft in three ways:

- Charging
- Sputtering
- Total ionizing dose and single-event phenomena

Spacecraft charging results when charges build up on different parts of a spacecraft as it moves through concentrated areas of charged particles. Discharge can occur with disastrous effect, such as damage to surface coatings, loss of power, degradation of solar panel.

Sputtering is a phenomenon caused by the high velocity particles which impact and damage spacecraft's thermal coating and sensors.

Single charged particles can penetrate deep into the guts of the spacecraft, resetting for example one part of a computer's memory from 1 to 0. Each abrupt disruption induced by an individual event is known as single event phenomenon (SEP).

1.1.5 Gravity

Spacecraft in space are subjected to low gravity effects. This does not mean that the distance with their planet's area of influence is high enough to set gravity to zero (from the universal law of gravity $F = \frac{Gm_1m_2}{r^2}$). In low-Earth orbit, for example, at an altitude of 300 km, the pull of gravity is still 91% of what it is on Earth surface.

What really differs is that astronauts are experiencing free falling effect. The gravity force is used to maintain the orbit, so they never touch Earth's surface and they do not act contact forces because the spacecraft has the same acceleration.

Weightlessness alters many observable phenomena within the physical and life sciences. It affects surface wetting and interfacial tension, multiphase flow and heat transfer and induces alteration in gene expression and aggregation of cells.

This phenomenon offers also many potential opportunities for space manufacturing.

In free fall we can mix material that will not mix on Earth, making exotic and useful metal alloy.

The drawback of microgravity is handling fluids in space. They are much harder to measure and pump in free fall.

1.1.6 Dust



*Figure 6 - A successful scoop of Martian regolith performed by NASA's Phoenix lander.
<https://www.universetoday.com/20360/lunar-regolith/>*

The surfaces of many planets and minor bodies of the Solar system are covered with dust created mainly over billions of years by continuous meteoric impacts.

CHAPTER 1 – SPACE ENVIRONMENT

This dust, combined with the microgravity, radiation and vacuum conditions, can cause problems both to the electronic components of the satellites and to the space suits of the astronauts, being very abrasive and with a high capacity to spread in closed places. The process of micrometeorite impacts on the Moon has made the dust particles very fine and sharp.

Another problem, considered important during the first space missions, was that being too fine, the dust was not able to carry the weight of astronauts and modules. In reality the first landing has shown the non-existence of this type of problem.

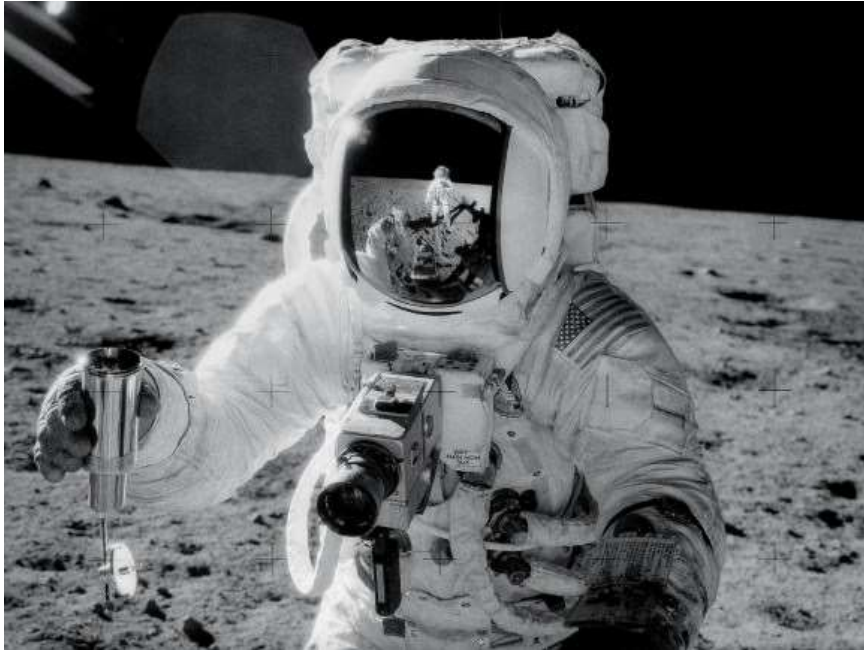


*Figure 7 - Alan Bean takes a sample of lunar regolith during the Apollo 12 mission.
<https://www.universetoday.com/20360/lunar-regolith/>*

1.2 Space environment simulation

As discussed above, the space environment is particularly complex and the effects on the space mission can be manifold.

It is therefore necessary to be able to test the various components of the environment in order to be able to validate the physical models used during the design phase, and to be able to verify the correspondence between the project and the real product.

In order to do this, many tests and prototypes are needed, together with the capability to correctly simulate the space operative environment on the Earth. More accurate simulations lead to more accurate results and to smaller margins to be used for the design phase.

It is not easy to accurately recreate the environmental conditions such as temperature, pressure, humidity, radiation and particles. However, thanks to adequate physical and technical knowledge of the phenomena involved, based on models and observations, it is possible to create ad hoc experiments in which only the most important parameters are simulated.

One of the most commonly used facilities for simulating these features is the environmental chamber.

CHAPTER 1 – SPACE ENVIRONMENT

Its purpose is to recreate the conditions under which machinery, materials and devices can be exposed during the life cycle. These conditions may include elements such as: temperature, vibration, radiation, weather, dust and vacuum.

To be able to include tests of any kind, these chambers can vary greatly in shape size and range of performances.

The following paragraphs will shortly describe a type of environmental chamber, that is, the vacuum-sealed chamber and the pumping systems used to reach and maintain the vacuum.

1.2.1 Thermo-vacuum chamber



Figure 8 - Chamber A located in the Space Environment Simulation Laboratory at NASA's Johnson Space Center in Houston.

The thermal vacuum chambers are used in many fields of physics, but the main use is in the engineering field, in particular aerospace. Being able to simulate the vacuum of the space environment is essential for example to describe the behaviour of a satellite from a thermal point of view and to be able to control the pressurized chamber seals.

We can classify vacuum levels as follows:

- rough vacuum (RV): from 10^3 to 10^{-3} mbar
- high vacuum (HV): from 10^{-4} to 10^{-8} mbar
- ultra high vacuum (UHV): from 10^{-9} to 10^{-12} mbar

The range between HV and UHV is the one used for space applications.

In order to achieve these vacuum levels, a rigid chamber with one or more pumps capable of removing internal gases is required. It is also possible to add a thermal machine to simulate the temperature profiles and a mass flow controller to replicate the atmospheres of the other planets.

Within the chamber it is also necessary to implement specific vacuum flanges in order to allow the installation of instruments without compromising the vacuum level.

1.2.2 Pumping system

Vacuum pumps are used to reduce the gas pressure in a monitored environment. There are basically two major classes of vacuum pumps, based on the different way that particles are moved away from the chamber:

- Vacuum pumps where the particles are pumped away, by means of displacement or pulse power, generally through compression stages.
- Vacuum pumps where the particles that must be removed are trapped to a solid surface by condensation or other bounding systems.

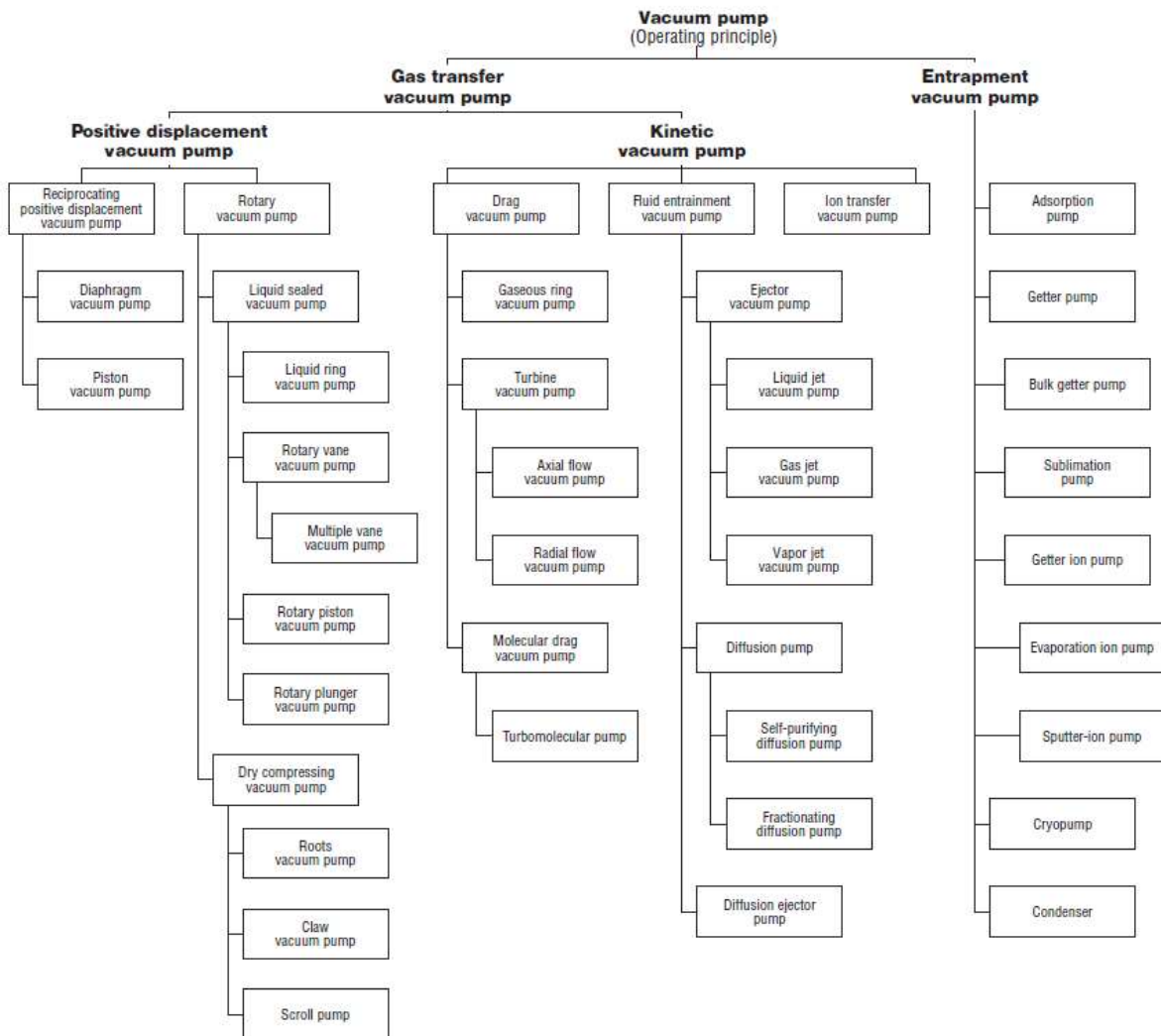


Figure 9 - Classification of vacuum pumps.
Leybold - Fundamentals of Vacuum Technology

Diaphragm pumps

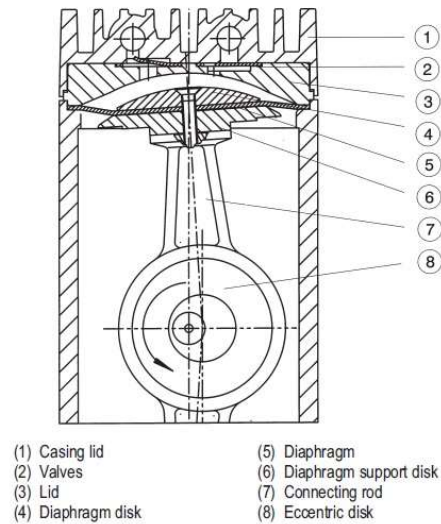


Figure 10 - Cross section of a diaphragm pump.
Leybold - Fundamentals of Vacuum Technology

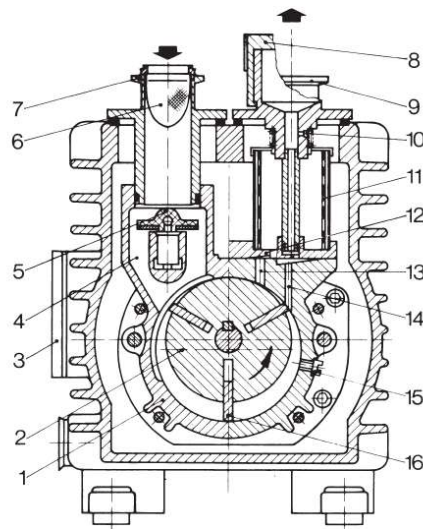
Diaphragm vacuum pumps are single or multi-stage dry compressing vacuum pumps. A diaphragm is tensioned between a pump head and the casing wall. It is moved in an oscillating way by means of a connecting rod and an eccentric.

The valves are arranged so that during the phase where the volume of the pumping chamber increases it is open to the intake line. During compression, the pumping chamber is linked to the exhaust line.

This type of pumps does not produce wastewater, saving the 90% of the cost compared to water jet pumps, and it is free of oil.

The problem is that diaphragm vacuum pumps are not capable of attaining a high vacuum level, the maximum reachable with a four-stage pump being about $5 * 10^{-1}$ mbar.

Rotary vane pumps



- | | |
|----------------------------|-----------------------|
| 1 Pump housing | 9 Exhaust port |
| 2 Rotor | 10 Air inlet silencer |
| 3 Oil-level sight glass | 11 Oil filter |
| 4 Suction duct | 12 Exhaust valve |
| 5 Anti-suckback valve | 13 Exhaust duct |
| 6 Dirt trap | 14 Gas ballast duct |
| 7 Intake port | 15 Oil injection |
| 8 Lid of gas ballast valve | 16 Vane |

*Figure 11 - Cross section of a rotary vane pump.
Leybold - Fundamentals of Vacuum Technology*

Rotary vane pumps consist of a cylindrical housing where the fluid is forced to move from the input vane by an eccentrically suspended and slotted rotor turns in the direction of the output of the system.

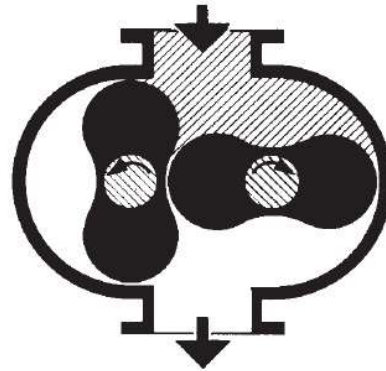
One of the problems of this method is the condensation of vapours in the pump chamber. If pumping water vapor, for example, at a pump temperature of 7°, the vapor may be compressed only to 312 mbar. Reached that point no overpressure is created until all the water vapor condense. So the water remains in the chamber and emulsifies with the pump's oil degrading its properties.

The solution to the problem is the gas ballast, which prevents the condensation of vapours in the pump chamber.

Before the actual compression process begins a precisely quantity of air is forced to the pumping chamber, the partial pressure of vapours goes down and they cannot condense.

The ultimate pressure reached by a two-stage pump is usually 10^{-4} mbar

Root pumps



- | | |
|-----------------|------------------|
| 1 Intake flange | 4 Exhaust flange |
| 2 Rotors | 5 Casing |
| 3 Chamber | |

*Figure 12 - Cross section of a root pump.
Leybold - Fundamentals of Vacuum Technology*

A root pump is a rotary positive-displacement type of a pump where two symmetrically shaped impellers rotate inside the pump casing past each other in proximity. They are synchronized by a toothed gear and the clearance between the rotors and the casing wall as well as between the rotors themselves is only few tenths of a millimetre. For this reason, they can operate at high speed without mechanical wear. The problem with root pumps is that they are not oil sealed, so only compression ratios in the range 10-100 mbar can be obtained.

Diffusion pumps

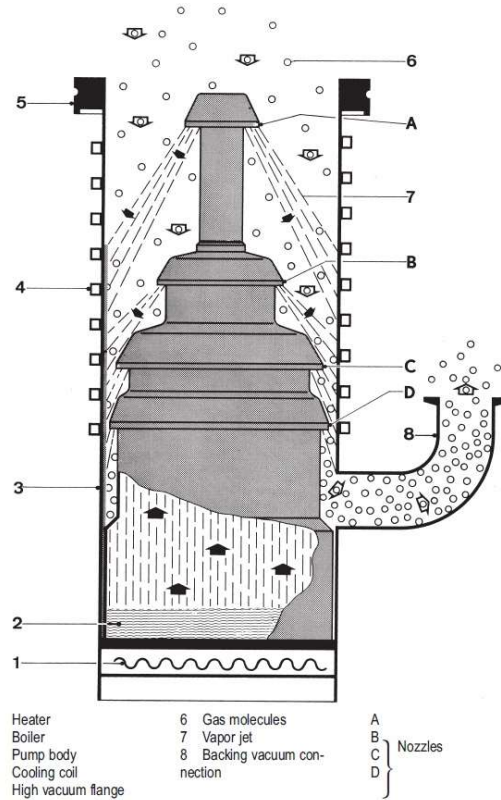
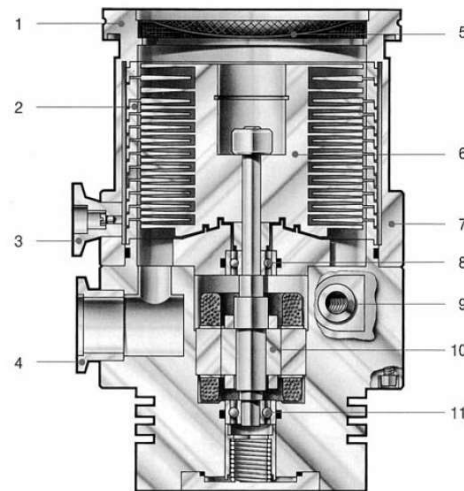


*Figure 13 - Cross section of a diffusion pump.
Leybold - Fundamentals of Vacuum Technology*

Diffusion pumps (Figure 13) operate by boiling a low vapor pressure, high molecular weight and inert fluid (usually oil) and forcing it through a vertical column. The pump fluid vapor streams through the rising tubes and emerges with supersonic speed from the ring-shaped nozzles. Gas molecules that randomly enter from the main chamber are pushed down by the flow from the nozzle.

Today they can reach ultimate pressure of 10^{-10} mbar order depending on the construction quality of the pump, the fluid used and the cleanliness of the vessel.

Turbomolecular pumps



1 High vacuum inlet flange	5 Splinter guard	9 Cooling water connection
2 Stator pack	6 Rotor	10 3-phase motor
3 Venting flange	7 Pump casing	11 Ball bearings
4 Forevacuum flange	8 Ball bearings	

*Figure 14 - Cross section of a molecular pump.
Leybold - Fundamentals of Vacuum Technology*

The principle of the molecular pump is that the gas particles receive, through impact with a rapidly moving surface of a rotor, an impulse in a required flow direction.

The design is turbine-like so with succession of rotor and stator surfaces.

The principal issue with this pump is that a turbomolecular pump can work only if molecules hit by the moving blades reach the stationary blades before colliding with other molecules on their way. The gap between moving blades and stationary blades must be close to or less than the mean free path.

Having 1 mm of gap, the minimum working pressure must be 0.10 mbar.

The main reason because they are used, is the versatility. In fact, they can generate different level of vacuum between 10^{-3} and 10^{-1} mbar

Sputter-ion pumps

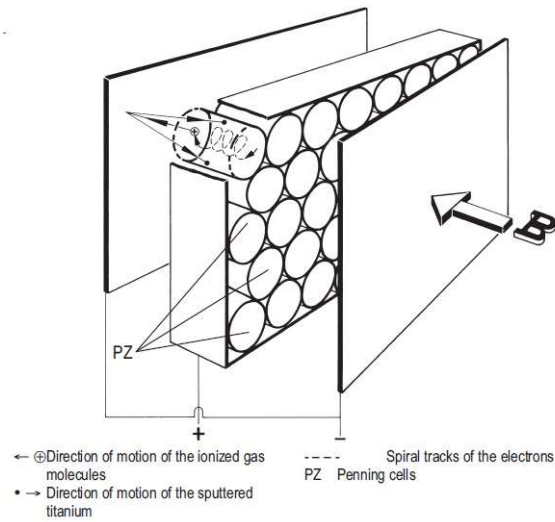


*Figure 15 - Cross section of a Sputter-ion pump.
Leybold - Fundamentals of Vacuum Technology*

The ions impinge upon the cathode of the cold cathode discharge electrode system and sputter the cathode material (titanium). The titanium deposited at other locations acts as a getter film and adsorbs reactive gas particles. These pumps do not have moving parts, and do not use oil so is not necessary a frequent maintenance. They can attain pressures of less than 10^{-11} mbar.

Cryopumps

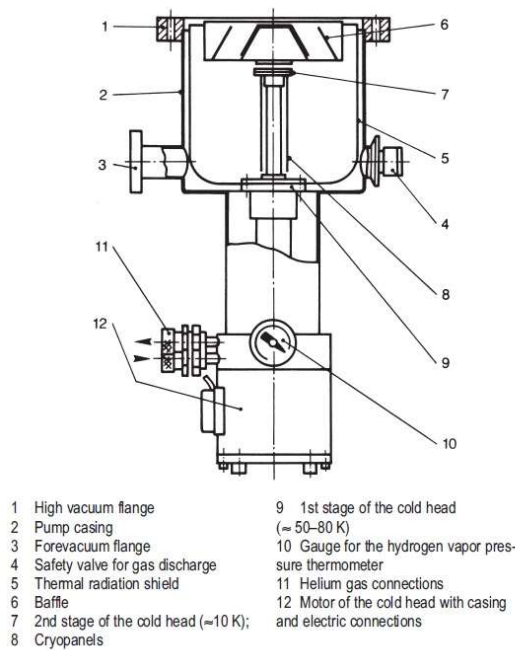


*Figure 16 - Cross section of a cryopump.
Leybold - Fundamentals of Vacuum Technology*

The effect of condensation of gases does not occur only at atmospheric pressure but also in vacuum.

The formation of condensate in a sealed space means that a large amount of gas molecules is removed from the volume. They remain located on the cold surface until they are removed for cleaning purpose of the pump.

There are basically three types of cryopumps.

In the case of **bath cryostats**, the pumping surface is cooled by direct contact with liquid nitrogen.

In **continuous flow cryopumps** the cold surface is designed to operate as heat exchanger.

Liquid helium is used to attain a sufficient low temperature. The waste gas of helium generated by the process is used to cool the baffle of a thermal radiation shield which protects the system from thermal radiation from the outside.

Refrigerator cryopumps are the most used today. They work like household refrigerator, but the thermodynamic cycles are obtained using helium.

The main problem with this type of pump is that they cannot work for an unlimited time. When the cold surface is becoming full of compensated gas molecules, the efficiency of the pump goes down, so it must be clean heating the surface and using a backup pump that blows away the particles.

1.3 Pressure sensors

Pressure sensors are one of the most important devices in a vacuum system. They are used to evaluate the various degrees of pressure in order to guarantee the tightness of a thermal vacuum chamber, and it is also necessary in the case in which some machines have precise ranges of operation.

There are basically three mechanism used to measure pressure in a closed environment, based on the working range.

Mechanical gauges work with diaphragms that move under the effect of the gas pressure. Their results are not affected by gas properties, but they cannot work below 10^{-5} Torr.

Gas property gauges are dependent on gas composition, because they measure properties like conductivity or viscosity. Working range is usually between 100 and 10^{-4} Torr.

Ionization gauges are used for high vacuum and UHV measurements, covering the pressure range from 10^{-4} Torr to 10^{-10} Torr. Gas molecules are ionized by electrons and the resulting ion current measured.

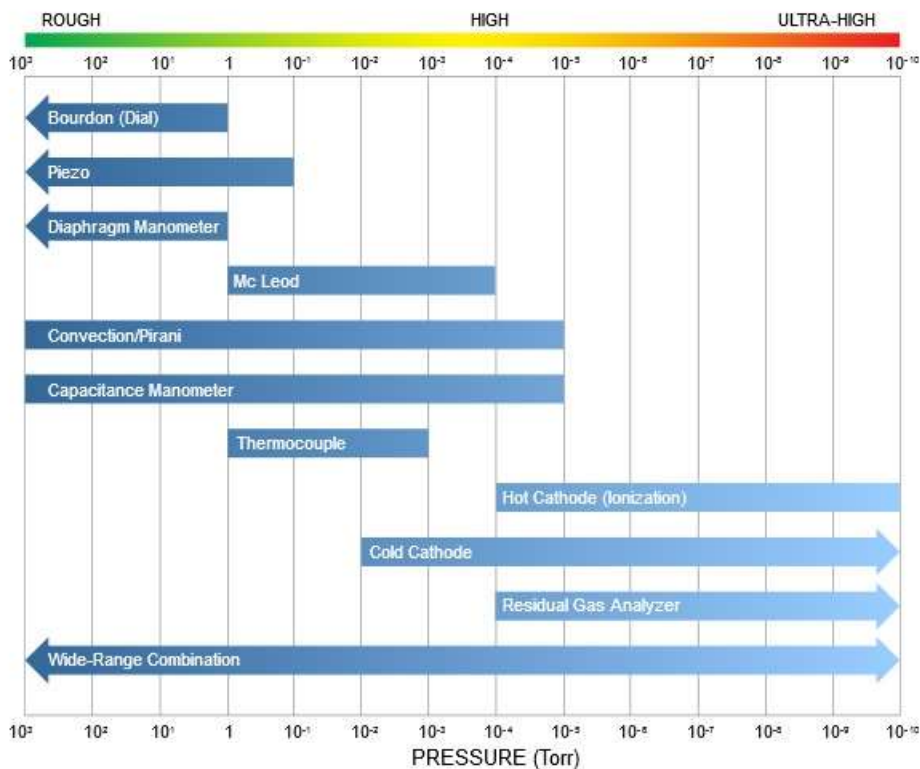


Figure 17 - Pressure Ranges of different Vacuum Gauges.
https://www.lesker.com/newweb/gauges/gauges_technicalnotes_1.cfm

1.3.1 Mechanical gauges

Bourdon

Mechanical Gauge Bourdon Tube

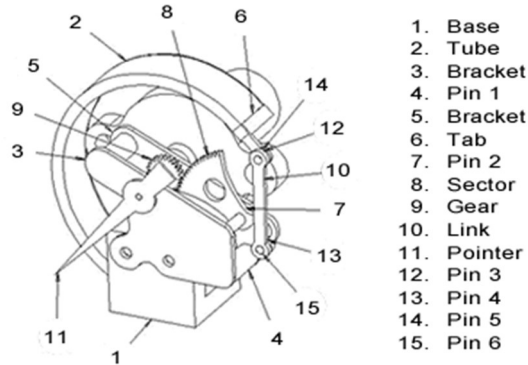


Figure 18 - Bourdon gauge.
<http://www.marshallinstruments.com/faqs/detail.cfm?id=22>

Bourdon gauges are mechanical pressure measuring instruments that consist of tubes bent into a coil or an arc. As pressure inside the tube increase, the coil unwinds. These sensors are widely used, but for pressure range from 0.6 to 6000 bar. There are also variations that can be used in the range between 1 to 760 Torr, but their accuracy is very low, so they are used only to sense if vacuum exists.

Piezo

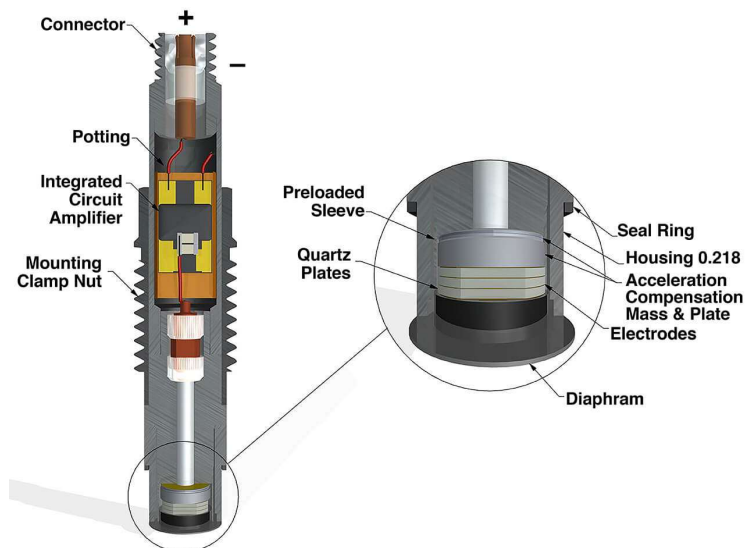


Figure 19 - Typical quartz pressure sensor cross section.
http://www.pcb.com/Resources/Technical-Information/Tech_Pres

Piezo pressure gauges are gas independent sensor that works between 0.1 to 1000 Torr thanks to the change of electrical resistance of piezo-resistive elements. This happens when the silicon crystal inside the sensor, built as a diaphragm, is deflected under pressure, causing the Wheatstone bridge network to move out of balance.

Capacitance Manometers

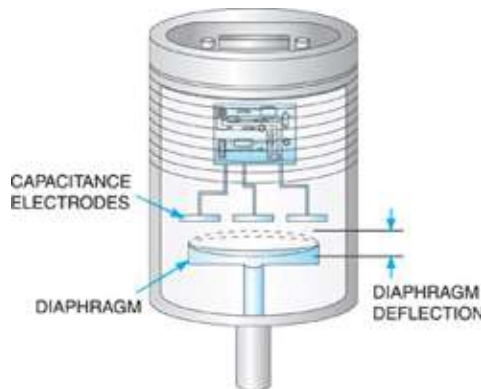


Figure 20 - Typical capacitance manometer cross section.
https://www.lesker.com/newweb/gauges/gauges_technicalnotes_1.cfm

Capacitance manometers are the only mechanical sensors that can reach pressure level of 10^{-5} Torr. They measure the difference between a known pressure and the unknown pressure through the deflection of a thin metal diaphragm cause by that. They are called capacitance manometer because the deflection is measured with an electrical capacitance.

Gauge ahead are specified by their maximum measured pressure, and each have a dynamic range of 10^4 Torr.

1.3.2 Gas property gauges

Pirani gauges

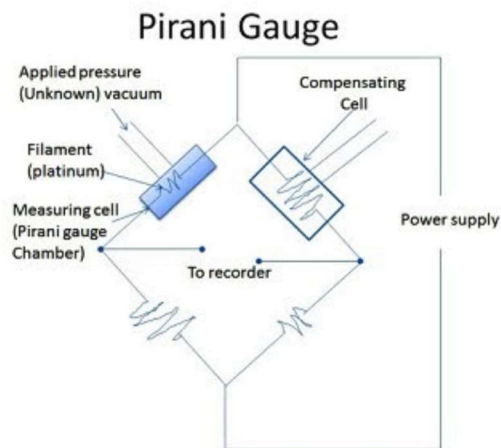


Figure 21 - Pirani gauge electrical scheme.
<http://instrumentationandcontrollers.blogspot.com/2012/03/pirani-gauge-thermal-conductivity-gauge.html>

The Pirani gauge consists of a metal filament (usually platinum) suspended in a tube which is connected to the system whose vacuum is to be measured.

A conducting wire (platinum filament) gets heated when electric current flows through it. This wire suspended in a gas will lose heat to the gas as its molecules collide with the wire and remove heat.

CHAPTER 1 – SPACE ENVIRONMENT

Measuring the heat loss is an indirect indication of pressure and a correction must be done if there are gasses other than air in the chamber.

The limits of this technology are that thermal conductivity is not a function of pressure in laminar flow range and that as the gas pressure is reduced (by the vacuum pumps) the number of molecules present will fall proportionately, the conductivity of the surrounding media will fall and the wire will lose heat more slowly. Below 10^{-4} hPa gasses do not influence anymore the heat output of the wire.

Over time, molecules will stick to the filament, causing an inaccurate measurement. Depending on what the gauge has been exposed to, the filament can be cleaned by pouring a small amount of solvent into the flange termination.

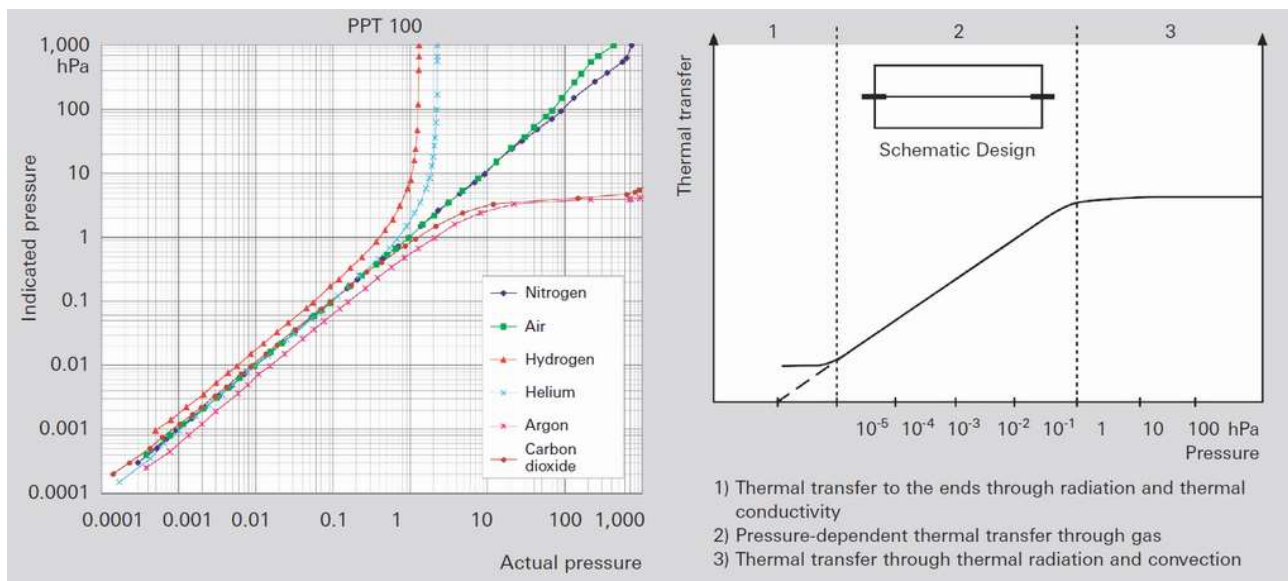


Figure 22 - Pirani gauge: indicated pressure over actual pressure for different gas species - Thermal transfer function. Sergio Calatroni. Copper for particle accelerators: electron stimulated desorption and study of hydrogen content measurement by laser ablation

Convection enhanced Pirani gauges

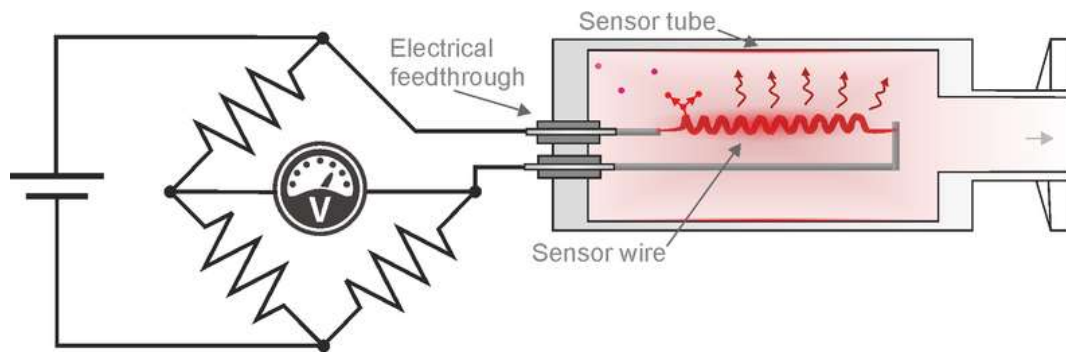


Figure 23 - Convection enhanced Pirani gauge scheme.
<https://sens4.com/pirani-working-principle.html>

As the Pirani gauge, the convection enhanced Pirani works applying current into a filament to maintain constant temperature. The specific design of this sensor causes a specific airflow inside that minimizes pockets of molecules sticking to a specific portion of the filament, providing more accurate reading. This helps maintain accuracy above 10 Torr.

1.3.3 Ionization Gauges

Hot Cathode Gauges

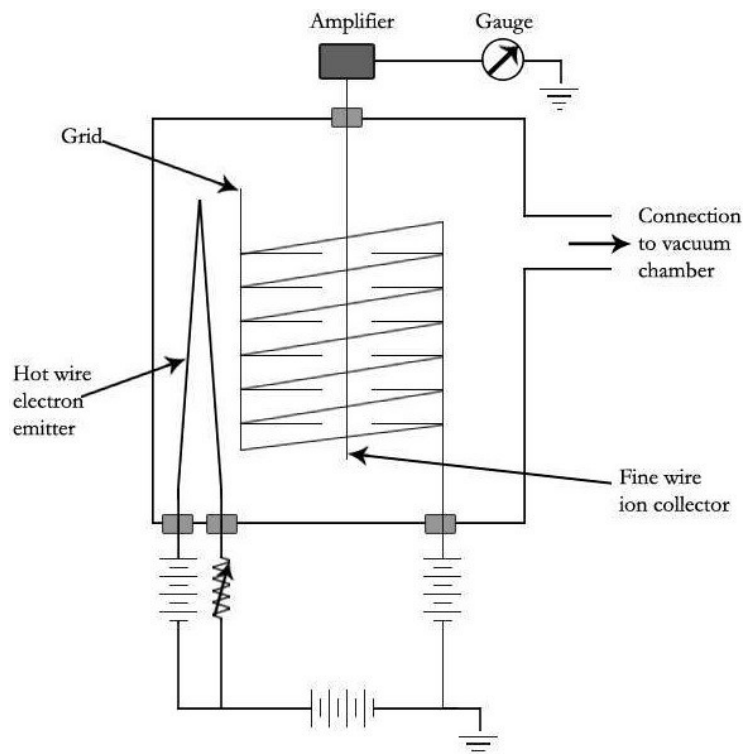


Figure 24 - Schematic of Hot Cathode Gauge.
<https://www.supervacoils.com/vacuum-gauges-explained/>

These sensors commonly use three electrodes. A hot cathode emits electrons which impinge on an anode. Electrons emitted from the filament move several times in back-and-forth movements around the grid before finally entering the grid. During these movements, some electrons collide with a gaseous molecule to form a pair of an ion and an electron (electron ionization). The number of these ions is proportional to the gaseous molecule density multiplied by the electron current emitted from the filament, and these ions pour into the collector to form an ion current. It is detected through the third electrode, the so-called ion detector, and this current is used as the signal which is proportional to the pressure. The hot cathode sensors which are mostly used today, are based on the Bayard-Alpert principle.

Bayard-Alpert ion gauges have a reasonably linear response from 10^{-4} Torr to 10^{-9} Torr, with gauge sensitivities from 5 to 20 Torr^{-1} . The low-pressure sensitivity of hot-cathode gauges is limited by the photoelectric effect. Electrons hitting the grid produce x-rays that produce photoelectric noise in the ion collector.

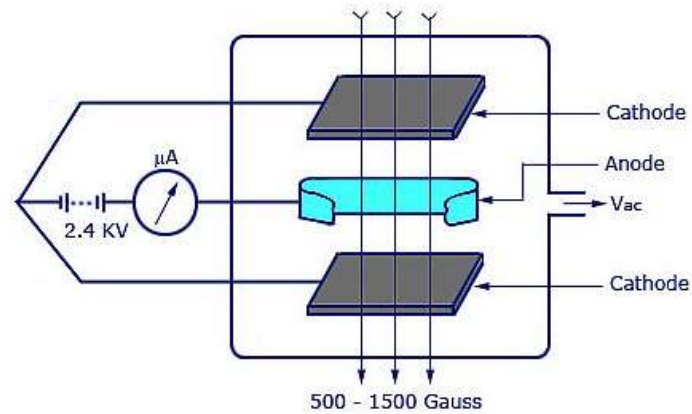
Cold Cathode Ionization Vacuum Gauge (Penning)

Figure 25 - Schematic of Cold Cathode Ionization Gauge.

<http://www.instrumentationtoday.com/ionization-gauge-cold-cathode-type/2012/01/>

In cold cathode gauges, ionizing electrons are part of a self-sufficient discharge (self-sustaining). However, since the CCG has no filaments, the discharge is triggered by stray field emissions or external events (cosmic rays or radioactive decay).

At low pressures, this can take up to a few minutes and CCGs are generally activated at high pressure (1^{-2} Torr or higher). The electric field of the meter forces the electrons into helical paths, providing long path lengths and therefore high probability of ionizing the residual gas. Ions are collected and measured to determine the gas pressure.

Many geometries of electrodes, cylinders, plates, rings, bars have been adopted, in various versions with the direction of the field and the force chosen to maximize the measured current. If the central or "final" electrodes of the meter are negative, the convention is to call this a magnetron. If the same electrodes are positive, the meter is called inverted magnetron.

The initial Magnetron, that was named Penning, design (cylindrical anode and end plate cathodes) was neither precise nor accurate and it was replaced by other geometries. However, the name Penning is still used even for magnetrons with central wire or ring cathodes. The operating voltage is limited to avoid field emission effects that cause increases in the ion current unrelated to pressure. While the newer magnetron designs are satisfactory, they are limited to the top of the high vacuum range and attract little commercial attention.

Inverted Magnetron design works into the UHV pressure range. Its axial central anode enters the cylinder/end plates cathode through voltage guard rings (to prevent field emission affecting the ion current measurement). The anode carries a much higher potential than the normal magnetron ($\sim 6\text{kV}$) and is parallel to the gauge's magnetic field. Some commercially available inverted magnetron designs have good linearity and operating characteristics down to 10^{-11} Torr. However, attempting to start one at such low pressures may take hours or days.

Unlike the hot filament gauge, the cold cathode gauge does not have the filaments or the grid to degas. Instead, some cold cathode gauges can be taken apart, exposing the ionization chamber and inside walls of the gauge. This exposure allows the user to literally scrub the inside walls of the cold cathode gauge, helping to remove molecules that have been "sputtered" onto the wall. This physical cleaning makes a cold cathode gauge generally more rugged than a hot filament gauge.

1.4 Temperature sensors

Being able to analyse the correct temperature of the components during a thermal vacuum test is as important as the pressure level. There are several ways to determine the temperature, related for example to the voltage difference at the ends of two metals, or more indirect measures such as the calculation of the radiation emitted by a given object.

The temperature sensors that work in contact, and those that do not touch, will then be analysed.

1.4.1 Contact temperature sensor

Thermocouples

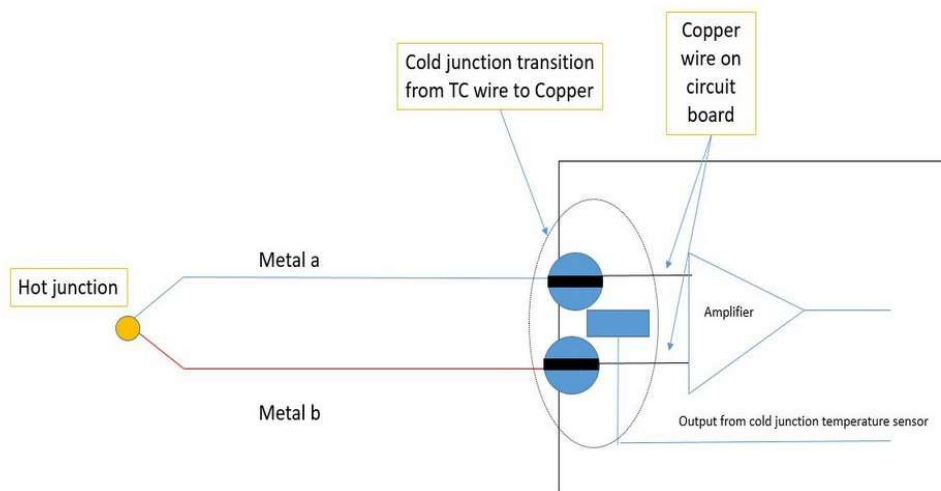


Figure 26 - Schematic of a thermocouple.

<https://www.flukeprocessinstruments.com/en-us/service-and-support/knowledge-center/thermal-profiling-technology/thermocouple-theory>

This sensor consists of two dissimilar metal wires, joined at one end, and connected to a thermocouple thermometer or other thermocouple-capable device at the other end. When different metals are joined and there is a thermal gradient at the extremities, it can be measured an electromotive force created by the Seebeck effect.

Each thermocouple type has its characteristic Seebeck voltage curve. The Seebeck curve is dependent on the metals used in the two wires of thermocouple and voltages generated are measured in mV.

Pressure can be calculated by the temperature information.

CHAPTER 1 – SPACE ENVIRONMENT

This gauge gives a differential measurement, so one of the temperatures must be hold constant, through an ice bath that set to 0 degrees the temperature, or with a circuit that compensate the difference of tension.

The second solution, that gives a more accurate response and is easier to build, requires a second temperature sensor.

There are many types of thermocouples given by the metals used, each with its own unique characteristics in terms of temperature range, durability, vibration resistance, chemical resistance, and application compatibility.

Thermocouple Type	Temperature Range (°C)				
	Short Term Use	Continuous Use	Class 1 Tolerance	Class 2 Tolerance	Class 3 Tolerance
Type E	-40 to +900	0 to +800	-40 to +800	-40 to +900	-200 to +40
Type J	-180 to +800	0 to +750	-40 to +750	-40 to +750	N/A
Type K	-180 to +1300	0 to +1100	-40 to +1000	-40 to +1200	-200 to +40
Type N	-270 to +1300	0 to +1100	-40 to +1000	-40 to +1200	-200 to +40
Type R	-50 to +1700	0 to +1600	0 to +1600	0 to +1600	N/A
Type S	-50 to +1750	0 to +1600	0 to +1600	0 to +1600	N/A
Type T	-250 to +400	-185 to +300	-40 to +350	-40 to +350	-200 to +40
Type B	0 to +1820	+200 to +1700	N/A	+600 to +1700	+600 to +1700

Figure 27 - Thermocouple Temperature range.
<https://www.sterlingsensors.co.uk/thermocouples>

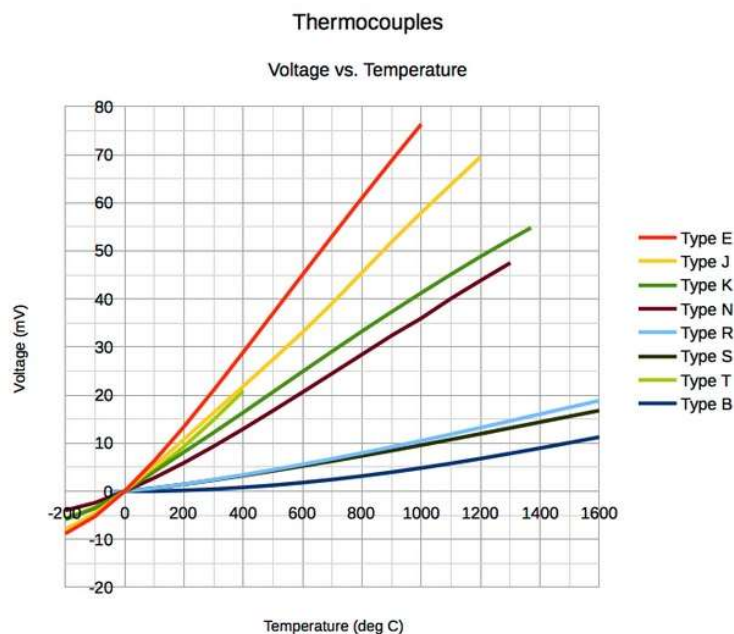


Figure 28 - Voltage function.
https://www.engineeringtoolbox.com/thermocouples-d_496.html

Resistance temperature detectors

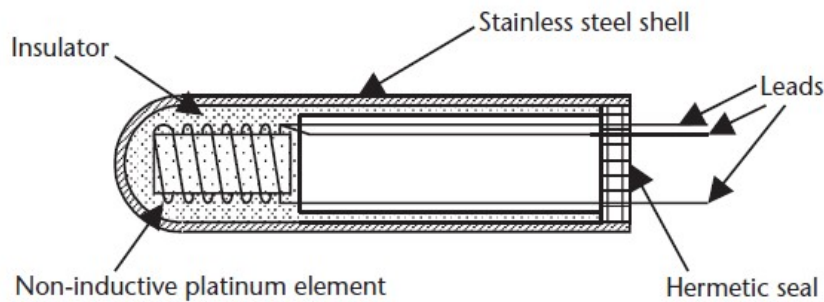


Figure 29 - Resistance temperature detector scheme.
<https://automationforum.co/resistance-temperature-detector-rtd/>

A Resistance Thermometer or Resistance Temperature Detector is a device which used to determine the temperature by measuring the resistance of pure electrical wire. The relationship between an RTD'S resistance and the surrounding temperature is highly predictable, allowing for accurate and consistent temperature measurement.

The variation of resistance of the metal with the variation of the temperature is given as:

$$R_t = R_0(1 + \alpha(t - t_0) + \beta(t - t_0)^2 + \dots)$$

Where, R_t and R_0 are the resistance values at t and t_0 C temperatures. α and β are the constants depends on the metals.

In RTD devices; Copper, Nickel and Platinum are widely used metals. These three metals are having different resistance variations with respective to the temperature variations. That is called resistance-temperature characteristics. Platinum has the temperature range of 650 °C, and then the Copper and Nickel have 120 °C and 300 °C respectively. For Platinum, its resistance changes by approximately 0.4 Ohm per degree Celsius of temperature.

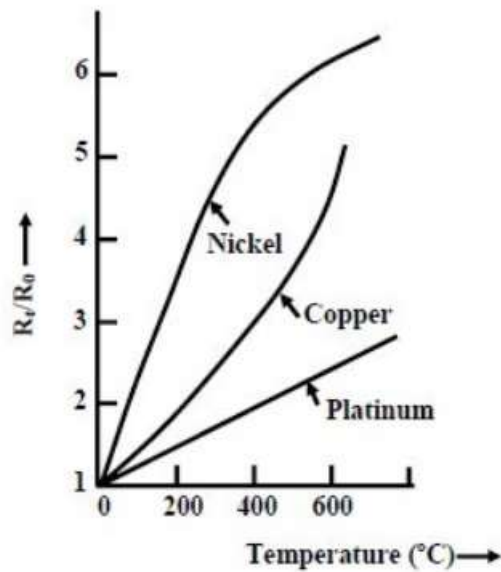


Figure 30 - Resistance function.

<https://www.electrical4u.com/resistance-temperature-detector-or-rtd-construction-and-working-principle/>

The purity of the materials platinum is checked by measuring $\frac{R_{100}}{R_0}$.

If it will not pure, it will deviate from the conventional resistance-temperature graph. So, α and β values will change depending upon the metals.

Thermistors

Thermistors

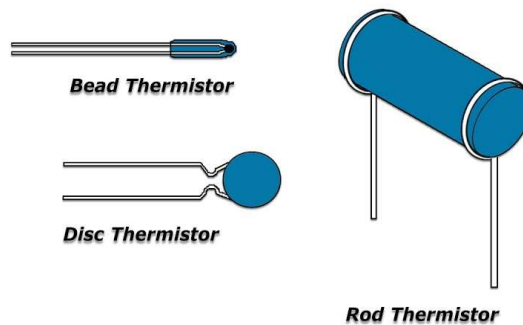


Figure 31 - Type of thermistors

Thermistors, derived from the term Thermally Sensitive Resistors, are a very accurate and cost- effective sensor for measuring temperature.

Thermistors are available in two types: those with Negative Temperature Coefficients (NTC thermistors) and those with Positive Temperature Coefficients (PTC thermistors).

CHAPTER 1 – SPACE ENVIRONMENT

NTC thermistors' resistance decreases as their temperature increases, while PTC thermistors' resistance increases as their temperature increases. Only NTC thermistors are commonly used in temperature measurement.

Thermistors work similar to RTD, with the difference that are made of semiconductors. As the temperature increases, an NTC thermistor's resistance will increase in a non-linear fashion, following a particular "curve." The shape of this resistance vs. temperature curve is determined by the properties of the materials that make up the thermistor.

Thermistors are available with a variety of base resistances and resistance vs. temperature curves.

Low-temperature applications (-55 to approx. 70°C) generally use lower resistance thermistors (2252 to 10,000Ω). Higher temperature applications generally use higher resistance thermistors (above 10,000Ω).

Some materials provide better stability than others. Resistances are normally specified at 25°C (77°F). Thermistors are accurate to approximately $\pm 0.2^\circ\text{C}$ within their specified temperature range. They're generally durable, long-lasting, and inexpensive.

Thermistors are often selected for applications where ruggedness, reliability and stability are important. They're well suited for use in environments with extreme conditions, or where electronic noise is present. They're available in a variety of shapes: the ideal shape for a particular application depends on whether the thermistor will be surface-mounted or embedded in a system, and on the type of material being measured.

Thermistors with epoxy coatings are available for use at lower temperatures [typically -50 to 150°C (-58 to 316°F)]; thermistors are also available with glass coatings for use at higher temperatures [typically -50 to 300°C (-58 to 572°F)]. These coatings protect the thermistor and its connecting wires from humidity, corrosion and mechanical stress.

1.4.2 Non-contact temperature sensors

Infrared thermometers and pyrometers



Figure 32 - Infrared thermometer

An infrared thermometer is a thermometer which infers temperature from a portion of the thermal radiation sometimes called black-body radiation emitted by the object being measured. They are also called laser thermometers as a laser is used to help aim the thermometer, or non-contact thermometers or temperature guns, to describe the device's ability to measure temperature from a distance.

By knowing the amount of infrared energy emitted by the object and its emissivity, the object's temperature can often be determined within a certain range of its actual temperature. Infrared thermometers are a subset of devices known as "thermal radiation thermometers".

Near ambient temperatures, readings may be subject to error due to the reflection of radiation from a hotter body rather than radiated by the object being measured, and to an incorrect assumed emissivity.

The design essentially consists of a lens to focus the infrared thermal radiation on to a detector, which converts the radiant power to an electrical signal that can be displayed in units of temperature after being compensated for ambient temperature. This permits temperature measurement from a distance without contact with the object to be measured.

A non-contact infrared thermometer is useful for measuring temperature under circumstances where thermocouples or other probe-type sensors cannot be used or do not produce accurate data for a variety of reasons.

1.5 Residual Gas Analysers

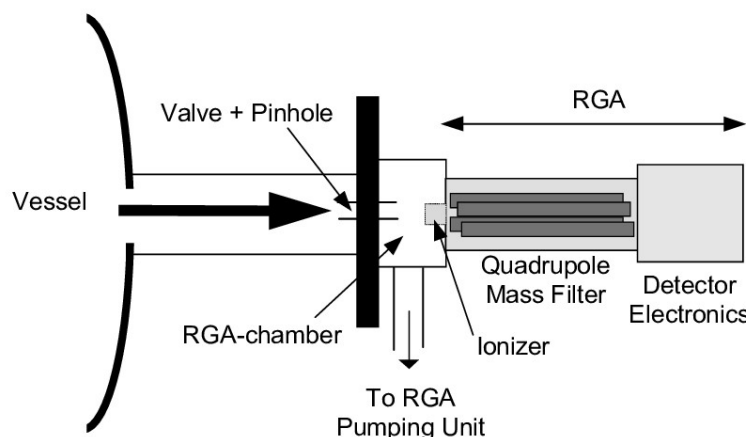


Figure 33 - The residual gas analyser and the connection to the vessel.
Ariel de Graaf. Deposition of CNH materials : plasma and film characterization

To be able to perform certain procedures, such as the bakeout procedure that will be discussed in more detail below, it may be useful to know the chemical species present in the thermal-vacuum chamber.

Special mass spectrometers designed to analyse gases remaining in a vacuum chamber are called residual gas analysers or RGAs. The wealth of information about experimental or process conditions offered by an RGA makes a permanently attached unit a convenient, often necessary, diagnostic device.

Quadrupole RGAs, named for the four rods used in the mass filter section, are powered by mixed RF/DC voltages.

The quadrupole analyser (or sensor head) bolts to the vacuum system. It consists of an ionizer (ion source) connected to the mass filter, which in turn is attached to an ion detector, all mounted on a UHV flange carrying the feedthroughs for power and signals. The combined RF/DC voltage is generated close to the sensor head.

From here, only main power voltage and returning signal information connect to the control chassis and display or desktop PC.

In the ionizer, neutral gas atoms and molecules are bombarded with 70eV electrons from a hot filament. The ionized species are extracted into the quadrupole, where only those ions with the appropriate mass-to-charge (m/e) ratio for the applied RF/DC voltages are transmitted. By varying the RF/DC voltage with time, the m/e ratios are scanned and the ion current at each mass is recorded as a spectrum.

Diagnosing vacuum problems with an RGA requires only a collection of fragmentation patterns from which the following may be quickly determined: the presence of air and water leaks; unacceptable levels of active gases such as O₂, H₂, and H₂O, pump oil back streaming, the presence of F₁ or Cl compounds; the regeneration requirements of a cryopump, and the purity of backfill gases.

Because an RGA operates at or below 10^{-4} Torr, high-pressure processes are analysed with the RGA installed in an auxiliary vacuum system, often a mobile cart moved to various vacuum stations.

2. CHAPTER 2 - PESCha



Figure 34 - PESCha overview

In order to study the various aspects of space environment the PEPS technological area was ideated to select and develop innovative and suitable technologies for space applications, as well as tools and instrumentations to verify materials and components in a representative aggressive environment.

The main facility of the PEPS technological area is PESCha, acronym of Planetary Environmental Simulation Chamber.

PESCha is a vacuum chamber, that can be use in multiples ways, but its main purpose is to simulate different environment, from outer space to planetary atmosphere.

A thermal range from -80°C to 140°C and a pressure level of 10^{-7} mbar can be obtained in order to test material and components for space application, or to accelerate the process of the outgassing of materials.

In this chapter it will be discussed how the whole facility works and which its the main components.

2.1 PESCha facility

The equipment of the PESCha facility located into two spaces, the PEPS laboratory and the thermal control system room:

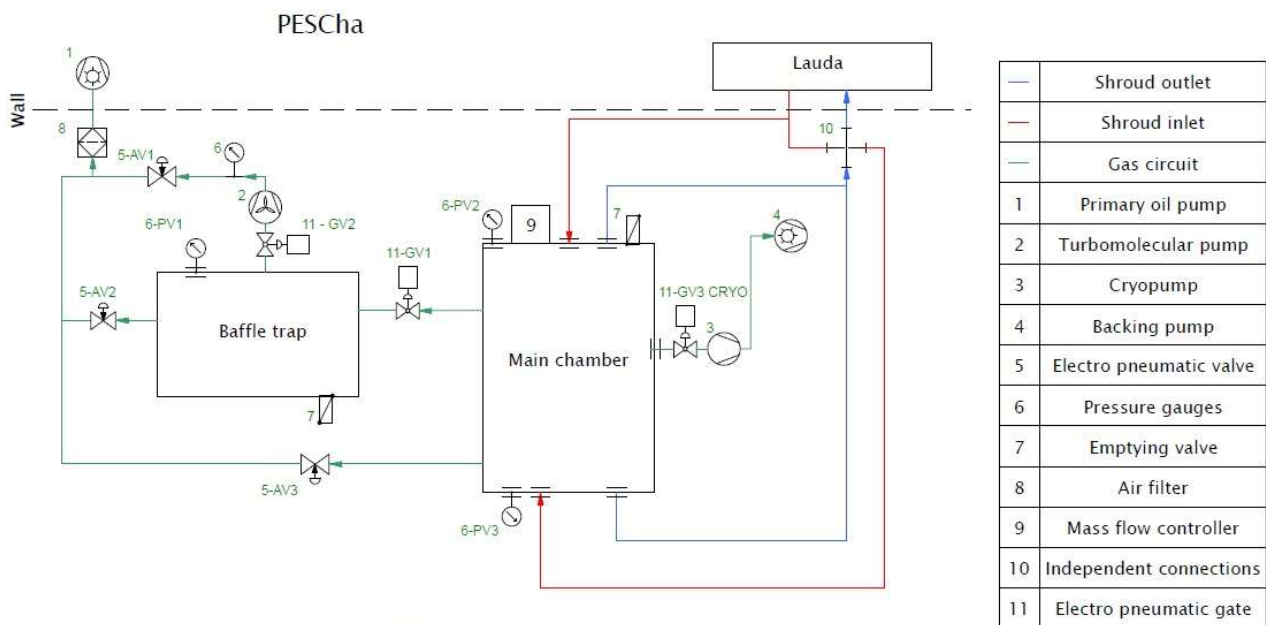
- In the laboratory are located the majority of the PESCha equipment's. In particular the PESCha vacuum chamber that is composed by two different chambers.

The main chamber is the largest cylindrical chamber where the tests are performed. The baffle chamber, positioned between the main and the turbomolecular pump, is useful in the case of dust tests, such as the Martian regolith, to avoid pump contamination.

The connection between the two chambers, like the connection between the baffle and the turbo, is managed by means of the electro-pneumatic controlled gates.

The primary pump is connected directly to both chambers, with electro-pneumatic valves that manage the passage of the air flow.

In this room there are the ends of the tubes with the operating liquid of the Lauda thermal machine, which pass through shrouds that are positioned inside the main chamber. In **Errore. L'origine riferimento non è stata trovata.** is reported the PESCha vacuum chamber functional diagram and in the table below are summarized its main components.



note: This is just a functional diagram, does not replicate the exact position of the sensors

Figure 35 - PESCha main room functional diagram

Component	Supplier	Model	Label
Primary oil pump	Oerlikon - Leybold	TRIVAC D40BCS	PP
Turbomolecular pump	Oerlikon - Leybold	TURBOVAC MAG W 2000 CT	TMP
Cryopump	Oerlikon - Leybold	COOLVAC iCL 2000	
Backing pump			
KF-40 electropneumatic valve	Agilent - Varian	L6282633	
Air filter-dust separator	Oerlikon - Leybold	AS 30-60	
Mass flow controller	MKS Instruments	1179B	MFC
Contamination-proof ISO-F 250 gate valve	1) Vacuum Research 2) Agilent - Varian	PCWA250ISON1EP VGA250IE24DP	GV1 GV2

Table 1 - PESCha components

- In the thermal control system are located the thermal control system, the primary pump and water-cooling system whose functional diagram is presented below.

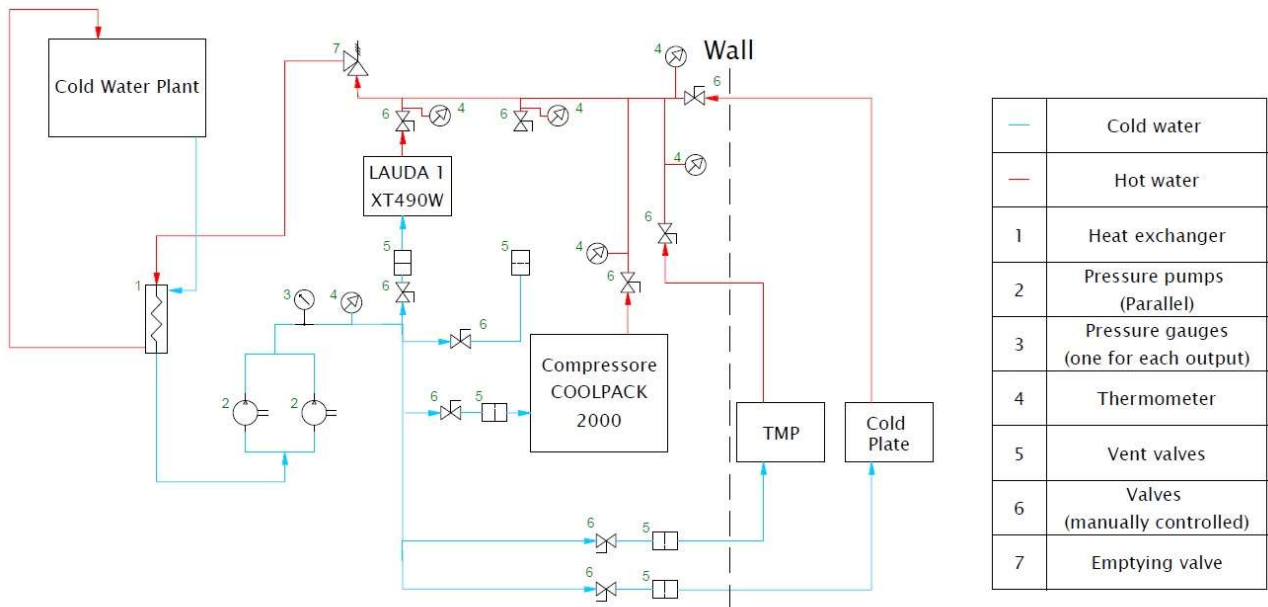


Figure 36 – Water cooling functional diagram

2.2 Components

2.2.1 Main chamber

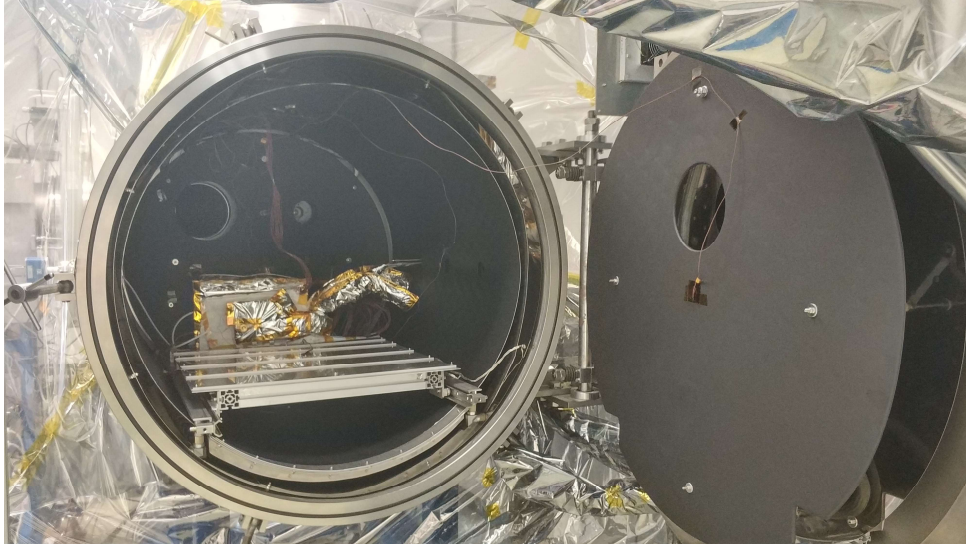


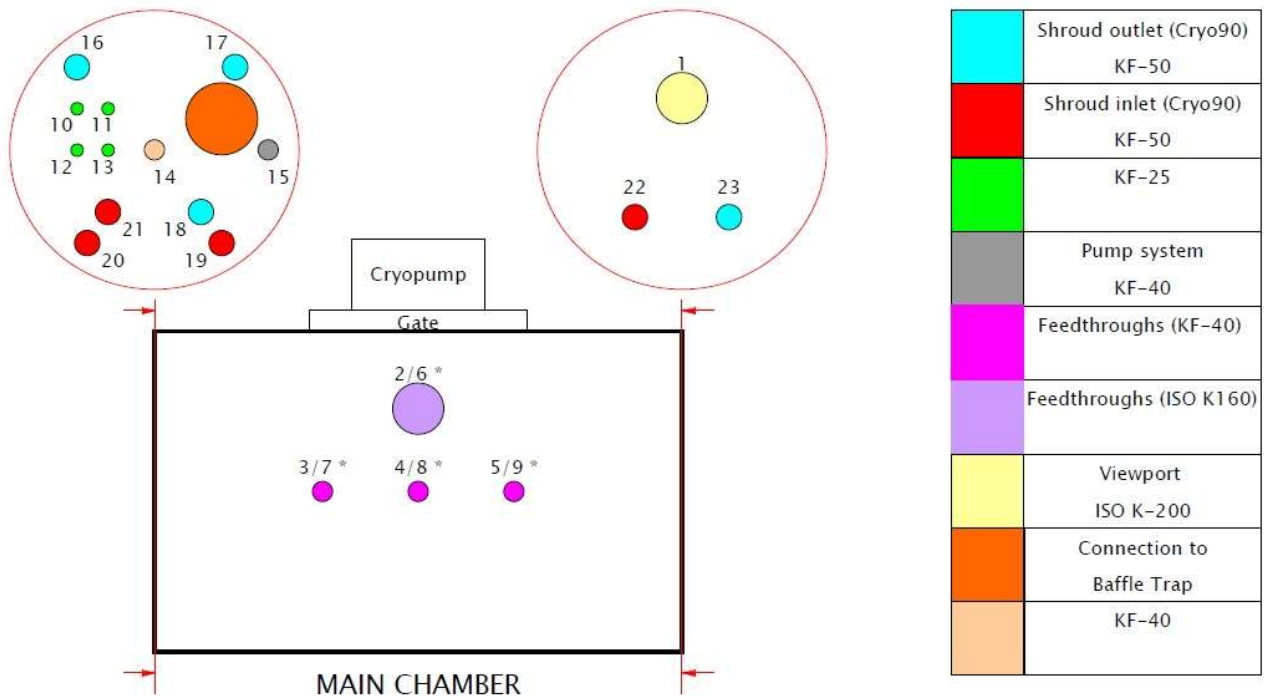
Figure 37 - Main chamber

The main structure is a rigid chamber whose goal is to limit a vacuum region. Many types of chamber are commercially available, depending on the shape of the structure, the material used and the magnetic shield that can be applied. The shape, which goes from spherical boxes to cylindrical ones, affects pressure range and constrains the type material to be used, such as stainless steel, brass or aluminium. PESCha main chamber has a cylindrical shape whose internal dimension is 1200 mm of length and 1100 mm of diameter. It is equipped with 4 different shrouds in order to control the thermal behaviour inside the chamber.

With the current configuration the following performance can be obtained:

- Minimum pressure: $5 * 10^{-7}$ mbar;
- Leak rate: 10^{-4} mbar*l/s;
- Temperature range: -80° C to 140° C;
- Max cooling rate: 1° C/minute.

This chamber has 24 different flanges of different dimension to allow the use of sensors and other equipment. In **Errore. L'origine riferimento non è stata trovata.** are listed the current allocation of the main chamber flanges and their typology.



* note: The left side is symmetrical with the right side, so the feedthroughs type is the same

Figure 38 - Main chamber feedthroughs

2.2.2 Baffle trap

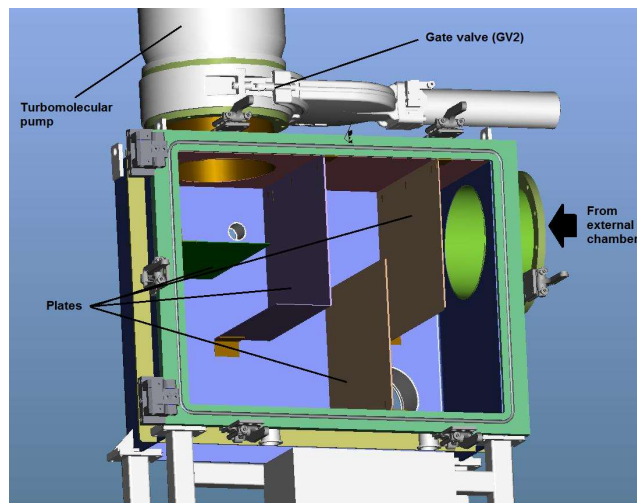


Figure 39 - Baffle trap

One of the main features of the PESCha facility is its capability to work with dust simulant, in order to do that it is necessary to avoid the contamination of the turbomolecular pump by dust particles.

The baffle trap is a small steel chamber between pumps and the main chamber. It is designed to create a difficult path for the outgoing gases that are forced to move around metallic plates. The few dust particles that could move away from the main chamber, get stuck against the plates.

So, the baffle trap acts as a filter, but its presence reduces pumping efficiency, because the articulated path makes it difficult for pumps to suck gases, therefore the metallic plates are not fixed and in case of a test without dust can be removed.

Like in the main chamber, there are available some sealed flange, to connect the turbomolecular pump, the primary pump, and the main chamber and finally for the sensors. In **Errore. L'origine riferimento non è stata trovata.** are listed the current allocation of the main chamber flanges and their typology

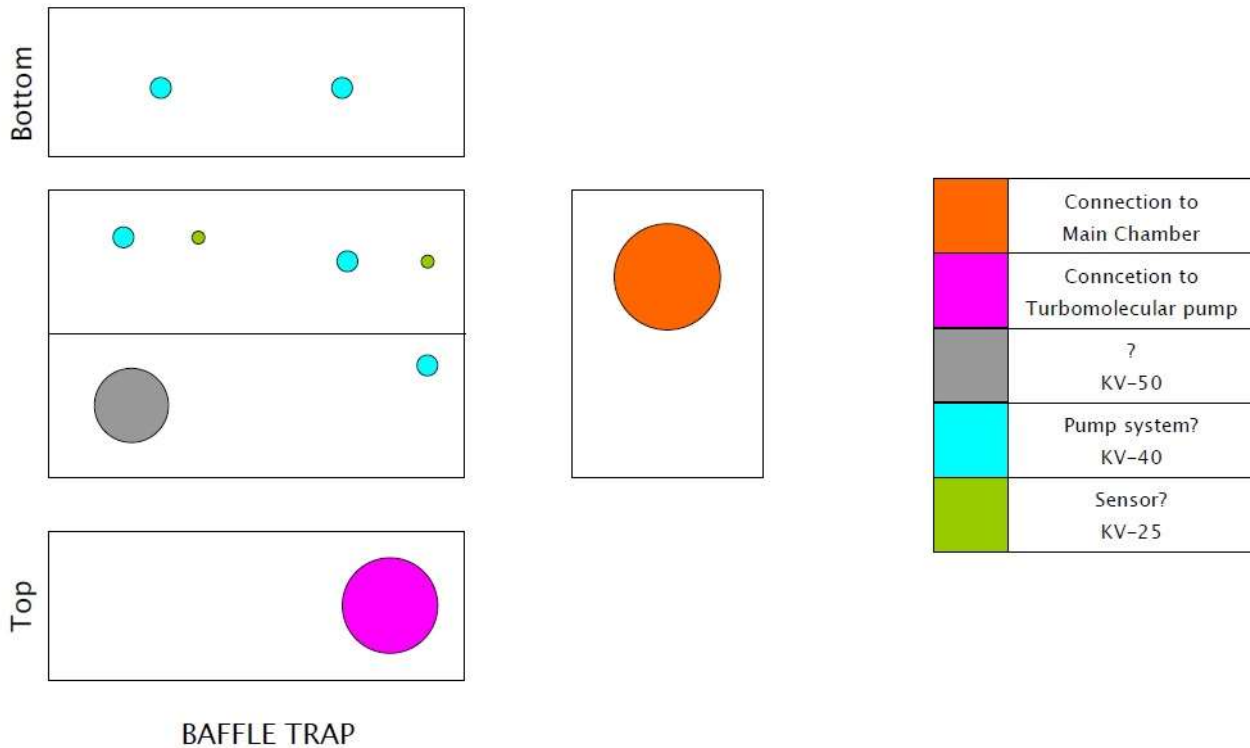


Figure 40 - Baffle trap feedthroughs

The baffle trap is smaller than the main chamber, and as can be seen from the schematic, it has fewer flanges. On the one hand, this has the disadvantage of being able to connect fewer sensors, but on the other hand it has the advantage of having fewer losses than the main chamber. This aspect will be exploited during the last test of the residual gas analyzer, which is discussed in the final chapter.

2.2.3 PESCha pumps

Three pumps assure different levels of vacuum in PESCha:

- Primary Pump
- Turbomolecular pump
- Cryopump

Their main features are described hereafter.

- **Primary Pump:** to start the vacuum process firstly the operator turns on the primary oil pump, a TRIVAC D40 BCS. It is an oil-sealed rotary vane pump with the gas ballast functionality which prevent reaching the ultimate pressure of the gas by admitting a very small amount of air into the pump chamber.



Figure 41 - TRIVAC D40 BCS

D 40 BCS		
Nominal pumping speed	46 (27.1)	$m^3 * h^{-1}$
Pumping speed	40 (23.6)	$m^3 * h^{-1}$
Ult. partial pr. without gas ballast	10^{-4}	mbar
Ultimate total pr. without gas ballast	$< 2 * 10^{-3}$	mbar
Ultimate total pr. with gas ballast	$< 5 * 10^{-3}$	mbar
Water vapour tolerance	40	mbar
Oil filling, min./max.	1.7/2.6	l
Admissible ambient temperature	12-40	°C
Motor power	2200	W
Speed (50 / 60 Hz)	1500/1800	rpm
Voltage range	50 Hz 218-242/380-420 60 Hz 230-277/414-480	V
Nom. current	50 Hz 9.9/5.7 60 Hz 8.5/4.9	A
Weight	68	Kg

Table 2 - Primary pump data sheet

- **Turbomolecular pump:** After reaching a pressure lower than $1.8 * 10^{-1}$ mbar the turbomolecular pump MAG 2000 CT can be turned on. In this pump the momentum transfer from the rapidly rotating rotor blades to the gas molecules transforms their initially non-directed thermal motion to a directed motion. This can be achieved only in the molecular flow range, where the mean free path is larger than the spacing between the rotor and stator blades so the molecules collide primarily with the rotor blades. At high pressure the turbomolecular pump cannot work because the effect of the rotor is impaired by the frequent collisions between the molecules. This pump is cooled by the water-cooling system of the facility.

An important thing that must be noticed and will be important for the next chapters is that turbomolecular pumps work better with heavier molecules, providing higher compression ratio. At a pressure of 10^{-6} mbar, just the molecules that weigh less than 44 Uma can be seen inside the chamber.



Figure 42 - MAG 2000 CT

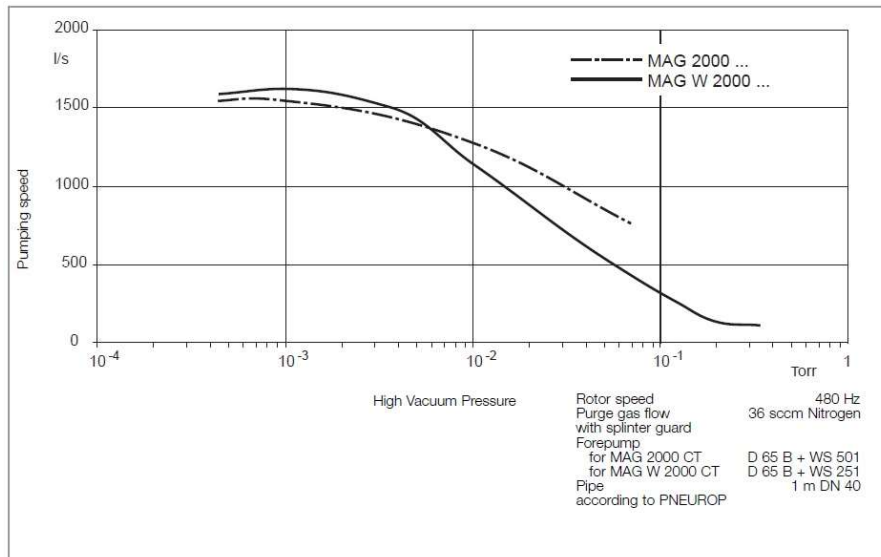


Figure 43 - Turbomolecular pumping speed

MAG 2000 C/CT		
High-vacuum connection flange	250 ISO-F	DN
Pumping speed for N2	1550	$l * s^{-1}$
Gas flow (continuous operation with Argon)	1300	sccm
Compression for N2	$> 10^8$	
Ultimate pressure	$< 10^{-8}$	mbar
Max. forevacuum pressure	1.6	mbar
Cooling water temperature	15 - 30	°C
Max. temperature of the high-vacuum flange	Short-time 85 Continuous operation 60	°C
Admissible ambient temperature	5-40	°C
Rotor Speed	28800	rpm
Max load	1800	W
Max Voltage	60	V
Max. current	20	A
Weight	68	Kg

Table 3 - Turbomolecular pump data sheet

- Cryopump:** the PESCha vacuum chamber is also equipped with a cryopump that can be used in conjunction with the turbomolecular pump in order to reach an higher vacuum level. The COOLVAC iCL 2000 works bounding gaseous substances to the cold surfaces within the pump by means of cry condensation. The advantages are that there are not any mechanically moving, oil or grease lubricated parts which lead to more compact low running cost system. One of the most critical downsides is that the performances decrease with the working time of the pump. A backing pump is required to clean the cold surfaces once the performances decrease too much.

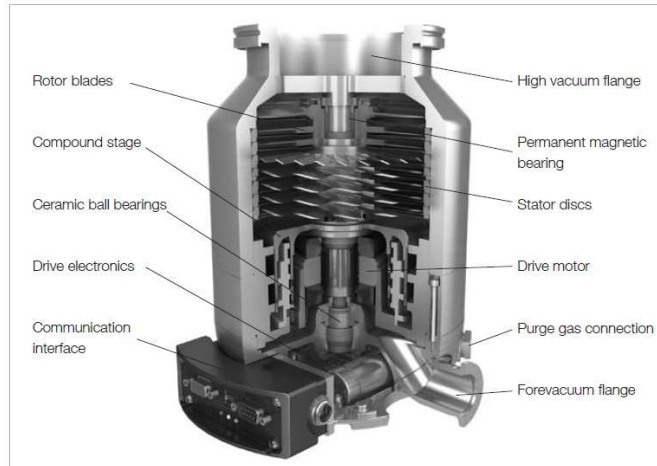


Figure 44 - COOLVAC iCL 2000

COOLVAC iCL 2000		
High-vacuum connection flange	250 ISO-F	DN
Pumping speed	H2O 7000 N2 1600 H2 3200	$l * s^{-1}$
Capacity	N2 1600 H2 15	Bar*l
Max. throughput	N2 12 H2 6	mbar x l/s
Heaters	1 st stage 160 2 nd stage 90	W
Weight	29	Kg

Table 4 - Cryopump data sheet

2.2.4 PESCha pressure sensors

The three main pressure sensors of PESCha TVC are identified with the name PV-1, PV-2, PV-3.

PV-1 checks the pressure inside the baffle trap, PV-2 and PV-3 inside the main chamber. Their output can be seen in the acquisition software, that also utilizes the data in the control logic that assure the correct working of the fluid's pumps. An example is that the gate between the baffle trap and the main chamber cannot be open if the pressure difference is greater than 30 mbar.

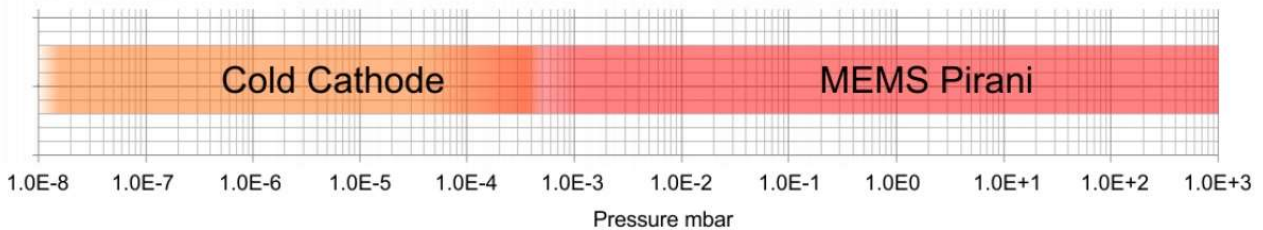
CHAPTER 2 - PESCha

It is notable that a variety of sensor types can be used to monitor the pressure in a vacuum chamber. A good combination is the one with sensors that work well in different pressure region.

At the time of writing this thesis, PTR90N pressure sensors are mounted on the PESCha vacuum chamber.

The peculiarity of this pressure sensor is that is the union of two different types of sensors, namely the Pirani and the Cold Cathode.

The MEMS Pirani automatically turns on the cold cathode at 6.7×10^{-4} mbar and turns it off at 1.1×10^{-3} mbar. Above 5.3×10^{-4} mbar, the combined reading is the MEMS Pirani pressure measurement and below 1.3×10^{-4} mbar it is the cold cathode pressure measurement. Between 1.3×10^{-4} and 5.3×10^{-4} mbar, the two measurements are smoothly integrated.



SLC: Low CC turn on pressure (6.7×10^{-4} mbar)
 SHC: High CC turn off pressure (1.1×10^{-3} mbar)
 SLP: Low CC/MP integration (1.3×10^{-4} mbar)
 SHP: High CC/MP integration (5.3×10^{-4} mbar)

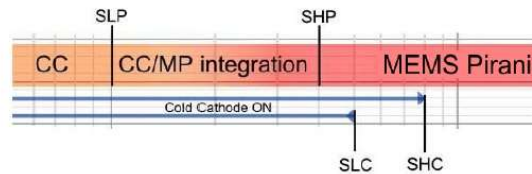


Figure 45 - PTR90N Pressure range

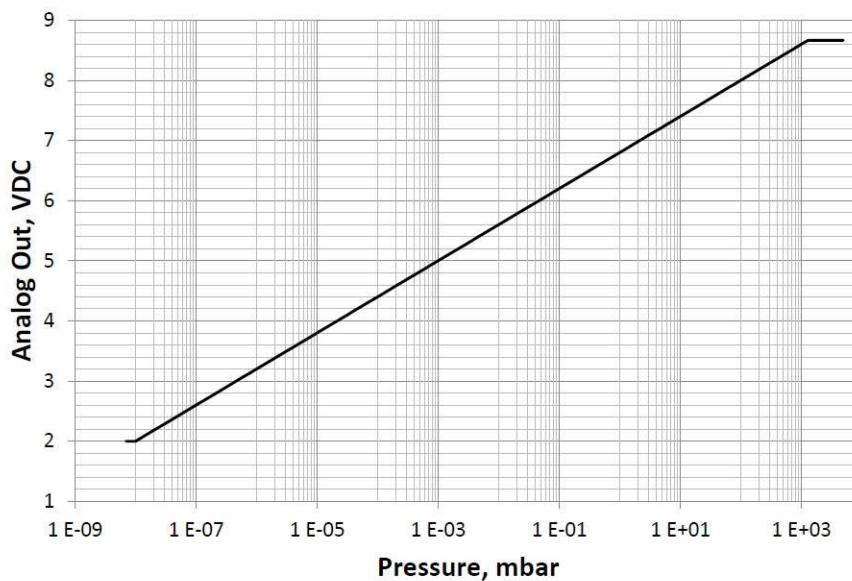


Figure 46 - PTR90N Output function

2.2.5 PESCha temperature sensors

PESCha facility provides different temperature sensors, not just to perform bake-out process but also different thermocouple that cover locally all the experiment that are performed in the chamber.

For controlling the bake-out process there is the main sensor at the output of the LAUDA temperature control system, there are different needle sensors at shrouds inlet and resistance temperature detectors attached with the shrouds for monitoring the actual temperature inside the main chamber.

The sensors used primarily within the chamber are of type j and k type thermocouples. The older Type K thermocouple has a Chromel positive leg and an Alumel (Nickel- 5% Aluminum and Silicon) negative leg. Type K is recommended for use in oxidizing and completely inert environments. One of the main problems of Type K is that should not be used in sulphurous atmospheres, in a vacuum or in low oxygen environments where selective oxidation will occur. The temperature range for Type K is $-200\text{ }^{\circ}\text{C}$ to $+1350\text{ }^{\circ}\text{C}$ and its wire colour code is yellow and red.

The Type T thermocouple has a Copper positive leg and a Constantan negative leg. Type T thermocouples can be used in oxidizing, reducing or inert atmospheres, except the copper leg restricts their use in air or oxidizing environments to 700°F or below. The temperature range for Type T is -200 to $350\text{ }^{\circ}\text{C}$ and its wire colour code is blue and red.

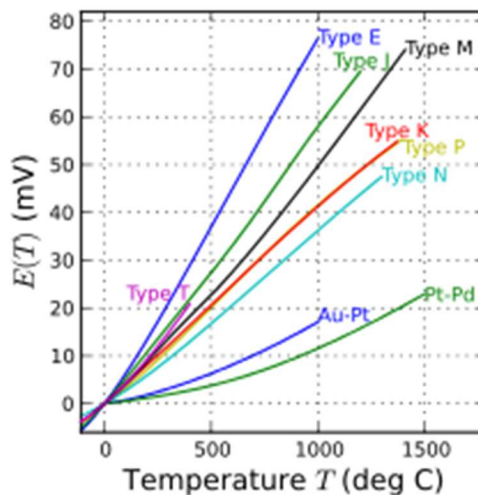


Figure 47 - Thermocouple Output.
Wikipedia

2.2.6 PESCha mass flow controller

The mass flow controller is a device that is used to manage the introduction of gases inside the chamber.

For example it allows to simulate the Martian atmosphere by injecting CO₂, or to carry out the controlled return to standard pressure of the chamber by entering pure N₂ and synthetic air to avoid contamination of the components that have been tested.

The flow rate of this device is managed in sccm (Standard Cubic Centimetres per Minute), a unit widely used in engineering and technical fields.

1 sccm corresponds to $0.001689 Pa \cdot \frac{m^3}{s}$

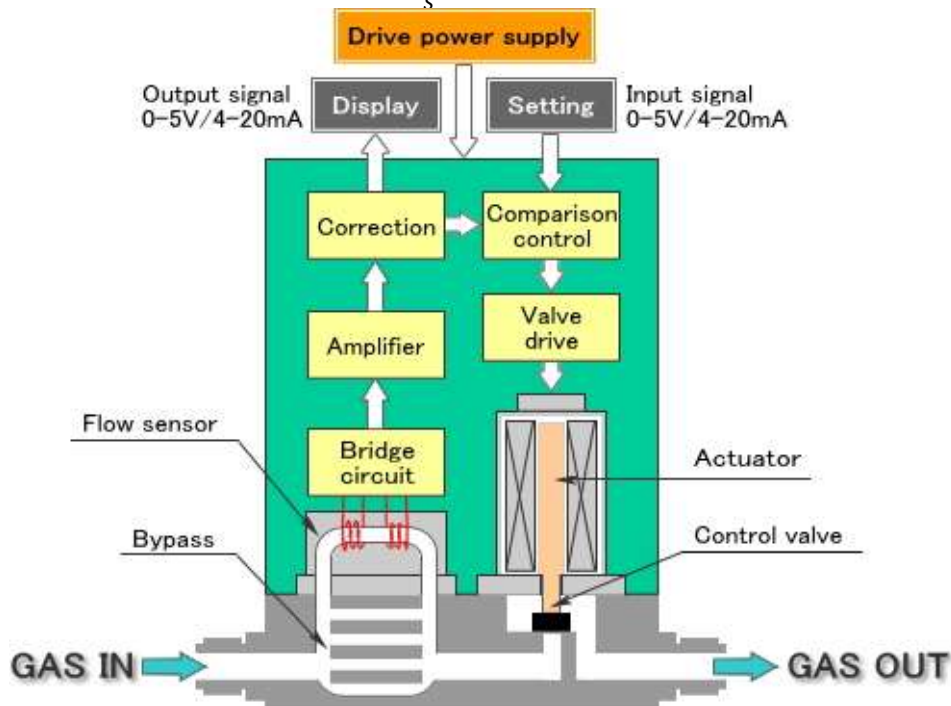


Figure 48 - Mass flow controller functional scheme.
www.fcon-inc.jp

PESCha's MFC is produced by MKS Instrument and its code is 1179B. Its operation is based on a sensor that can measure flows of the order of 10 sccm. The output is an analog signal in the range between 0V and 5V.

CHAPTER 2 - PESCha

The control circuit is of the PID type, which manages the opening of a solenoid valve.

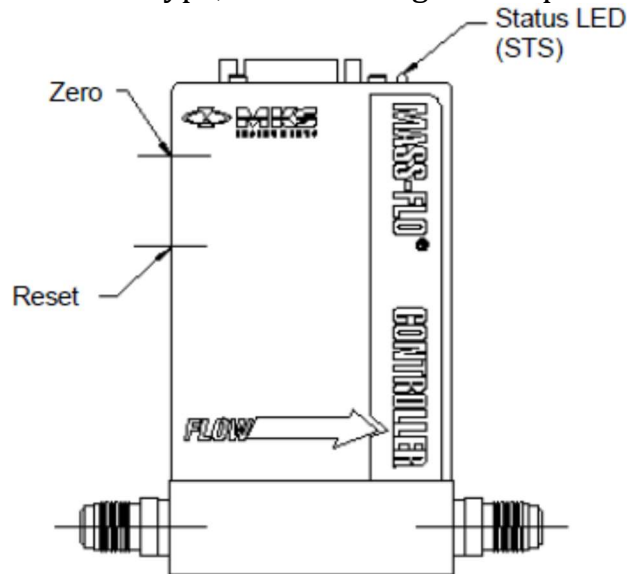


Figure 49 - MKS 1179B

Accuracy	
Analog and Profibus version:	0,5 % of reading plus 0,2 % of full scale
Control Range	2,0 % to 100% of full scale
Controller Settling Time	typically < 0,8 seconds (to within 2 % of set point)
Full Scale Ranges (nitrogen equivalent)	10, 20, 50, 100, 200, 500, 1000, 2000, 5000, 10.000, 20.000 sccm
Maximum Inlet Pressure	150 psig
Operational Differential Pressure	
≤ 5000 sccm	0,7 bar (g) to 2,8 bar (g)
10.000 to 20.000 sccm	1 bar (g) to 2,8 bar (g)
Repeatability	± 0,2 % of full scale
Resolution (measurement)	0,1 % of full scale
Warm Up Time	15 minutes
Operating Temperature	0° to 50° C (32° to 122° F)
Input Voltage/Current Required	20,5 to 31,5 VDC ²
Maximum at Start Up (first 5 seconds)	@ 200 mA
Typical at Steady State	@ 100 mA
Output Impedance	< 1 Ω
Output Signal/Minimum Load	0 to + 5 VDC into > 10 kΩ
Set Point Command Signal (not for type 179B)	0 to + 5 VDC from < 20 kΩ
Leak Integrity (mbar·l/s He)	
External	< 1 x 10 ⁻⁹
Through closed Valve (MFC only)	< 1 x 10 ⁻⁴
Mass	≤ 0,9 kg (1,9 lbs)

Table 5 - MFC data sheet

2.2.7 PESCha temperature control system



Figure 50 - LAUDA XT49W

The temperature of the main chamber can be controlled by two autonomous systems:

- IR lamps
- Thermal shroud

The first system based on IR lamps allows to heat different location separately. Its main limitation is that can only perform a temperature rising

The second system is based on a high-performance process thermostat for temperature control “Lauda XT490W”.

Its operation is based on modifying the temperature of an operating liquid through a cooling or heating cycle.

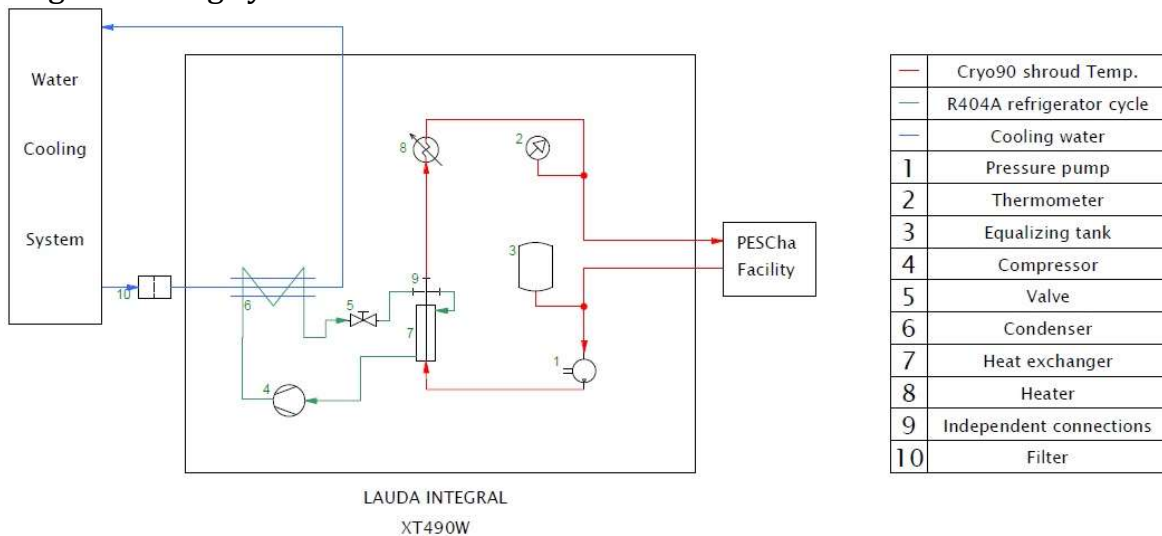


Figure 51 - LAUDA functional scheme

It can set the temperature of the chamber at a range of -80° to 160° C.

With this range, PESCha facility can better simulate some aspect of space and planetary environment and test the behaviour of the components during thermal cycles.

The working fluid flows through a complete shroud.

The shroud consists of four stainless steel skins that cover the internal surface of the chamber with internal cavities which allow a fluid to circulate and set a thermal profile inside the chamber.

LAUDA XT 490 W			
Operating temperature		°C	-80;160(cryo90)
Ambient temp. range		°C	5-40
Setting resolution		°C	0.01
Filling volume, minimum		L	9.5
Additional filling volume in the expansion vessel		L	17.4
Refrigerant			R404A & R508A
Cooling refrigerant unit			Water
Cooling air temperature range, without performance loss		°C	10-40
Cooling water temperature range, without performance loss		°C	10-30/10-15
Cooling water pressure		bar	3-10
Cooling water consumption temperature 15°C, pressure 3 bar		L/h	1200
Heat power / Power consumption 200 V; 50/60 Hz		kW	5.3/8.6
Pump capacity water 20°C	Discharge pressure max.	bar	2.9
	Flow rate max.	L/min	45

Table 6 - Lauda data sheet

The following screen, available in the control pad of the Lauda, contains the operational status of the camera.

It is possible to display on the right the temperature set with the control system, the temperature detected in the case of an external sensor, and the oil outlet temperature from the thermal process.

At the centre of the screen, on the other hand, it is possible to view information on the pressure inside the circuit, the level of oil contained in the tank of the hydraulic pump and its operating status. Finally, on the left side you can see which thermal process is in progress, the cooling or heating of the operating liquid.



Figure 52 - Lauda controlling Pad

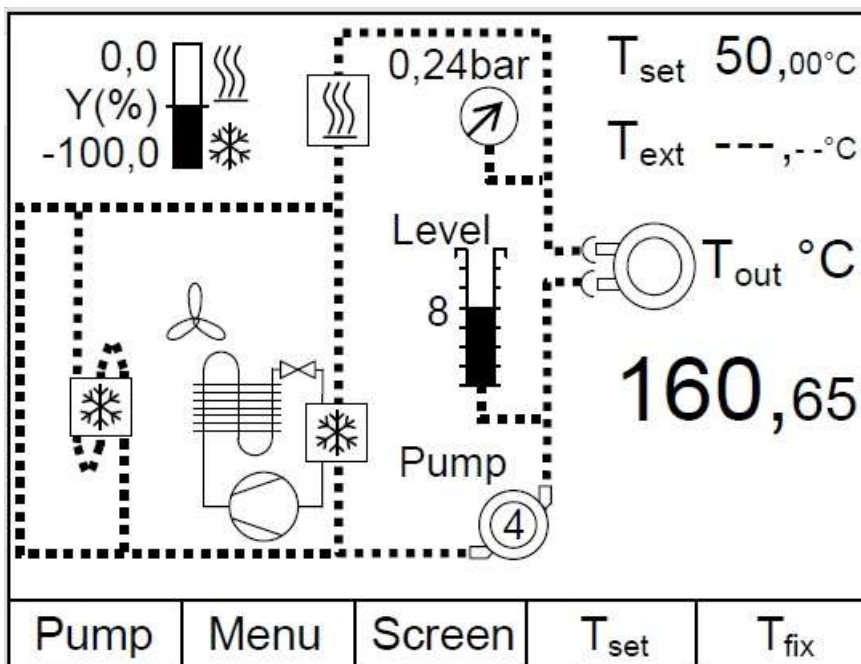


Figure 53 - Lauda controlling Pad view

2.2.8 Water cooling circuit

A water-cooling circuit is available in the PESCha facility. This is used to cool all the utilities needed to keep the chamber operational.

The water circuit is kept running through two pumps connected in parallel.

It is therefore possible to monitor the pressure and temperature of the general circuit, and of all the subsystems, such as the turbomolecular pump, or the cold plate, essential for the TQCM.

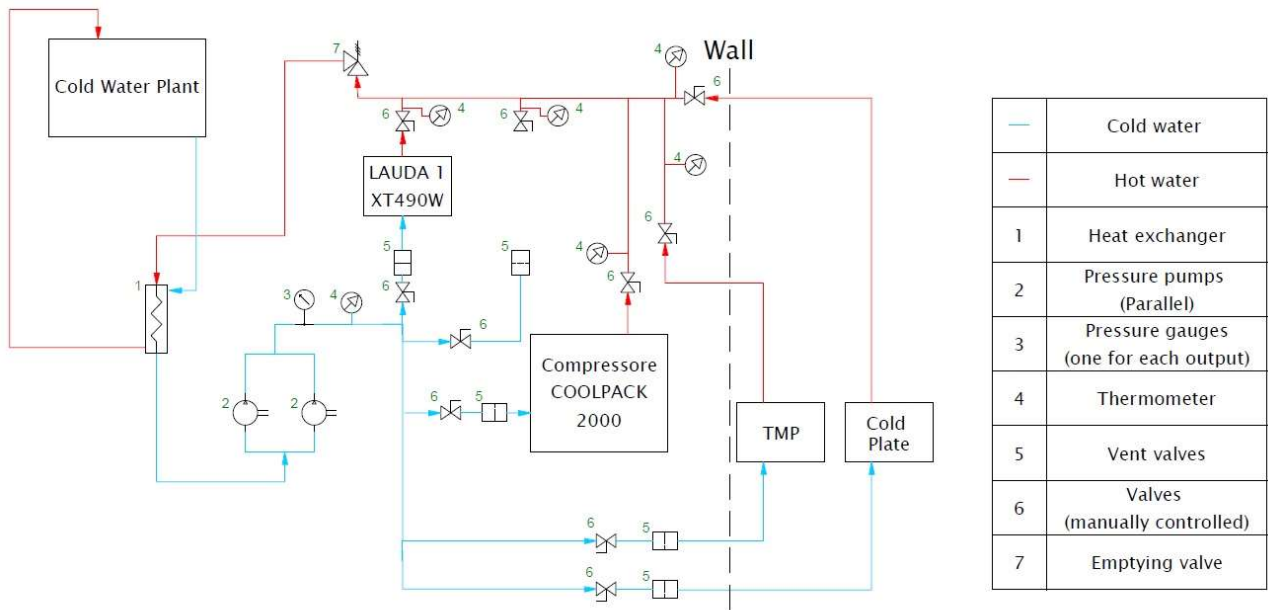


Figure 54 - Water cooling system functional scheme

2.2.9 PESCha venting valves

The venting valve is a valve used to bring the interior of the chamber back to atmospheric pressure, after having carried out the tests. This valve is not always usable because, unlike the MFC, it connects the chamber directly with the external environment, thus allowing access to contaminants.

However, this procedure is faster, so it is convenient when no critical hardware is tested. PESCha has two venting valves, the Varian Agilent L6280 model, one for the baffle, and one for the main chamber.



Figure 55 - VARIAN AGILENT L6280

2.3 Other components

2.3.1 TQCM

The QCM (quartz crystal microbalance) is a precision instrument for measuring surface contamination as a function of temperature in a space simulation chamber. The QCM uses a quartz crystal oscillator to measure mass loading while the set temperature of the crystal is automatically controlled.

One of the problems with this type of sensor is high temperature. When the temperature rises there is a different adsorbance of the gases with the quartz crystal, and this leads to incorrect readings. In order to solve this problem, a TQCM or a microbalance with thermal control is used.

The TQCM uses a two-stage thermoelectric device to actively control the temperature of the crystal between -59°C and $+100^{\circ}\text{C}$ to $\pm 0.1^{\circ}\text{C}$.

In order to measure the mass load, two 15 MHz crystals are used. The first crystal is kept in view of the chamber, while the second is used as a reference. During the acquisition the crystals are usually kept at a temperature of -20°C . The two crystals are made to vibrate and the frequency difference between the two crystals gives us the degree of the material attached on the exposed crystal and therefore of the outgassing of materials within the test chamber. The output recorded by the software that control the TQCM is the difference between the frequency the reference crystal and the crystal exposed to the outgassing in the vacuum chamber.

The sensor cannot be used indefinitely. Over time, the exposed crystal will excessively decrease its oscillation frequency down to zero, due to too the amount of deposited particles.

When the sensor is saturated, in order to continue the measure , it is necessary to bake out the crystal, usually bringing its temperature at 80 ° C for a few hours.

2.3.2 RGA (VQM)

The Vacuum Quality Monitor (VQM) System is a gas analysis instrument consisting of:

- VQM Controller,
- Ion Trap Mass Spectrometer Gauge (MS Gauge)
- Controller-to-MS Gauge Interconnect Cable
- VQM Viewer Software.

The MS Gauge is a specially engineered form of an Auto resonant Trap Mass Spectrometer (ART MS) sensor that connects directly to a high vacuum system and operates at gas pressures between UHV and 10^{-5} Torr.

The MS Gauge uses purely electrostatic fields to store ionized gas molecules within a cylindrical ion trap. Ions are generated directly inside the trap by electron impact of gas molecules. An an harmonic trapping potential well confines the ion trajectories of all ion masses, and a wide range of initial energies to stable oscillatory motions along the axis of the trap.

Mass selective ejection is achieved through an auto resonant energy pumping process. The mass spectrometer has unlimited mass range, is capable of achieving high sensitivity at high and ultrahigh vacuum levels, is capable of fast scan rates, is very compact, and requires extremely low power to operate as it uses only static bias potentials and very small RF signal levels (<100 mV).

The MS Gauge sensor is natively a ratiometric measurement device that provides detailed compositional analysis of a gas mixture. To measure absolute partial pressure readings, the VQM System requires an auxiliary total pressure measurements from an ionization gauge and an advanced data analysis built into the VQM Viewer Software.

The sensor consists of three major parts:

- The Ionizer
- The Auto resonant Ion Trap
- The Ion Detector.



Figure 56 - MS Gauge

The three parts reside inside the vacuum space where the gas analysis measurements need to be made. For MS Gauges in a demountable envelope, a stainless steel tube covers the probe assembly and provides electrical isolation from other ion sources in the high vacuum system.

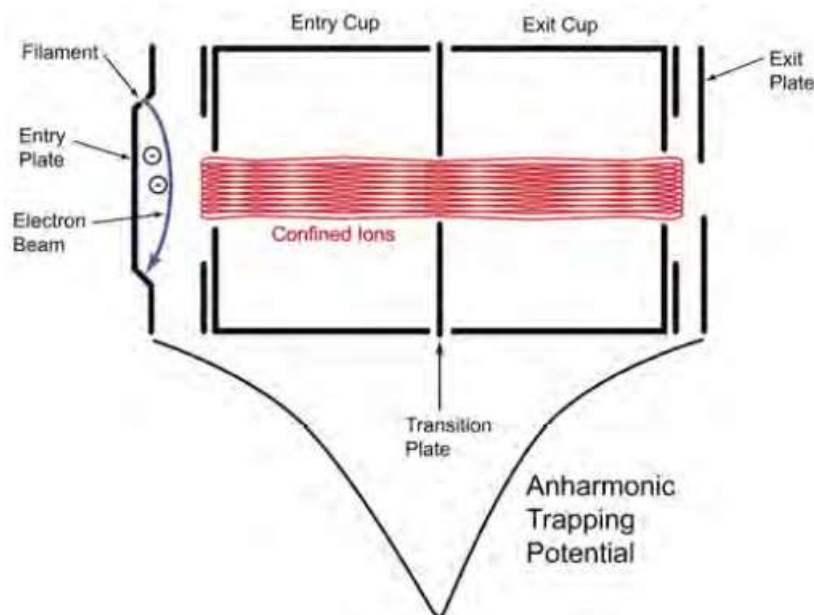


Figure 57 - Cross Section of MS Gauge and Electrostatic Trapping Potential Well

The ionizer works forming positive ions directly inside the Ion Trap volume by continuously bombarding gas molecules with energetic electrons generated from a heated filament (i.e., thermionic emission). A fraction of the ions formed inside the ion trap are confined into oscillatory motions and contribute to the mass spectral output of the gauge (auto resonant ejection).

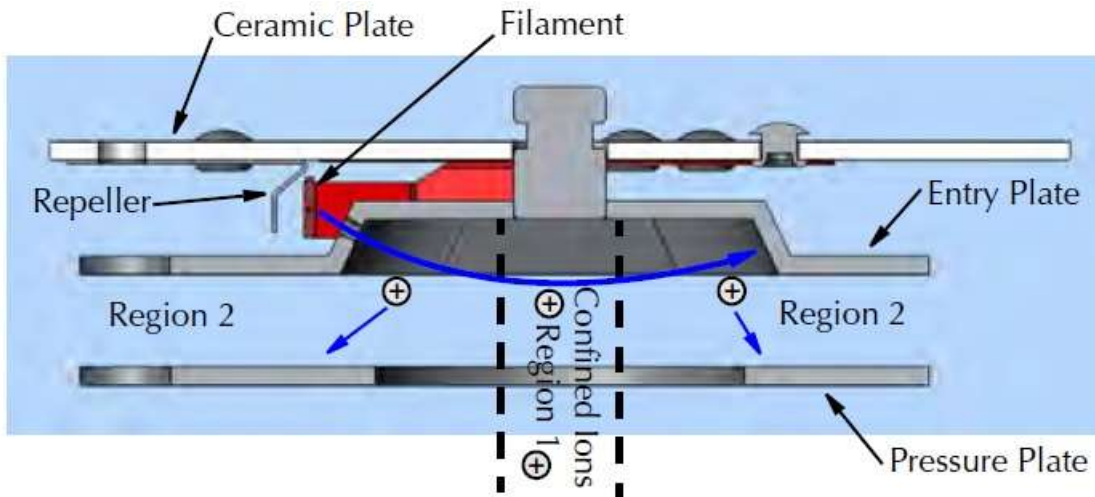


Figure 58 - VQM MS Gauge Ionizer

The blue arrow traces the ionization path of an off-axis electron beam and defines two regions where ions are created between the entry plate and entry cup. Ions formed in the region close to the axis of the trap (Region 1) are confined into oscillatory motion and contribute to the mass spectrometer signal. Ions formed away from the axis (Region 2) are directed towards the pressure plate and do not contribute to the mass spectrum since they are neutralized on impact.

Excited ions are ejected from the trap through the exit plate's gridded aperture and are detected by the electron multiplier detector to produce a mass spectrum.

Since ion ejection frequencies are strictly proportional to the inverse of the square root of mass-to-charge ratio, M/q , mass axis calibration is very straight forward: mass calibration is performed on a single mass peak of the spectrum, mathematically linking its ejection frequency to the square root of the mass, $f_e = \frac{K}{\sqrt{\left(\frac{M}{q}\right)}}$. The calculated factor, K ,

is then used to assign masses to all other peaks in the spectrum based on their unique ejection frequencies. The dependence of ejection frequency on square root (M/q) is strongly dependent on the shape of the trapping potential well which is a function of trap geometry, and bias voltages applied to the electrodes.

CHAPTER 2 - PESCha

Below are reported some screenshots of the VQM data management program.

In the upper part it is possible to select several functions, as:

- Connect is used for connecting VQM devices to the program
- Scan is the main function that allows the sensor to work, by clicking on it you can also switch off the sensor or put it in Standby
- Auto tune is one of the functions necessary for the preliminary setup of the machine
- Summary, Trend and Leak give us an idea of the gases present in the room, with their percentages and their trends over time
- Settings is the function that allows us to have a real-time histogram of the species present in the room
- Tune is the function where it is possible to calibrate the sensor and see the spectrum and the gas
- Log data allows us to save the data of the machine in a definite time space of the user
- Save instead provides an instant data backup

The **Errore. L'origine riferimento non è stata trovata.** is related to the “Tune” function. In this view it is possible to change the characteristic parameters of the sensor in order to obtain more or less accentuated signals. One of these parameters is the EM Bias, which allows us to raise the peaks, then to be able to see more clearly molecules less present, at the cost of a more intensive use of the electron multiplier, thereby decreasing its life cycle.

On the right side we can see the gas spectrum instead. It is possible to display it both as amperage and as partial pressure, and to change the scale from linear to logarithmic.

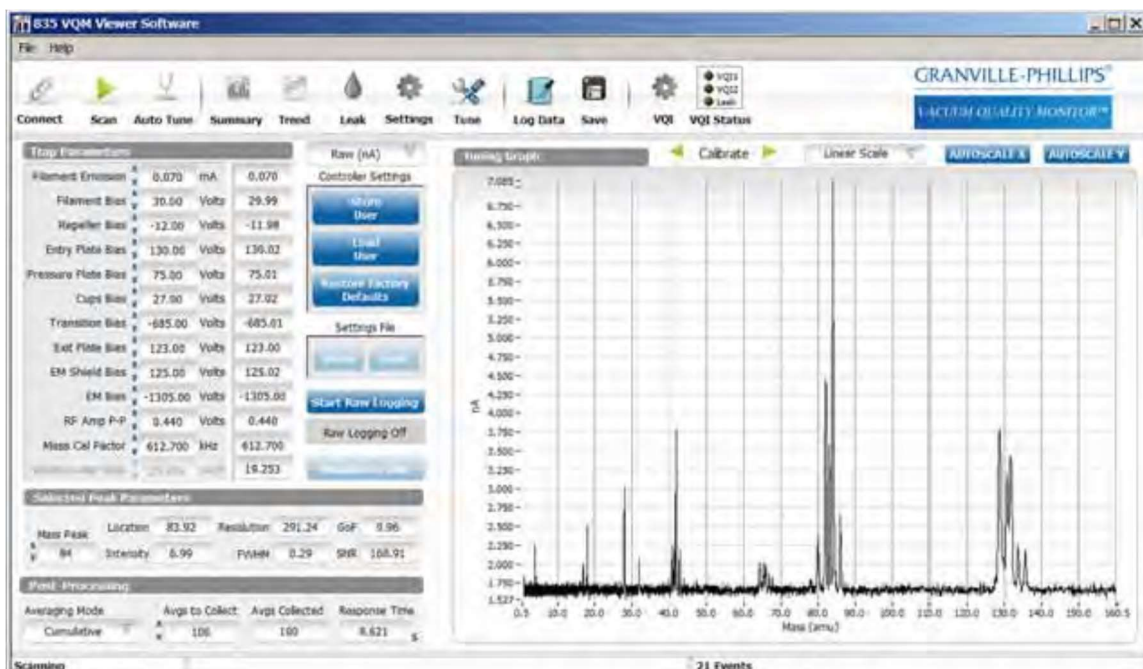


Figure 59 - VQM Viewer Tune screen

CHAPTER 2 - PESCha

The Summary function allows us to have on the left a table with the atomic masses detected by the VQM with the relative percentages, on the right two graphs with the time trend of the percentages of the gases, and an instant histogram with the masses detected.



Figure 60 - VQM Viewer Summary screen

The third image gives us the possibility to visualize the histogram with the percentages of gas, combined with two very useful functions.

The first allows us to insert in the graph an arbitrary gas spectrum so that it is possible to recognize if there are known species.

The second one allows to vary the display range in terms of atomic mass. Once the range shrinks or widens, the percentages of gas change, because they refer to the specific selected spectrum range.

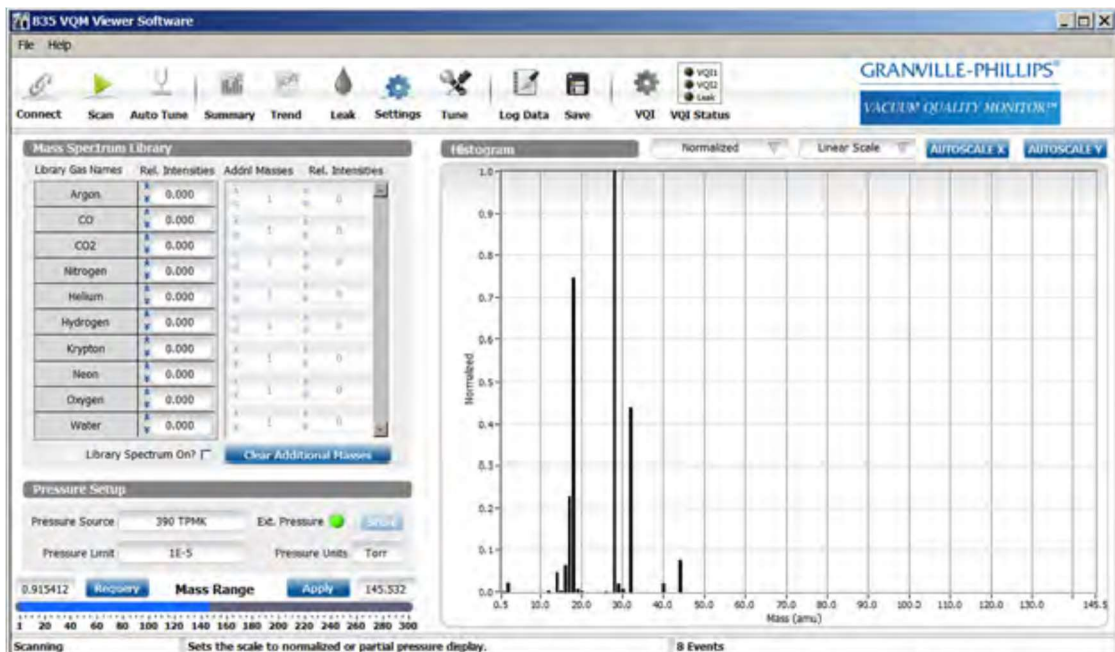


Figure 61 - VQM Viewer Settings screen

2.4 Software

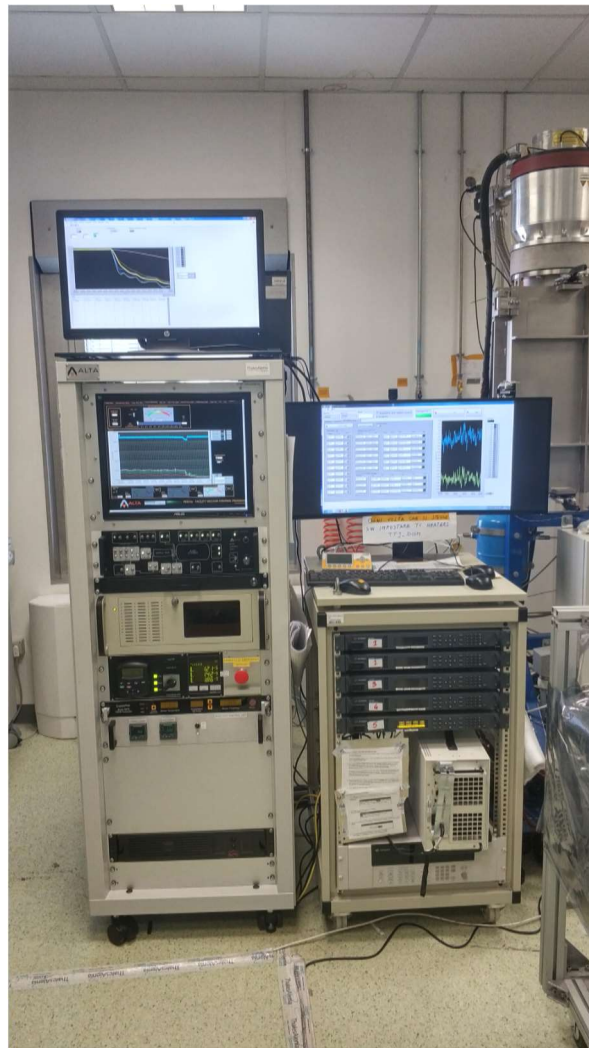


Figure 62 - PESCha facility controlling screens

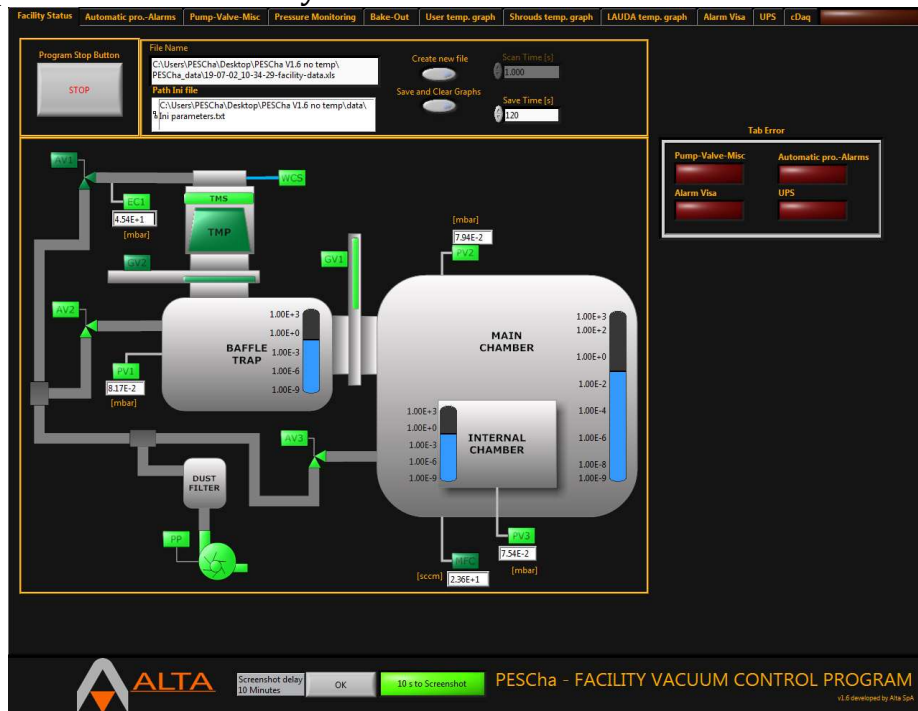
PESCha facility is controlled by a software that has been developed by ALTA s.p.a., the company that built the entire facility, and that is based on Nation Instrument LabVIEW.

This software provides the monitoring and control of the system, with both automatic and manual procedure. A wide range of controls are implemented in order to assure the safety of the operators.

2.4.1 Control and data acquisition software

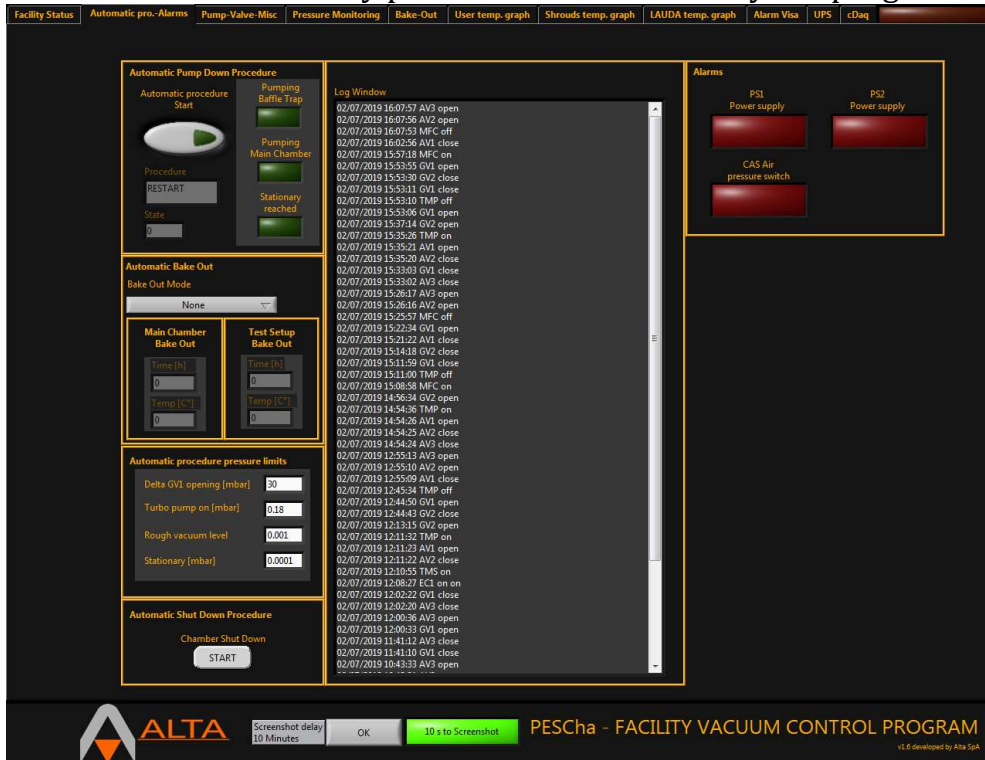
The graphical user interface of the control software consists of various windows, where the users can control all the procedures and monitor the main components, such as the vacuum pumps:

- The first window provides a simplified image of PESCha facility with its main components. In light green it is possible to view the components that are active and the pressures detected by the 3 main sensors PV1-2-3.



CHAPTER 2 - PESCha

- In the second window you can view the log of PESCha operations. Any action that is carried out such as the opening of a specific valve or the ignition of a pump is recorded. You can also view any problems encountered by the program.



- The third window is very important because it is the screen where it is possible to manage the switching on and off the primary and turbomolecular pumps, as well close and open the valves and the gates accordingly.



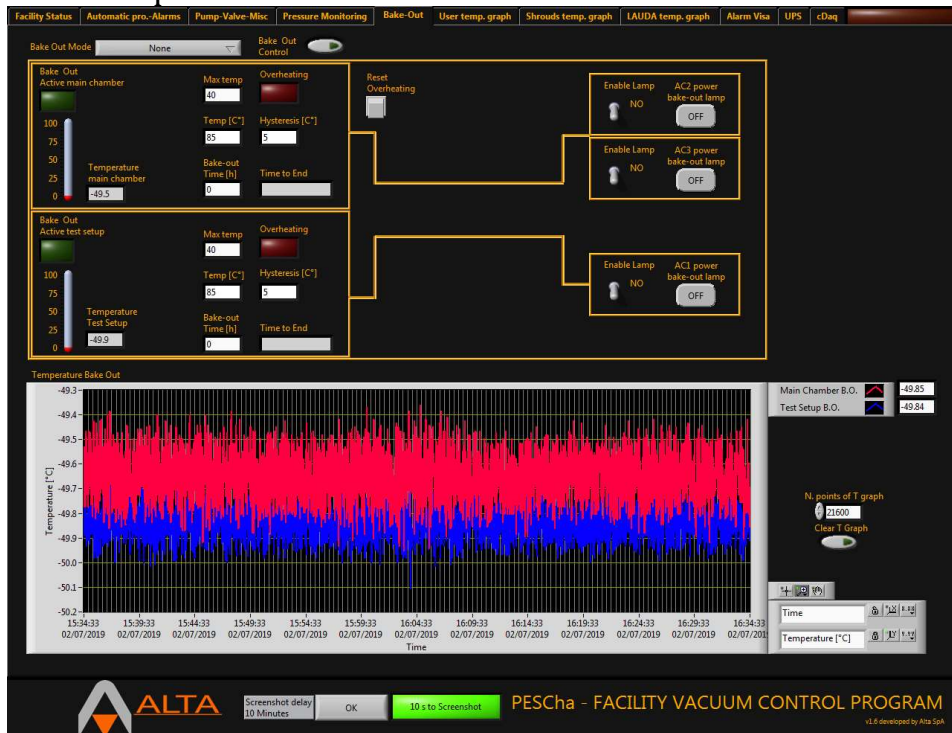
CHAPTER 2 - PESCha

- The fourth window has three features:
 - In the first one it is possible to adjust the switching on and off of the mass flow control, and adjust the flow rate
 - In the second one there is a graph showing the pressures recorded by the three sensors. For example in particular, in the figure below, it can be noted that the baffle trap was vacuumed (the red line is relative to pressure sensor PV1 That is mounted on the baffle chamber), after having performed a spectrum analysis via RGA the gate connecting the baffle from the main chamber was opened and helium was inserted through MFC.
 - The third feature instead concerns the control of the room's leak rate.



CHAPTER 2 - PESCha

- The fifth window concerns the management of the bakeout of the room, with the control of the temperature sensors.

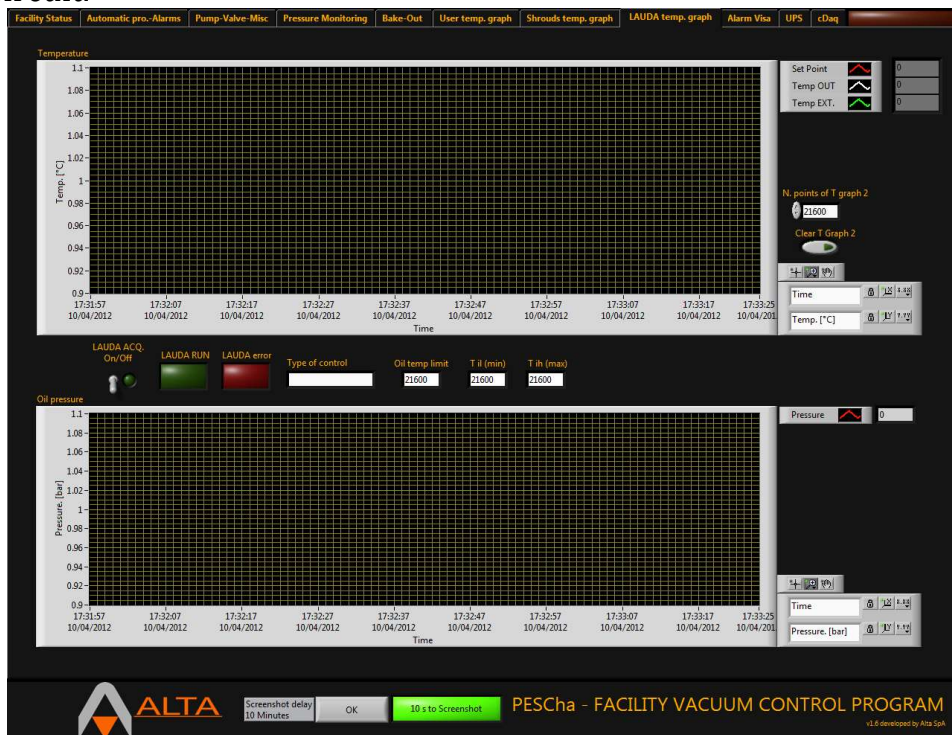


- In the sixth window it is possible to check the temperature of the 4 shrouds.



CHAPTER 2 - PESCha

- The seventh window shows us the trend of pressure and temperature of the Lauda circuit.



3. CHAPTER 3 – PESCha FACILITY: APPLICATIONS ANALYSIS AND PROCEDURES

This chapter deals with two of the main activities that were carried out in the PESCha facility.

The first paragraph will describe the process to reach high vacuum into the chamber and the relevant procedures which make use of the experimental data obtained from the facility sensors. The operation of the Lauda thermal control machine will also be presented.

The second paragraph will focus on the bakeout procedures, with specific attention on data collection and processing.

3.1 Vacuum procedure

The procedures for reaching the vacuum both directly and in a step process are standardized, but the response of the chamber can vary significantly from experiment to experiment.

In particular, the presence of leaks due to flanges or valves not perfectly sealed, the outgassing characteristics of the hardware under testing and a non-perfect internal cleaning due to the presence of contaminants changes the times necessary to reach the desired vacuum conditions and the different degree of vacuum that the chamber can achieve.

For example, the presence of a single fingerprint in a small chamber may lead to a vacuum difference of an order of magnitude, and the presence of leakages can lead to a significant increase of the vacuum processes by several hours.

In order to reach high vacuum, several steps are typically required. The process for reaching the higher vacuum level, turning on all three pumps is described hereafter.

The first step is to check the status of the utilities (e.g., the N₂ supply to the turbomolecular pump, water cooling temperature and flow in the cooling circuit).

After checking the status of the utilities, the primary pump is switched on. This pump is not able to reach high vacuum levels, but it is used as backing pump, to reach the minimum operational level required by the turbomolecular pump. During this phase the AV2 and AV3 valves are opened as well as the Gate number 1 that connects the main chamber with the baffle trap. If the pressure difference between the baffle and the main chamber is higher than 30 mbar, a control system does not allow to open the gate, so it is necessary to wait for the pressure to normalize.

When a vacuum of $1.8 \cdot 10^{-1}$ mbar is reached, it is possible to switch on the turbomolecular pump (after the MAG drive control system and the Thermal Management System (TMS) Turbo have been switched on).

Once the AV2 and AV3 valves are closed and the AV1 valve is open, the turbomolecular pump can be turned on. From here on, the subsequent steps require opening the gate of the turbomolecular when the rotation speed reaches 100 Hz and opening the N₂ circuit, necessary for cleaning the rotating blades at 240 Hz.

The pressure will start to fall very quickly, until reaching vacuum levels between 10^{-5} and 10^{-6} mbar, depending on the presence of leaks. A cryopump can be activated to further decrease the pressure that can be reached by the turbomolecular pump.

When it is necessary to work with even lower pressures, the Lauda thermal machine can be used to lower the internal temperature of the chamber. The isochoric transformation in fact guarantees a direct lowering of the pressure.

The graph shown hereafter gives an example of a typical thermal vacuum process. At the beginning, the vacuum process started with the primary pump. The pressure jump that can be seen on the day 29/5/2019 at 10 am is due to the turning on of the turbomolecular pump. After a pressure lower than 10^{-4} mbar was reached, heating cycles have been carried out to clean the chamber and thus to reach lower pressures. On the 30th of May, at 12 am, the chamber was then cooled to allow the use of the Residual Gas Analyzer.

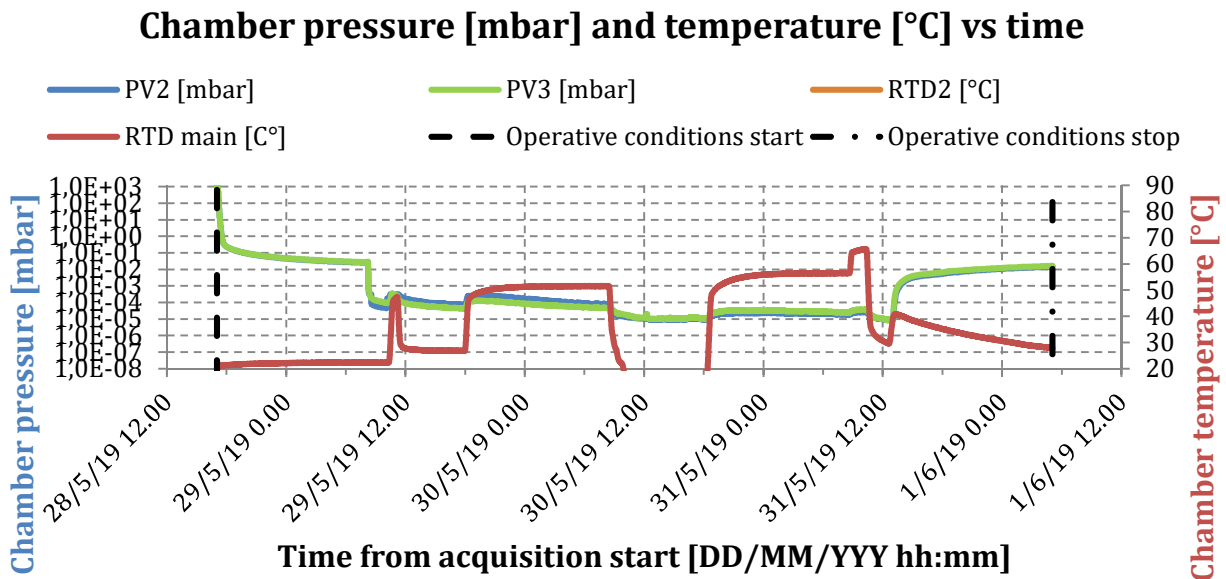


Figure 63 - Test sample

3.2 BAKEOUT procedure

In the presence of vacuum environment, the gas that was dissolved, trapped, or absorbed in materials tends to be released in a process called outgassing.

Outgassing products can be harmful for a spacecraft mission because they can condense onto optical elements, thermal radiators, or solar cells and obscure them.

This process is related to vapor pressure so high temperatures can increase the releasing ratio.

To solve this problem many components of the spacecraft are artificially outgassed in a process called bake-out.

The effectiveness of reducing the contamination level of a particular material depends on many factors, such as temperature and duration of the bake out or the outgassing characteristic of all material present.

The outgassing rate is initially fast but decrease over time, till to become linear in time.

Measurements are made using a temperature-controlled quartz crystal microbalance (TQCM). A quartz crystal is made to resonate, and the change to his frequency is related to the amount of deposition on the sensor and so to the outgassing of the hardware.

Stopping criteria like rate reduction can lead to different results depending of the heating rate of the hardware, so different requirements are made to assure an optimal bake-out.

In this thesis will be discussed a method that uses a physical model based on a paper called “Analysis of bake-out monitoring data” from ESA Estec.

The outgassing characteristic, like the frequency of the TQCM, is given by a sum of exponential decay functions:

$$f(t) = \sum_i a_i (1 - e^{-\frac{t}{\tau_i}})$$

Where a_i gives the contribution of outgassing species i to the total outgassing characteristic and τ_i the residence time.

It is important to notice that a TQCM cannot discriminate the different outgassing species.

From this function we can derive the outgassing rate and the change of the rate:

$$f'(t) = \sum_i \frac{a_i}{\tau_i} e^{-\frac{t}{\tau_i}}$$

$$f''(t) = \sum_i \frac{a_i}{\tau_i^2} e^{-\frac{t}{\tau_i}}$$

The deviation from linearity per unit of time can be defined as:

$$\zeta' = \left| \frac{f''(t)}{f'(t)} \right| = \frac{\sum_i \frac{a_i}{\tau_i^2} e^{-\frac{t}{\tau_i}}}{\sum_i \frac{a_i}{\tau_i} e^{-\frac{t}{\tau_i}}}$$

The time at which a deviation from linearity of less than 1 %/hour is reached does depend on the distribution of outgassing species after a certain bake-out time. It does not depend on the total amount of outgassing mass from the hardware or on the heating

rate of the facility, since the analysis is valid only for the isothermal part of the bake-out. Setting a stopping criterion below a deviation from linearity of 1 %/hour thus ensures that a “best effort” has been reached.

Something that must be considered is that fluctuation in the hardware temperature can generate changes in the outgassing rate that obscure the reduction rate.

One requirement related to this problem prescribes that temperature fluctuation shall have a root mean square variation of no more than 1°C in an hour and no more than 2°C in a day.

In order to not allow fluctuations in the outgassing rate, it is required to have at least 48 hours of isothermal data. This is not always possible because one of the problems that may occur is QCM saturation, so the instrument is no longer capable to read changes in outgassing rate. During saturation, it is necessary to keep QCM sensor at 80° C until the outgassing rate has decreased to a level where it can be measured within a reasonable amount of time.

How can be achieved a fitting procedure, giving the equations mentioned before?

The purpose of curve-fitting is not to discriminate the residence times of all the species outgassing. The aim is “to provide an accurate description of the measured data in such a way that the first and second derivative can be calculated from the fit-curve, in a way that minimizes systematic fitting errors”. By adding enough terms to the exponential equation, any function can be simulated.

In practice just 4 terms, different from zero, are sufficient to describe bake-out data.

The fitting method used is the least-squares, it consists of minimizing a parameter called χ^2 that is the sum of the square differences between the data points f_i and the fit curve y_i :

$$\chi^2 = \sum (f_i - y_i)^2$$

This method has been implemented in Matlab environment, whose code is listed in the Appendix A. Find the absolute minimum of a function with 8 parameters is not analytically passible, so has been implemented a method the search for the nearest relative minimum of several random initial parameters. Between this minimum the lowest is chosen. The number of random sets can be chosen in order to choose between accuracy or time of simulation.

Below is presented an example of curve fitting, using data of an old experiment. In the first screen can be seen the data output of the TQCM so the difference of frequency of the quartz crystals and the temperature of the sensor. As can be seen, it was necessary to heat the sensor several times to prevent it from saturating within 48 hours. The last cycle was therefore useful for permitting continuous use of the sensor.

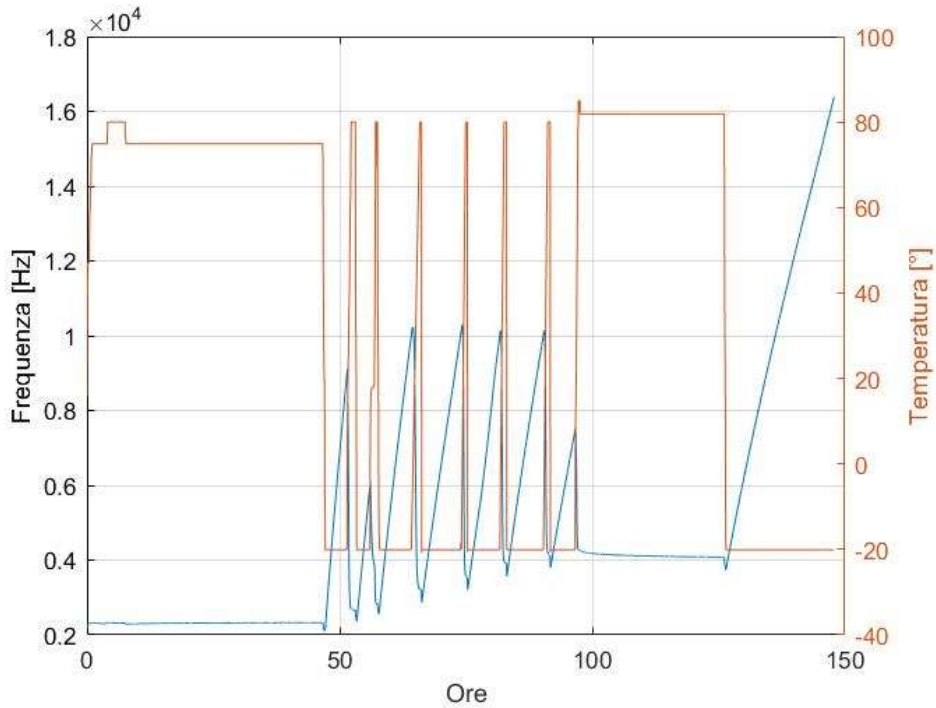


Figure 64 - TQCM data output

The second screen shows the frequency function measured by the instrument and the interpolating function. The difference is barely notable.

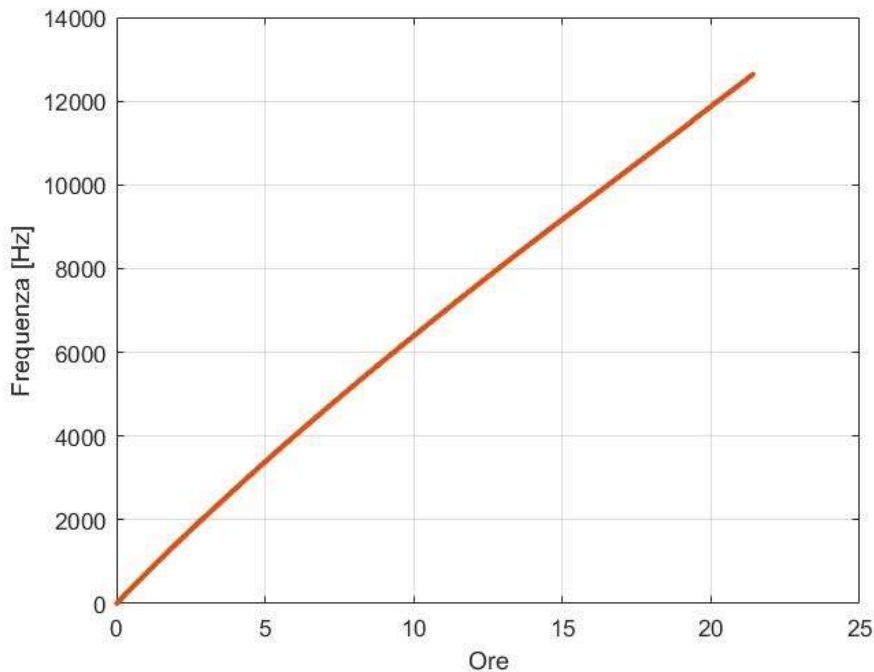


Figure 65 - TQCM frequency function with interpolation

In the third screen can be seen the 4 functions used to interpolate the curve. The third function has coefficient slightly higher than zero.

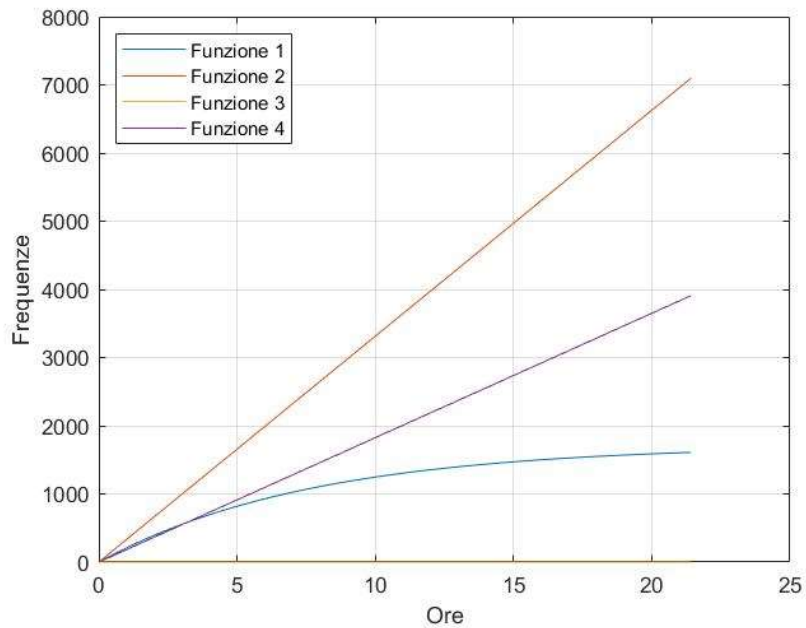


Figure 66 - Function included in the sum

The following screens show the derivatives of the function and the relationship between the second derivative with the first. When this parameter goes below 10^{-3} the bakeout process can be considered terminated.

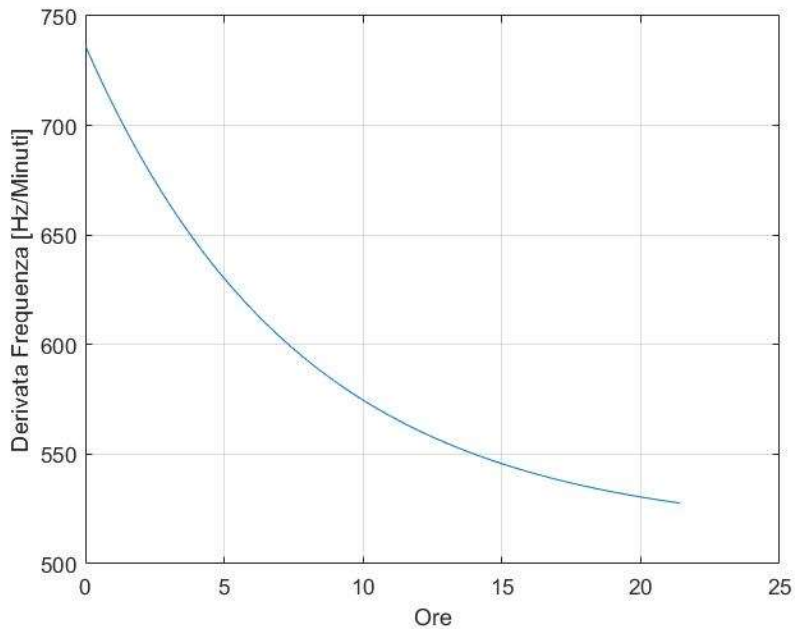


Figure 67 - Frequency first derivative

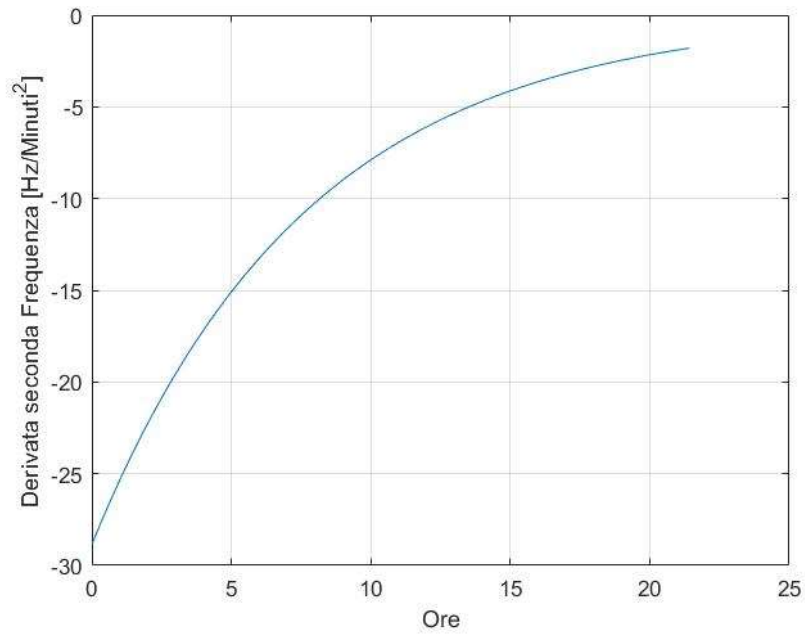


Figure 68 - Frequency second derivative

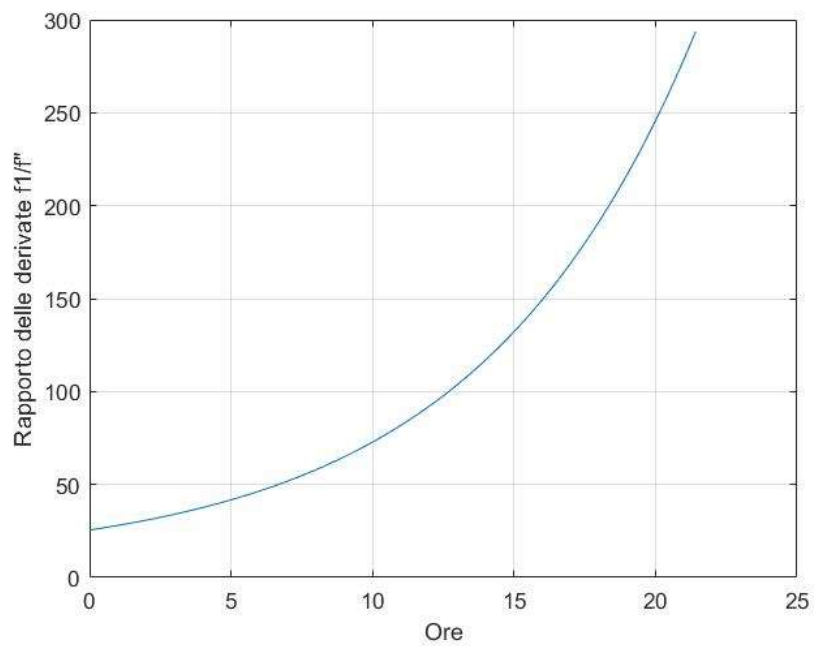


Figure 69 - Relationship between first derivative and second derivative

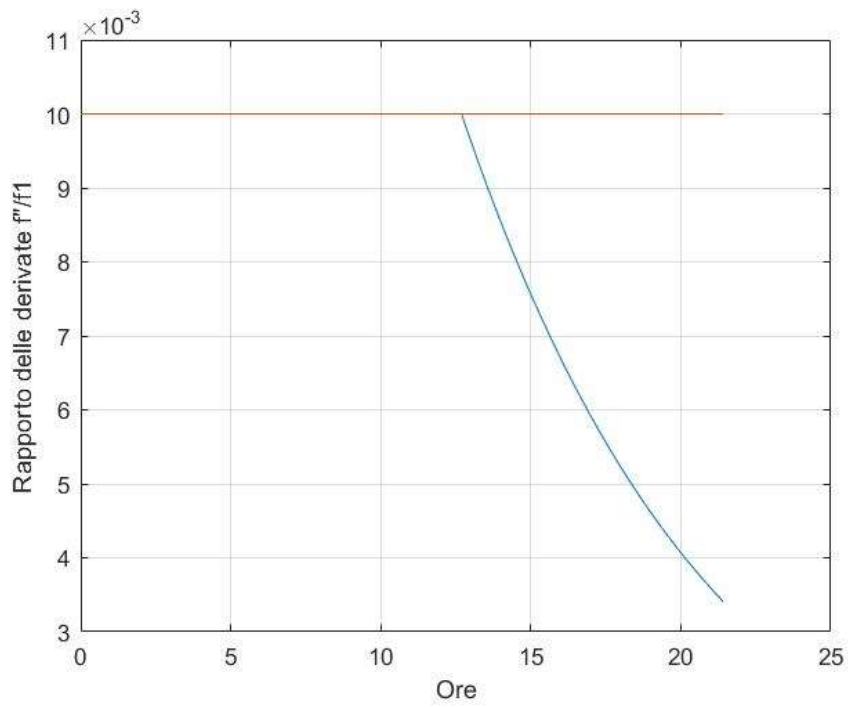


Figure 70 - - Relationship between second derivative and first derivative

4. CHAPTER 4 – PESCha facility: Sensors implementation

In this chapter are presented in detail the activity performed in the context of this Thesis work related to:

- the PESCha thermal control upgrade;
- the RGA set-up development and testing;

while the activity related to the TQCM data post processing was presented in the previous chapter)

4.1 Thermal control

This chapter deals with the implementation of a feedback thermal control for the PESCha facility. In the first part are presented the reasoning for the implementation of type of control, instead in the second part is presented a possible modeling and simulation of the system from the physical point of view, in order to have an immediate indication on the effect of the controller parameters on the system and therefore to be able to predict its behavior in advance.

The Lauda thermal machine provides a purely proportional thermal control by default, as well as the implementation via external sensor of two PID and P cascade controllers. The purely proportional system provides direct control over the temperature of the operating liquid that heats the machine. This system is very simple, but can lead to a very slow heating process if is not continuously monitored by an operator.

In fact, the components inside the chamber, under vacuum conditions, are heated only by radiation so only the oil temperature will quickly reach the Tset.

However, this system has the advantage of not having an overshoot of the temperature of the materials to be tested.

The system with PID control on the other hand is faster, allowing more direct control over what happens inside the chamber. The difficulty is in managing the configuration parameters.

The PT100 sensor can be integrated to use the feedback function on the thermal control inside the chamber.

The control system in this case consists of two controllers in cascade, in particular a PID as "master" and a P type as "slave".

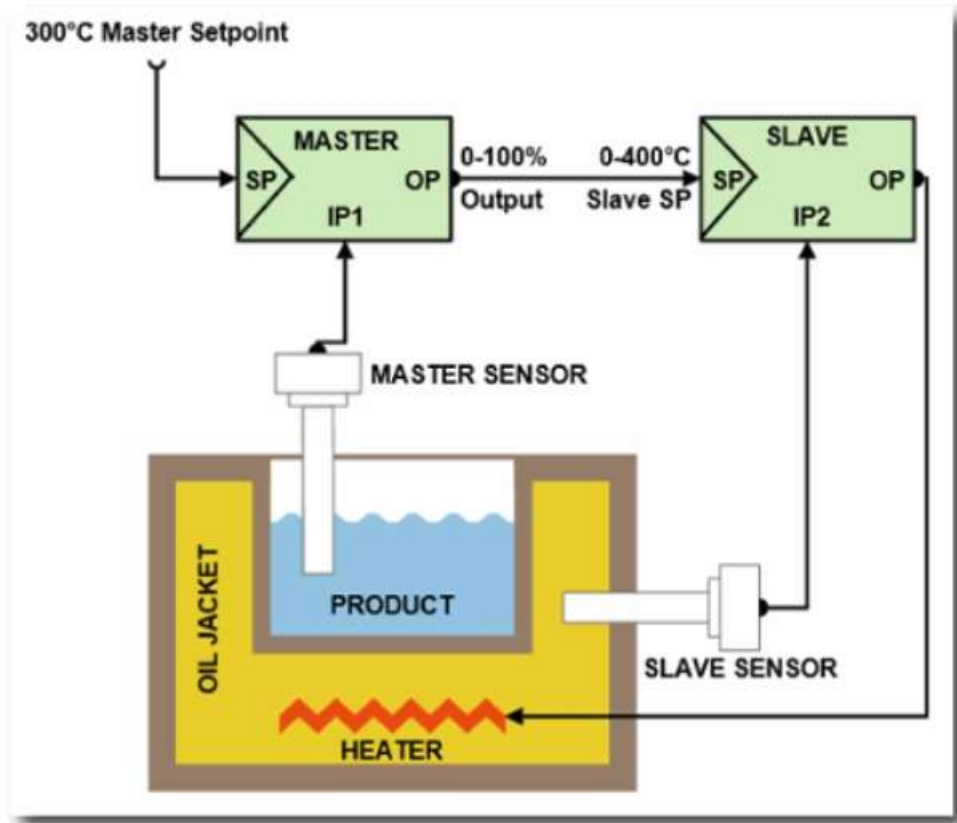


Figure 71 - Master-Slave controller example.
<https://www.west-cs.com/news/how-does-cascade-control-work/>

A temperature command is sent to the first controller, to command the desired temperature at a particular point of the chamber, the error with respect to the measurement made, is manipulated by the controller which gives a voltage response. The output is therefore converted into temperature and compared to the actual temperature of the operative oil, here a proportional controller command the heat exchanger of the machine to cool or heat the oil.

This system allows a faster heating of the test components. For the software implementation below the various schemes of Lauda are reported, with the various parameters modified.

The problem with this system, from the machine user point of view, is that it only controls the PID parameters of the two controllers (therefore manipulating the proportional, derivative and integrative ratio of the error)

So how is it possible to model the system physically?

In the context of this thesis a thermodynamic model was developed, in which the three main components are represented:

- The shrouds which are the interface component between the oil heated by the Lauda and the chamber;
- A pt100 sensor to verify the increase in its temperature with respect to the environment;
- A test material placed inside the chamber.

The following equations have been written to identify the behaviour of the system, under the hypothesis that inside the chamber only a radiative heat exchange can take place:

$$\rho_s c_s V_s \left(\frac{\delta T_s}{\delta t} \right) = h(T_{liquid} - T_s)S_s - \epsilon_s \sigma T_s^4 S_s + \alpha_s T_{PT100}^4 S_s + \alpha_t T_t^4 S_s$$

$$\rho_{PT100} c_{PT100} V_{PT100} \left(\frac{\delta T_{PT100}}{\delta t} \right) = \alpha_{PT100} T_s^4 S_{PT100} - \epsilon_{PT100} \sigma T_{PT100}^4 S_{PT100}$$

$$\rho_t c_t V_t \left(\frac{\delta T_t}{\delta t} \right) = \alpha_t T_s^4 S_t - \epsilon_t \sigma T_t^4 S_t$$

Where each parameter is listed in this table:

	Unit	Chamber (Steel)	Sensor (Platinum)	Test (Steel)
ρ (density)	$\frac{Kg}{m^3}$	7700	21450	7700
c (thermal capacity)	-	500	130	500
T (temperature)	K	-	-	-
t (time)	s	-	-	-
h (convective coefficient)	$\frac{W}{m^2 * K}$	900	-	-
S (surface)	m^2	$2 * 1.1 * \pi$	$0.1 * 0.01 * \pi$	$0.3 * 0.3 * 6$
V (Volume)	m^3	$2 * 0.025^2 * \pi$	$0.1 * 0.01^2 * \pi$	0.3^3
ϵ (emissivity)	-	0.65	0.08	0.65
σ (Stefan-Boltzmann coefficient)	$\frac{W}{m^2 * K^4}$	$5.67 * 10^{-8}$	$5.67 * 10^{-8}$	$5.67 * 10^{-8}$
α (absorbivity)	-	0.65	0.08	0.65

Table 7 - Equations parameters

The chamber is approximated as a cylindrical surface with a diameter of 1.1 meters, while the test hardware is modeled as a cube of side 0.3 meters positioned in the center of the chamber.

It is possible to solve this system of differential equations through the simulink program The block diagram of the code developed is shown below:

CHAPTER 4 – PESCha facility: Sensors implementation

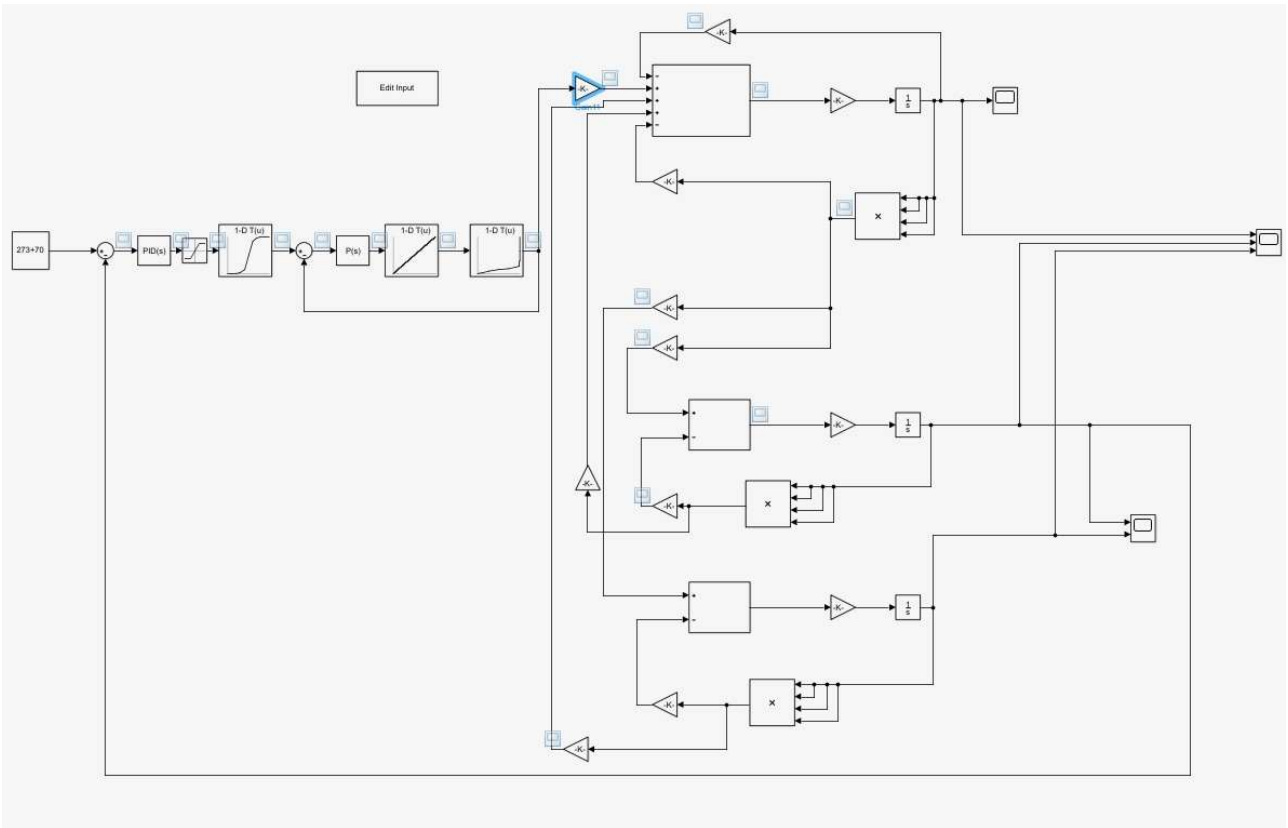


Figure 72 - Block scheme

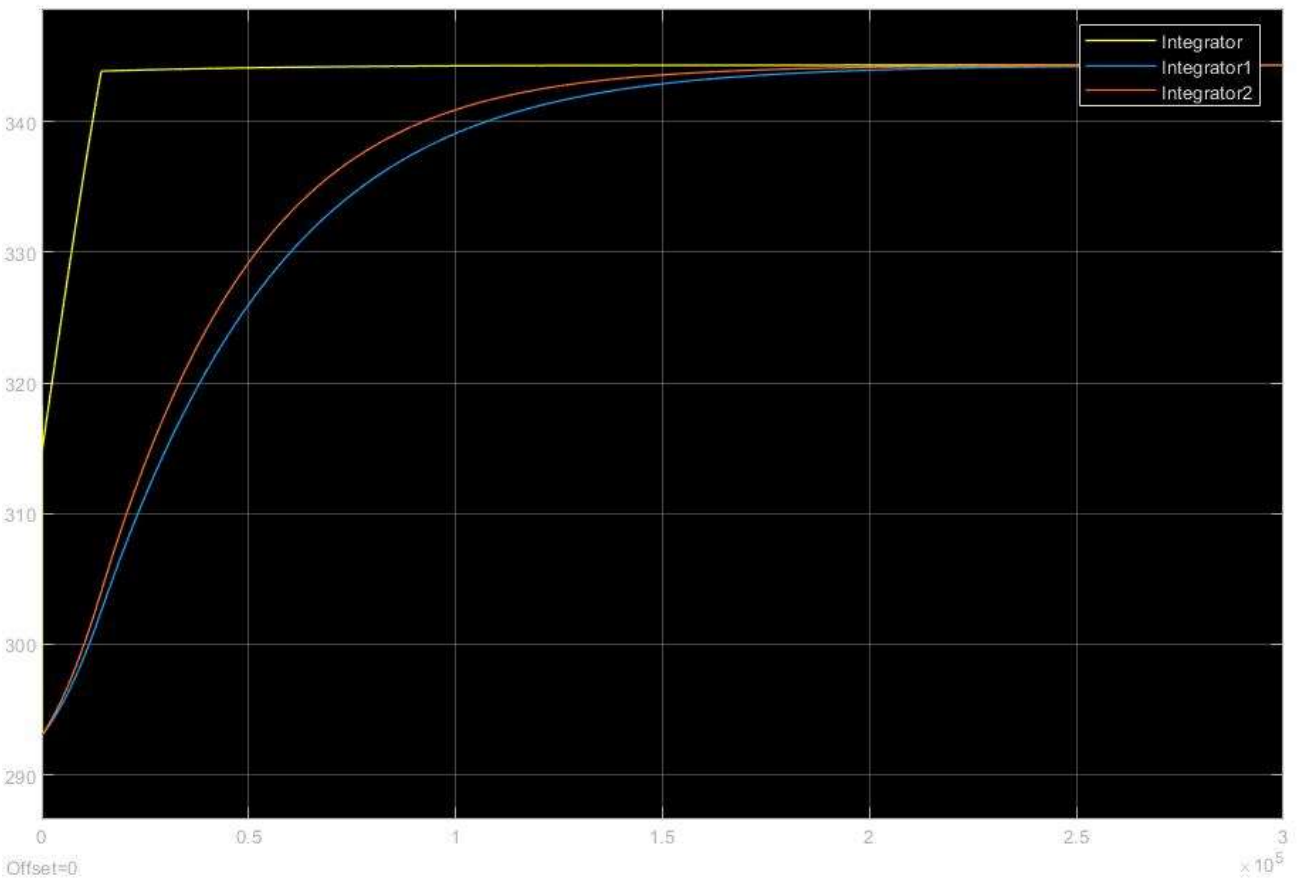


Figure 73 - Temperature functions

CHAPTER 4 – PESCha facility: Sensors implementation

These results were obtained through the following parameters of the PID controller:

- Proportional: 1.5
- Integral: 1.5 / 200
- Derivative: 1.5 * 164

The equilibrium temperature (360 K) is reached in 55 hours, too high but this is due both to the parameters of the controller inserted and to the in-depth analysis of the parameters of the single objects, which should be more carefully selected.

The yellow curve represents the trend of the chamber temperature, the blue curve the temperature of the sensor, while the orange curve the temperature of the test.

It should be noted that the sensor heats up less than the test due to the low surface area and emissivity.

The graphs obtained lead us to these results.

It is important to notice that it was not possible to correctly simulate the heating of the oil by the Lauda because the data for the conversion of current consumed and temperature produced are not available.

These results will therefore lead to a faster implementation of the system, which will consist of a pt100 sensor, vacuum cables, flange, air cables and connector with Lauda, allowing a software test of the experiments done in the room.

So how can you manage the PID controller and change the software?

Through the Lauda Control Pad it is possible to select the parameter control mode.

These parameters are:

- The gain of the controller: K_{pe}
- The proportional range: Prop_E
- The reset time: T_{ne}
- The derivative time: T_{ve}
- The damping Time: T_{de}

• the proportional time

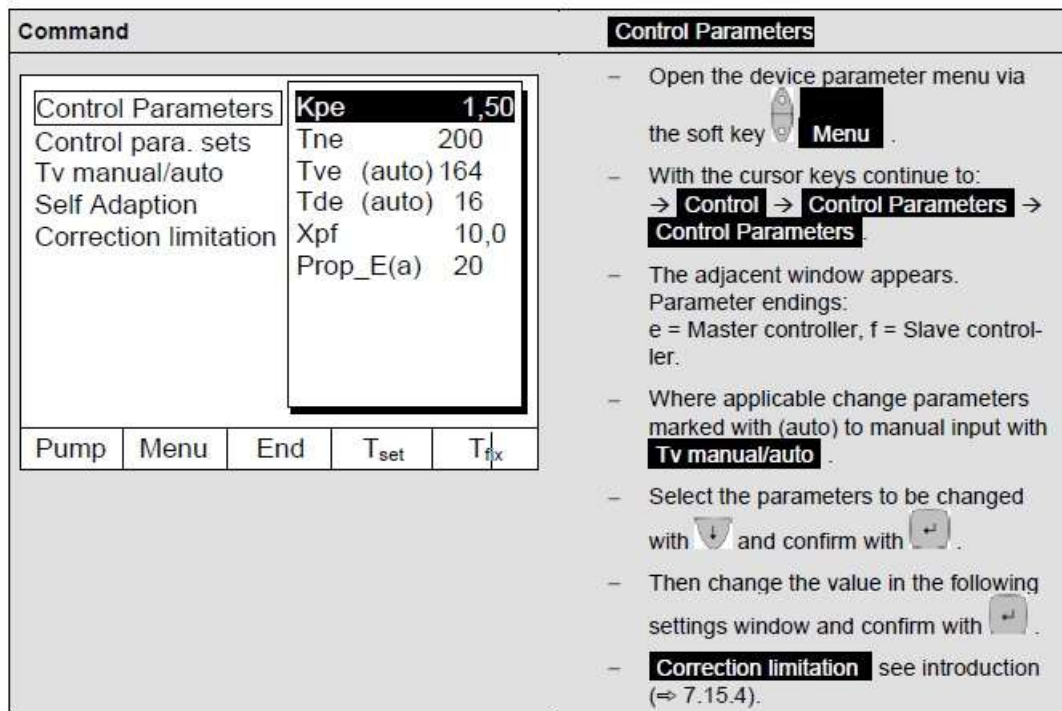


Figure 74 - Lauda Control Parameters settings

The following procedure is the one recommended by the manufacturer to try to obtain optimal values for the room, in case it is not possible to have an external simulation:

1. Alter the setpoint by 5°C and record the outflow temperature and the external temperature for a sufficient length of time (approx.. 20-40 min)
2. If the external temperature oscillates (>0.1 K), then reduce Kpe until the oscillation dies away. Always wait a sufficient length of time between the changes (at least 2 oscillation periods).
3. +20 K setpoint change, await transient response;
-20 K setpoint change, await transient response.
4. Asses transient responses:
 - if an overshoot is to be reduced, then slowly increase Tve (until about 90% of Tne)
 - vice versa, reduce Tve to about 60% of Tne
 - if doing this, adjust Tde. Tde=20% of Tve
 - continue at 3) after each change: Carry out and evaluate +- 20 K setpoint change.
5. If the response takes too long, then Tve can be reduced. Similarly reduce Tve. Tde as a percentage. Reduce Kpe to 150...200% so that the system oscillates. Then continue from Point 2
6. If the tendency to oscillate increases without the overshoot being acceptably reduced,
 - a) Kpe can be slightly reduced; continue with Point 3
 - b) is a larger time constant need to be chosen: Kpe to 150...200% so that the system oscillates. The continue from Point 2.

4.2 Residual Gas analysis

In this chapter is presented the work performed to develop a set-up for the use of the RGA, the related procedures and the results of various tests carried out to check the effectiveness of the sensor, and to have a clear idea of its operation.

In the first part are discussed the procedures that have been created to allow the correct functioning of the RGA, while in the second part the various experiments are analyzed in detail, with the respective data obtained.

The procedures listed below have been created for the correct operation of the VQM 835 sensor.

Procedure for the first application of VQM sensor used for Residual Gas Analysis			
Preliminary operation			
A	Checklist	<p style="text-align: center;">Equipment check:</p> <ol style="list-style-type: none"> 1. Mass Spectrometer VQM (in a vacuum-sealed metalized bag) 2. VQM Control unit 3. Interconnect cable between the Control unit and the mass Spectrometer 4. Interconnect cable (USB type) between the Control unit and the computer 5. Power supply (AC to 24 Vdc) 6. Micro-Ion ATM Total Pressure Measurement Gauge 7. Interconnect cable between the Control unit and pressure sensor 8. Heater Jacket for the Mass Spectrometer Gauge 9. Ground wire 	Page 31
2A	Assembly and status check	<ol style="list-style-type: none"> 1. Determine the best placement for the MS gauge, if possible, far from magnetic fields (preferable flanges 4-5-8-9) 2. Break the hermetic seal of the metalized Bag and remove the hard-plastic shell that mechanically protects the MS Gauge 3. Remove the MS Gauge from its hard-plastic shell. Do not breath directly into an open vacuum port. (wear a mask to prevent contamination) 4. Prior to mounting remove the plastic cylinder that protects the electrode 5. Hold the MS Gauge in an upright position and visually inspect both end of the cylindrical unit checking for possible damages 6. Position the copper gasket, align the holes in both flanges and tighten the six-bolt following this procedure: Finger tighten all 6 bolts, then continue tightening each about 1/8 turn in crisscross order, until the flanges are in contact. After contact, further tighten each bolt about 1/16 turn 7. Connect the spectrometer to the chamber 8. Connect through the interconnection cable the spectrometer to the control unit 9. Rotate the connector once inserted to ensure closure 	Page 33-35

CHAPTER 4 – PESCha facility: Sensors implementation

Procedure for the first application of VQM sensor used for Residual Gas Analysis			
3A	(Optional) Pressure sensor assembly	<ol style="list-style-type: none"> 1. Determine the best placement for the pressure sensor, preferably near the Spectrometer, far from heat source and gas inlets 2. Connect the sensor to the chamber 3. Connect through the interconnection cable the control unit to the sensor 4. Calibrate the sensor at atmospheric pressure 	Page 32
4A	Procedure for cable connection and grounding	<ol style="list-style-type: none"> 1. Connect the 24 Vdc power supply to the back panel of the VQM Controller. Plug in the DC power plug on the rear panel of the VQM Controller (24 Vdc, 75 W connector), but do NOT plug in the AC power supply at this time. 2. Connect a ground wire from the ground lug on the rear panel of the control unit to a known Earth ground. Do NOT connect a ground wire directly between the control unit and the vacuum chamber 3. Plug in the power supply 4. Do NOT turn ON the control unit 5. Test with a multimeter for both DC and AC voltages between the metal parts of the vacuum chamber and the control unit chassis. <ul style="list-style-type: none"> • If no voltages exist, measure the resistance that should not exceed 2 Ohms <ul style="list-style-type: none"> • If AC or DC voltages exist and are less than 10 volts, shunt the meter with a 10 Ohm/10 Watt resistor. Repeat the voltage measurement. With the shunt in place across the meter, if the voltage remains at 83% or more of the unshunted value, commonality of the ground is implied 6. Plug the power supply to a AC plug 	Page 41-43
5A	First depressurization	<ol style="list-style-type: none"> 1. Reach inside the main chamber a pressure lesser than 10^{-5} Torr (1.33×10^{-5} mbar), temperature must remain between 0° and 50° C 2. Turn on the control unit. Look the table below for verify if it is working properly 	
6A	Mass Spectrometer Bakeout (optional)	<p style="text-align: center;">To be carried out:</p> <ul style="list-style-type: none"> • After the first installation of the spectrometer • After the spectrometer is left open for a long time • When there are obvious signs of contamination • When there is a noticeable drop in performance <ol style="list-style-type: none"> 1. Turn off the mass spectrometer and unplug it from the control unit 2. Attach the heating jacket. Do NOT exceed 200° C with any heating system. 3. Make sure the chamber pressure is below 1×10^{-5} Torr (1.33×10^{-5} mbar) 4. Establish, if possible, a slow flow of dry N2 gas in the vacuum chamber 5. Bake the probe for at least 12 hours 6. Remove the heating jacket and wait for the sensor to cool to room temperature 7. Connect the MS Gauge to the control unit and wait for the pressure to drop below 10^{-5} Torr (1.33×10^{-5} mbar) and reach the targeted base pressure 	Page 126

Procedure for the first application of VQM sensor used for Residual Gas Analysis		
7A	Filament Outgassing and Electron Multiplier Preconditioning	<p style="text-align: center;">Filament Outgassing To be carried out:</p> <ul style="list-style-type: none"> • The first time power is given to the spectrometer after installation <ul style="list-style-type: none"> • After a long period in which it is stored in its container • Each time the filament or Electron Multiplier is replaced <ol style="list-style-type: none"> 1. Connect and apply power to the control unit 2. Turn on the control unit, but NOT the gauge 3. Connect the control unit to the host pc through the USB cable 4. Launch the VQM Viewer software and connect it through the “Connect” Icon 5. Click the gauge operating mode Off and click STANDBY. <p style="text-align: center;">WARNING: If the pressure sensor is connected and the pressure is higher than 10^{-5} Torr, the system will not work</p> <ol style="list-style-type: none"> 6. Wait 2 hours. If the pressure sensor is NOT connected, the process must be physically monitored. <hr/> <p style="text-align: center;">Electron Multiplier Preconditioning To be carried out:</p> <ul style="list-style-type: none"> • Every time the room is not cleaned <ol style="list-style-type: none"> 1. Go to the settings screen and select “390 TPML” as the Pressure Source so the software recognizes the pressure sensor 2. On the Tune screen, change the gauge operating mode from Standby to Off by clicking the Standby button on the top bar and selecting Off from the drop-down menu 3. Set the EM Bias voltage to -750 V 4. Change the gauge operating mode from Off to Scan in the drop-down menu 5. On the Tune screen, select the Raw(Na) view 6. Change the EM Bias setting by clicking to the right of the 10s digit, then use the Down arrow to decrease the voltage -20 V every 1 minute(or 10 V every 30 seconds) until; (1) the Em bias voltage reaches -900 V or (2) any of the peaks in the mass spectrum reaches a 20 nA amplitude 7. Wait 2 hours
8A	Auto Tune	<p style="text-align: center;">To be carried out:</p> <ul style="list-style-type: none"> • Every time a new spectrometer is installed • Each time the filaments or the electron multiplier are replaced • After finding a loss in definition of the instrument due to its degradation <ul style="list-style-type: none"> • After a long period at ambient conditions • After the number of peaks in the spectrum has increased or decreased significantly since the last procedure <ol style="list-style-type: none"> 1. Assure that the chamber pressure is reasonably stable, it is also advisable to set an 90 % N₂ atmosphere with a pressure of $3 \cdot 10^{-7}$ Torr 2. Click the Auto Tune icon at the top of the Viewer Application. Select Auto Tune 3. Upon successful Auto Tune completion, choose to continue without storing the data from the message that appears

CHAPTER 4 – PESCha facility: Sensors implementation

Procedure for the first application of VQM sensor used for Residual Gas Analysis			
9A	Mass axis calibration	<p>To be carried out:</p> <ul style="list-style-type: none"> during the first installation each time the parameters are changed by the VQM Viewer software <ol style="list-style-type: none"> Access the Tune screen display of the VQM Viewer Software and select the Normalized view Change the gauge operating mode to Scan Set the averaging mode and number of buffers so the peak to be used for calibration is reliably fitted Type the integer value of the calibration peak into the Mass Peak field of the Selected Peak Parameters Click the Calibration arrow to move the peaks so that they coincide 	
10A	Save the options	Click "Store User"	
11A	Environmental constraint	<p>In order to work properly, the MS Gauge has these constraints:</p> <ol style="list-style-type: none"> Pressure: must be less than 10^{-5} Torr, and the optimal point of operation is $2 * 10^{-7}$ Torr Temperatures: The spectrometer must operate between 0°C and 50°C. while the temperature sensor cannot operate at 40°C Initializing time: The starting time of the sensor is about 5 minutes, and it is the time required by the power generator to ensure stable voltage and current. 	Page 128-129

The most important procedures to be performed during the first sensor installation are the following:

- **Mass Spectrometer Bakeout:** is an optional procedure that should be done in operating situations with vacuum of the order of 10^{-7} mbar or when is detected an high a presence of water vapor in the reading spectrum. It consists in heating the sensor, bringing it to a temperature of 180 degrees, for 12 hours in conditions of high vacuum (optional)
- **Filament Outgassing and Electron Multiplier Preconditioning:** These two procedures are used to perform a further bakeout, but they are related to the filament that generates the electrons and at the electron Multiplier. The gases present in the material in this case do not only affect the correct reading of the spectrum but can also compromise the operational life of the sensor, leading to peaks of deleterious voltages for the material.
- **Auto Tune:** This procedure is performed to synchronize the peaks
- **Mass axis calibration:** This procedure is carried out to be able to calibrate the peaks, which could be slightly shifted with respect to the reference axis. It is usually done by taking as a reference the gas most present in chambers, such as nitrogen or water vapor.

TEST 1 - EMPTY CHAMBER

In the first test it was decided to perform an analysis with the empty test chamber. This was done both to get an idea of which gas can outgas from room under standard conditions, and to be able to verify the correct functioning of the sensor.

The data that are expected from this first test are similar to standard atmosphere, so with gases such as nitrogen, oxygen and carbon dioxide, with the presence of water vapor.

All the preliminary procedures have been carried out, for the calibration and for the cleaning of the various components of the sensor.

It was not possible to bakeout the spectrometer because the support provided by the manufacturer was the relative to a smaller model of RGA, and therefore was not applicable to the RGA in use in the PESCha facility.

The data obtained were used to develop the following graphs.

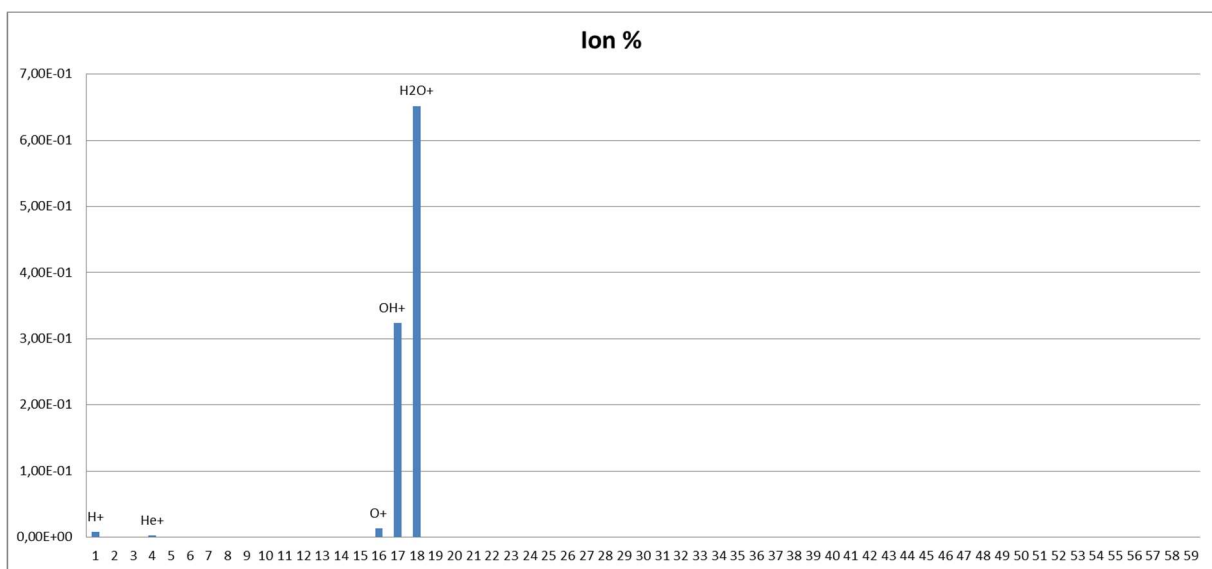


Figure 75 - Empty chamber mass spectrum

As can be seen in the figure above the spectral analysis shows an evident concentration of water vapor. The ions that have been created are all related to water (H₂O⁺, OH⁺, O⁺).

Given the lack of other gases, the test can lead to two conclusions:

- The sensor has been incorrectly calibrated or is not working properly, in this case the calibration procedure should be re-done or the correct operation of the same verified
- The sensor is valid and the atmosphere inside the room is not composed of the gases we expected to find.

In order to verify the other theories experiments have been designed with the introduction of different gases inside the chamber.

TEST 2 - CO2

The first gas to be tested is carbon dioxide.

This gas is available in the PESCha facility where is used for the simulation of interplanetary environments, specifically the Martian one. It was not possible to directly inject the gas during the operation of the sensor, this because the molecular turbopump is not able to immediately compensate for the increase in pressure due to the intake of gas (the RGA can be operated only below $1.33E-5$ mbar). Therefore, a small amount of CO₂ was then introduced through the MFC, then the pump was pumped down the chamber bringing the internal pressure to the chamber to acceptable values to operating the RGA.

The graphs produced are as follows:

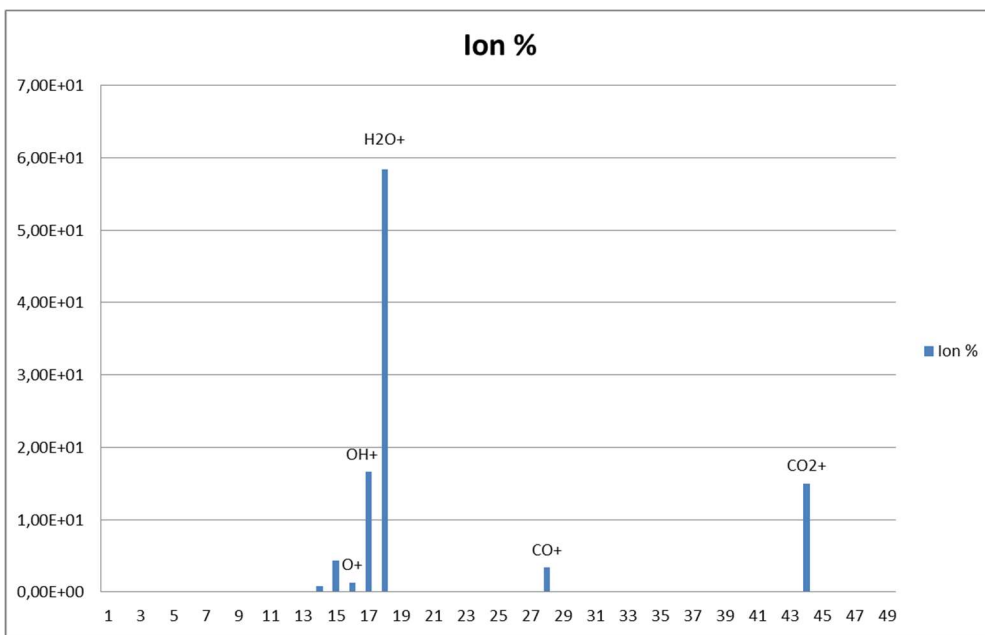


Figure 76 - CO2 mass spectrum

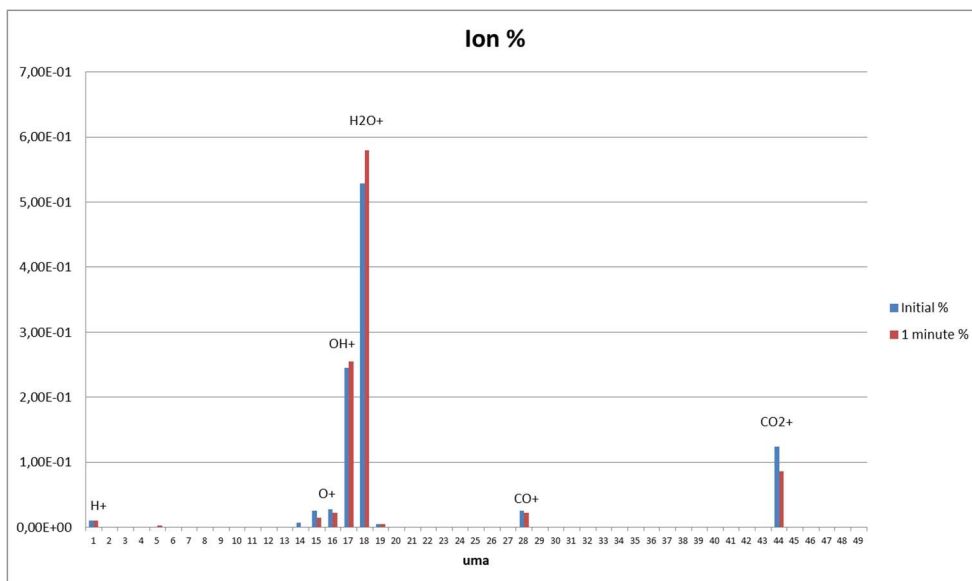


Figure 77 - CO2 mass spectrum (1 minute delay)

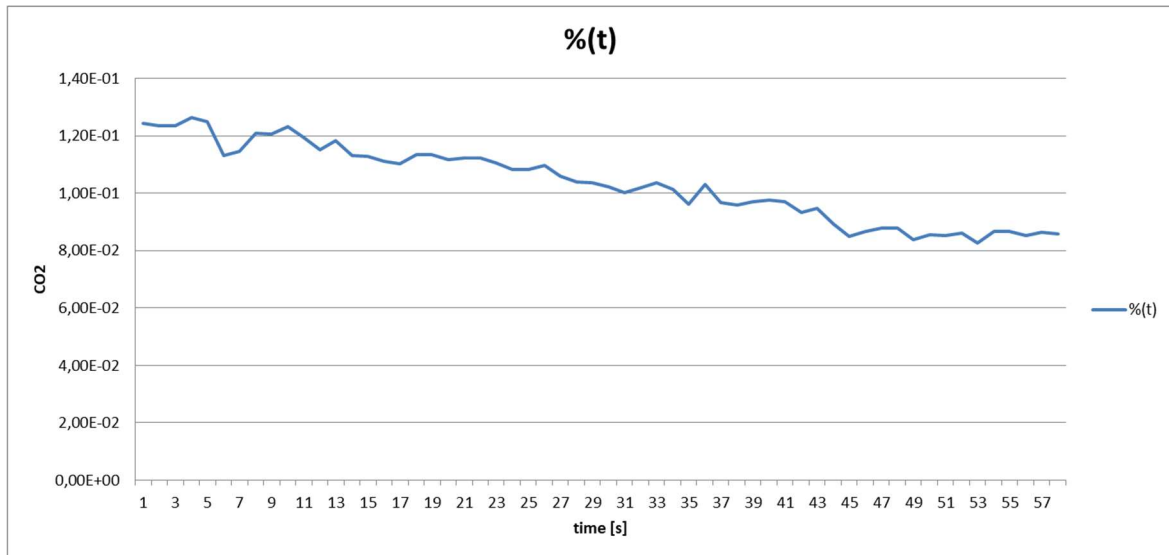


Figure 78 - CO2 time function

The first scan shows a presence of CO2 in the RGA spectrum. This data confirms that the sensor is operating correctly.

The other two graphs show the distribution of gas with a detection carried out after 1 minute and the specific trend in the CO2 time. It can be noted a marked decrease of CO2 over time.

What can this be caused by?

The first possible cause is motivated by the continuous presence of water vapor inside the spectrometer readings. A datum that, through the research in various documents inherent to this type of analysis, is a common result. This is because the chamber and the sensor outgases mainly water vapor. This directly affects the percentage composition of the gases inside the chamber, leading to the lowering of the other gases present.

This motivation, however, was considered insufficient, the gas in fact decreases too quickly, and in any case other types of gas should also be detected.

In order to prove this assumption, it was decided to introduce another gas, this time in bigger quantities in order to better monitor the behaviour. The results of this third test are presented in the following paragraph.

TEST 3 - N2

During this test it was decided to introduce another gas available in the PESCha facility, that is the N2, used mainly for the maintenance and correct operation of the vacuum pumps and for the pressurisation after back out test. In order to guarantee a higher gas supply, it was verified that the turbomolecular pump could compensate for nitrogen inlet. In fact, the PESCha system is designed to switch off the pump if the operating limit of the pump is reached, i.e. 10^{-1} mbar. With the MFC control at minimum it was seen that the pressure did not rise more than 10^{-3} so it was possible to introduce a good amount of nitrogen.

The graphs produced are as follows:

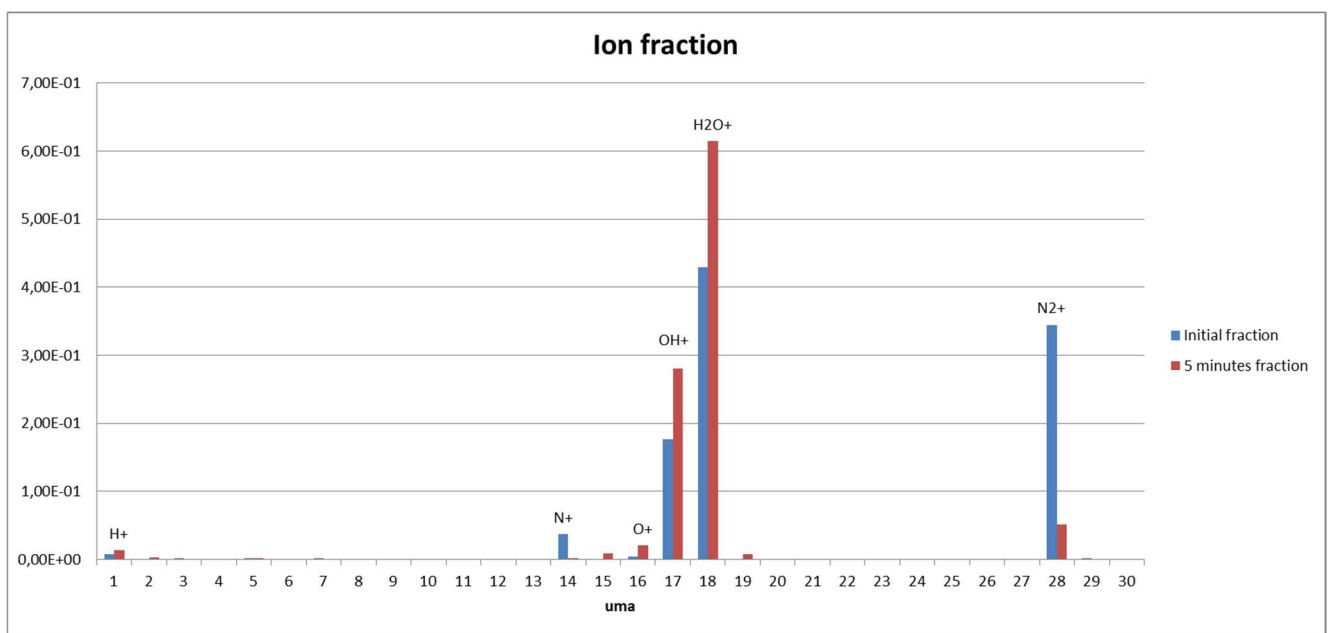


Figure 79 - N2 mass spectrum

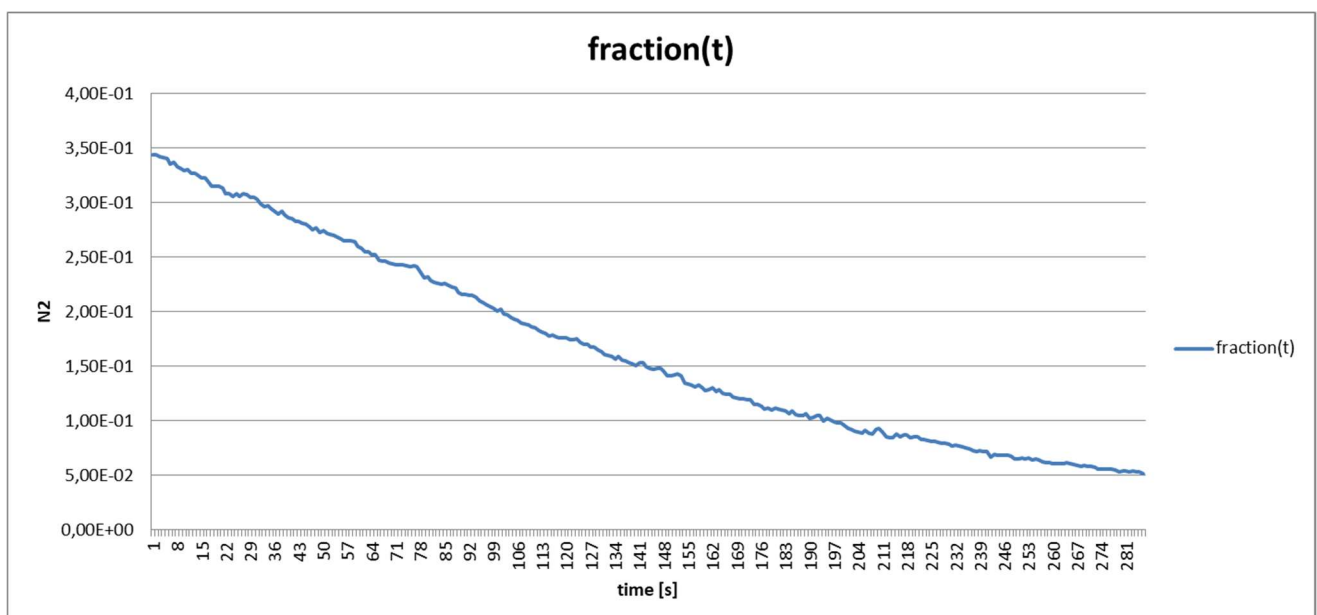


Figure 80 - N2 time function

CHAPTER 4 – PESCha facility: Sensors implementation

A remarkable presence of nitrogen can be noted, which however, as in the case of CO₂, decreases over time.

The hypothesis that has been made in this case is that, in addition to the introduction of water vapor present in the materials, something favours the removal of gasses.

The peculiarity is that the heavier gases are not present or are decreasing in a very short time. Could this be due to a behaviour of the pumps?

Checking the manuals, and the operation of the various pumps, the fault fell to the turbomolecular pump. In fact, we have seen that turbomolecular pump has different compression ratios based on the molecular weight of operating gases, it works better with heavier molecules, which therefore disappear more quickly at higher vacuum levels. This phenomenon is positive with regards to the use of thermal vacuum chambers, because the possible presence of hydrocarbons that could damage the chamber itself or the experiments would be avoided by the operation of the pump.

Although it is therefore justified from the theoretical point of view, it was decided to verify this behaviour anyway through the introduction of lighter gases, and this will be discussed in the next test.

TEST 4 - He

The helium test was performed by connecting the RGA sensor to the baffle trap. This is because a high leak was found in the main chamber that made the procedure to reach the high vacuum difficult.

The chamber was first brought to a pressure of 0.01 mbar, then helium was inserted up to atmospheric pressure.

The graph obtained is the following:

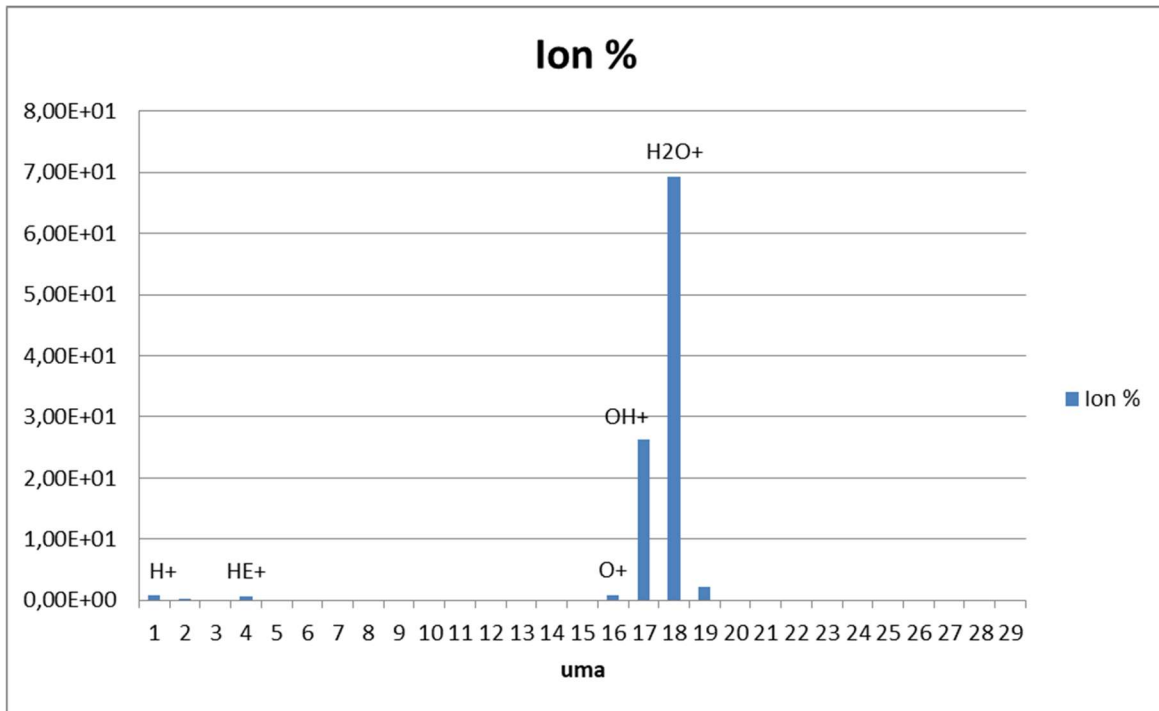


Figure 81 - He mass spectrum

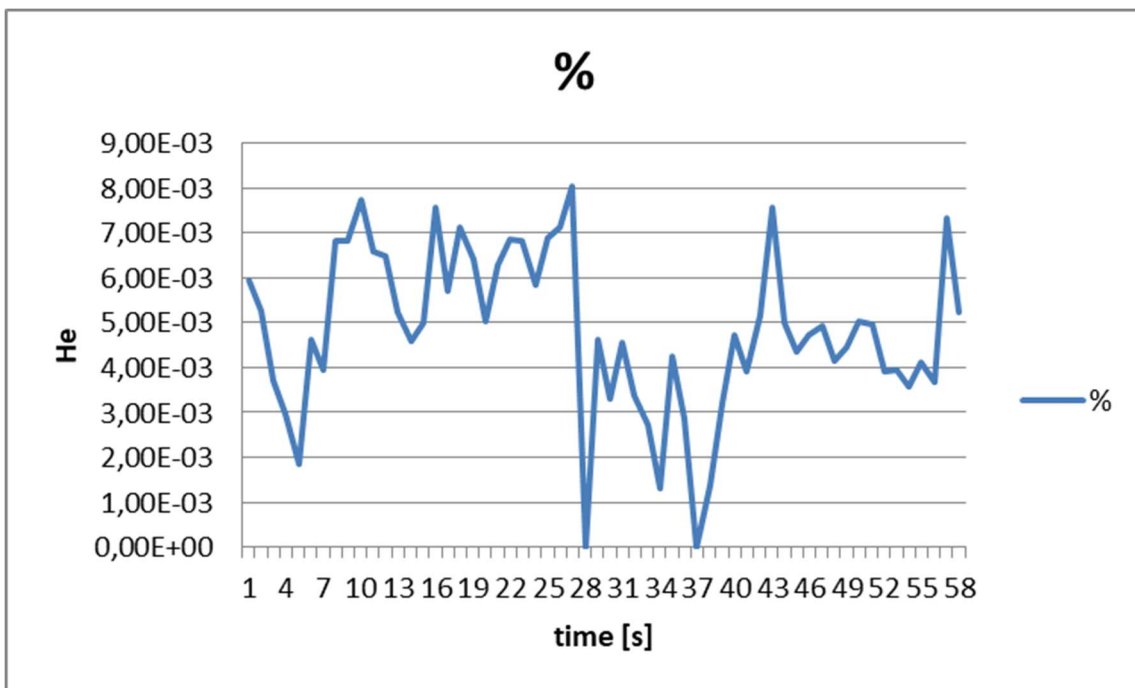


Figure 82 - He time function

CHAPTER 4 – PESCha facility: Sensors implementation

A small amount of helium is visible, not constant in time, but even in this case it is obscured by the large amount of water. These results made clear the outgassing is therefore much more important than expected.

Another possible explanation may be linked to the fact that at higher pressures the collisions between the molecules dominate, therefore the lighter gases tend to remain in the upper parts. When the gate of the turbomolecular pump is opened, positioned at the top of the chamber, the lighter gases are the first to leave, until the pressure drops enough to dominate the effect of the pump, which instead works more efficiently with heavier gases.

TEST 5 - Outgassing

A series of experiments were performed to see if it was possible to view the outgassing of materials inserted into the chamber.

Tests were carried out on the following materials:

- Kapton
- Kevlar
- Scotch-Weld

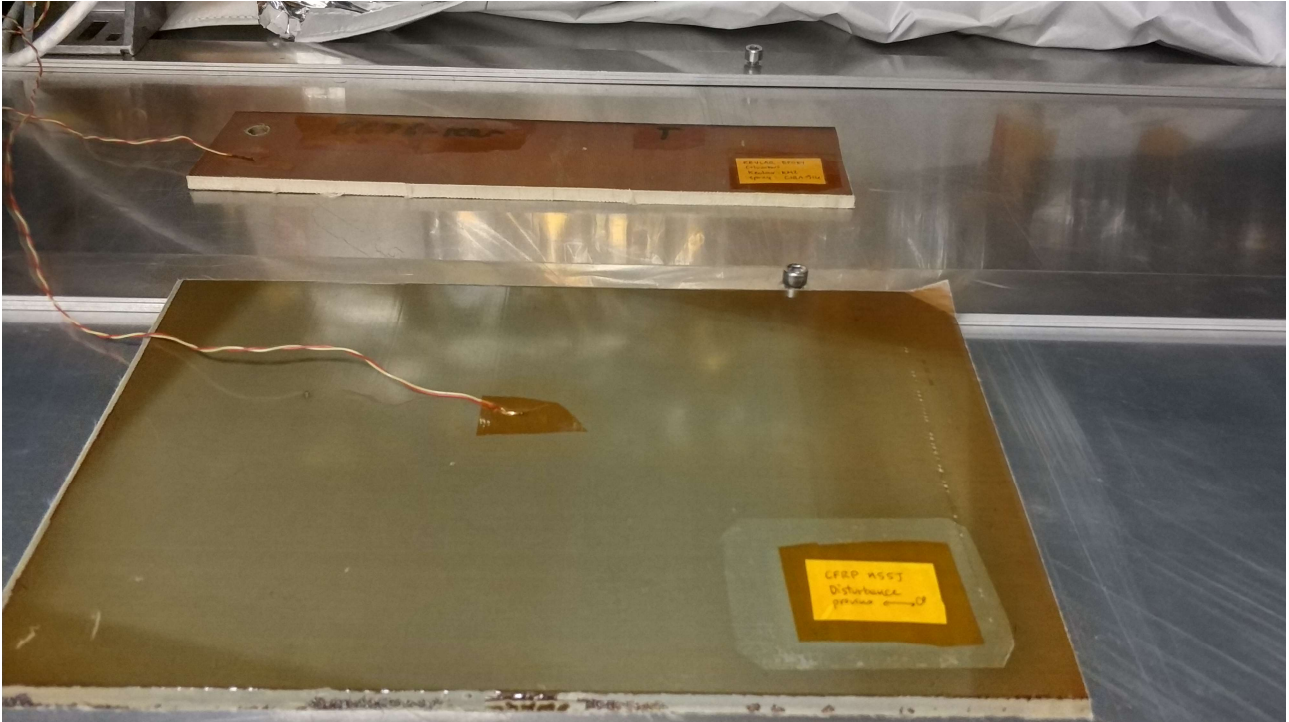


Figure 83 - Kevlar experiment

It was possible to heat these materials only indirectly, by increasing the chamber temperature, with maximum temperatures of 80 ° C so as not to compromise the operation of the various sensors.

CHAPTER 4 – PESCha facility: Sensors implementation

The graph that was obtained for scotch weld is the following:

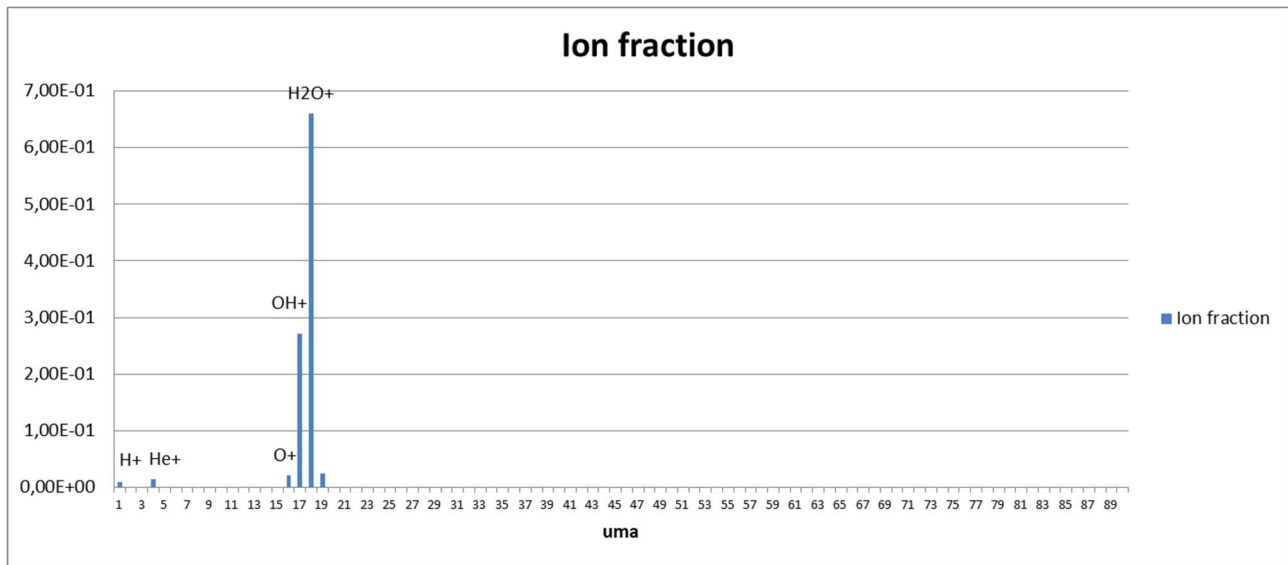


Figure 84 - Scotch weld mass spectrum

The following materials should outgrow heavy particles.

The following elements should be present in the scotch weld spectrum:

- 57, 71, 85 hydrocarbons
- 73, 267, 281, 355 siloxanes
- 60, 43, 41, 129 carboxylic acids
- 59, 72, 255 amides
- 213, 228, 119 Bisphenol A (epoxide precursor)
- 149, 279 phthalate derivatives

None of these elements is visible.

The two main reasons found are the too much presence of water that obscures the reading and the fact that the particles that are outgrowing are very few and are immediately taken away by the turbomolecular pump, making it therefore difficult for the sensor to be readable.

Helium is detected because the experiment was carried out after the previous experiment.

TEST 6 - BAKING

In the previous tests it was not possible to make a bakeout of the spectrometer, due to problems related to the support provided by the manufacturer.

It was therefore decided to build a device to heat the sensor.

The device that has been built consists of two parallel heaters and two thermocouples to monitor the actual temperature of the spectrometer. These components were sealed through aluminized Kapton and an additional layer of insulating material resistant to high temperatures in order to avoid heat dispersion towards the outside. This step is fundamental because of the voltage limit that the heaters can withstand. If the dispersion were high it would not be possible to reach high temperatures without increasing the tension.

The whole system was therefore connected to a threshold type controller, that allows to set the minimum and the maximum temperature that. If the temperature monitored by the sensors is not above the High Temperature Limit set by the user the heater is switched off via a relay, which instead activates the sensor if the temperature is not high enough. This system is not very efficient because it produces very high temperature spikes, even of 10 degrees. In the future it may be necessary to implement a system with a more efficient type of controller, such as a PID.

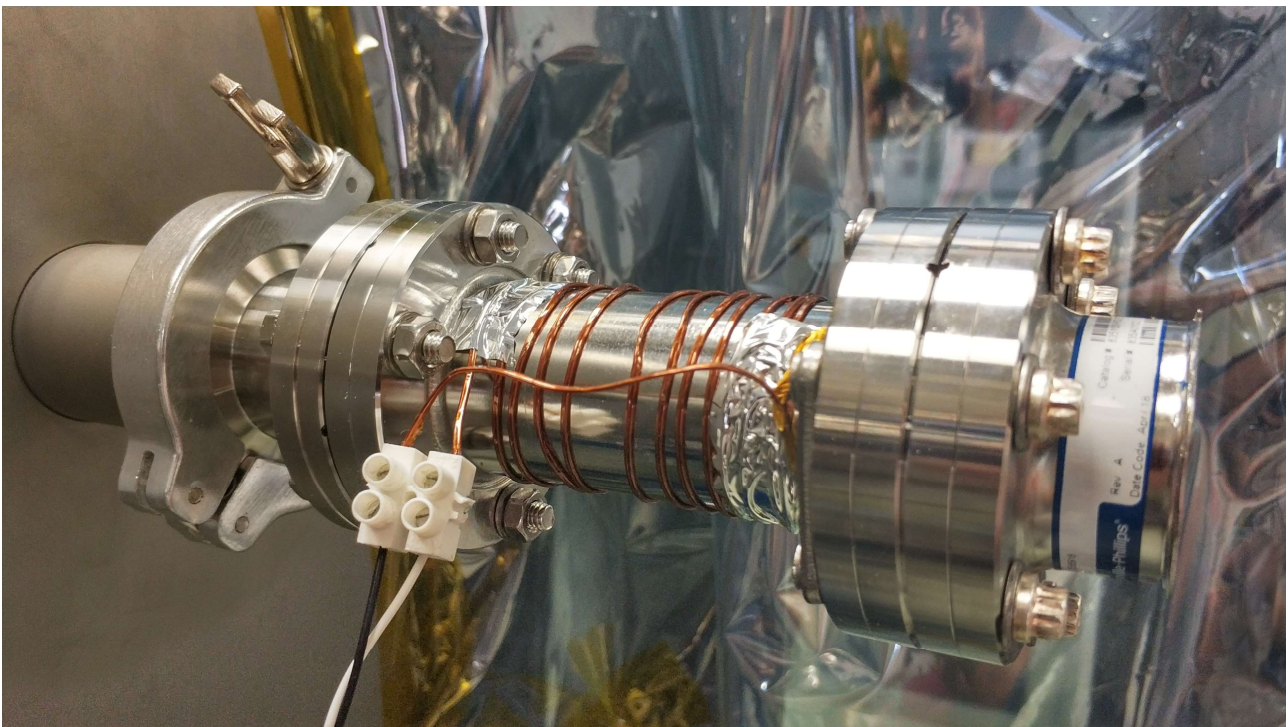


Figure 85 - RGA bakeout - Heater and thermocouple

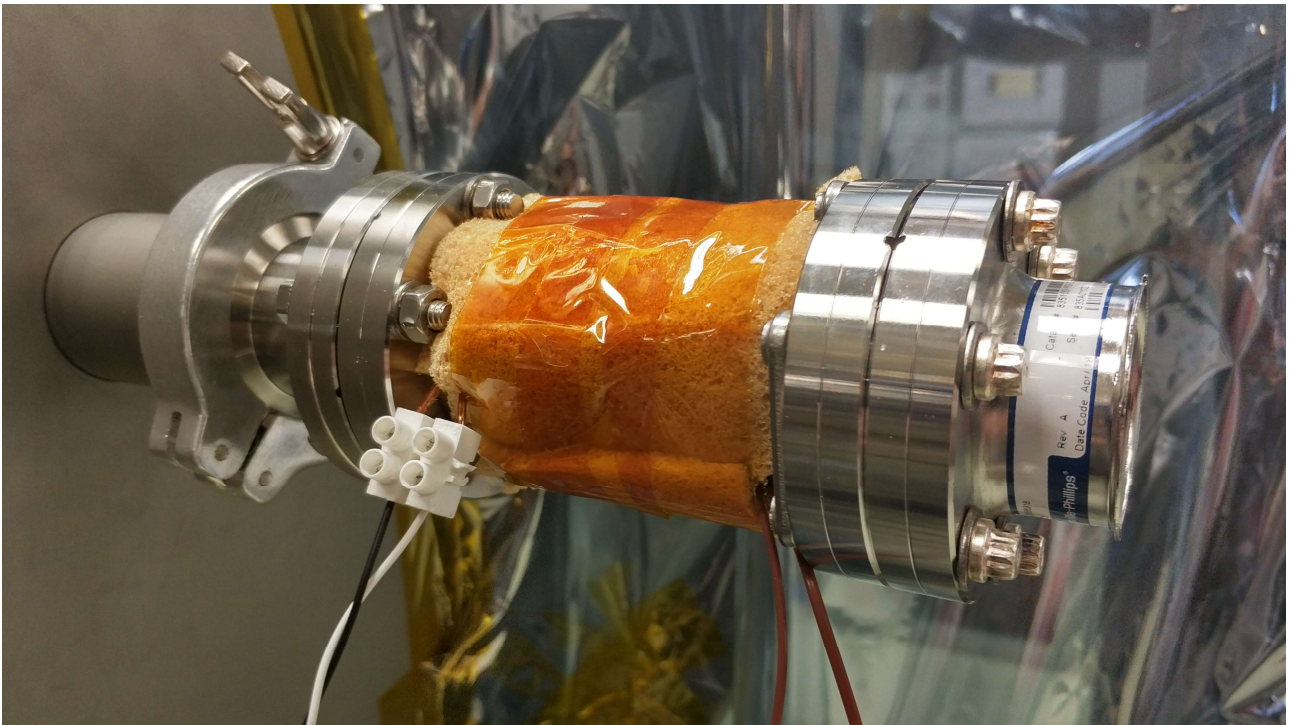


Figure 86 - RGA bakeout - Protection

To be able to reach a temperature of 180 degrees, necessary for the correct outgassing of the sensor, 18 V of power supply of the heaters have been set, with a limit of 2 A to the current.

A 6-hour bakeout was performed, and the graph that was obtained is as follows:

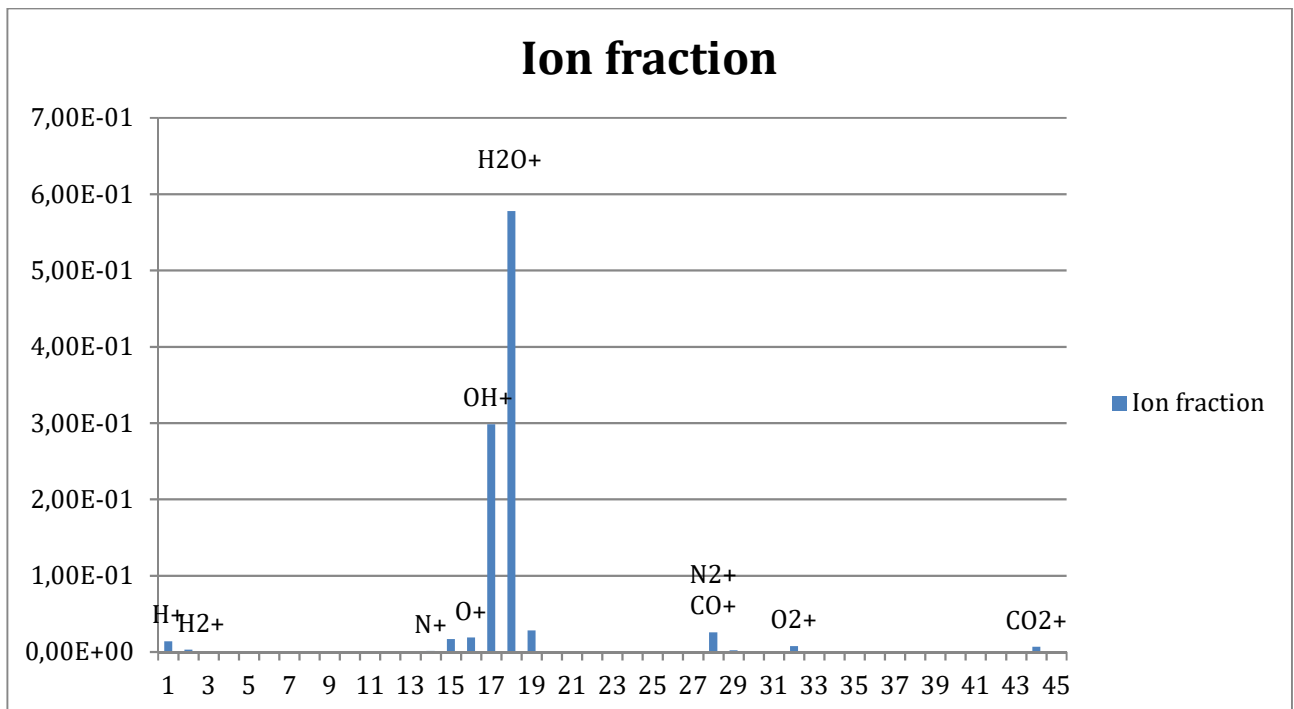


Figure 87 - Bakeout mass spectrum

CHAPTER 4 – PESCha facility: Sensors implementation

The effect of bakeout is the one expected. The relative amount of water detected by the instrument has decreased, and more molecules have appeared within the spectrum.

The presence of carbon dioxide, oxygen and nitrogen can be noted.

This is an excellent result, because it demonstrates how an adequate bakeout process can improve the reading of the spectrum and therefore the correct understanding of the internal atmosphere of the room.

The limit of this type of approach is due to the fact that, in case of malfunction of the thermocouples used to control the switching on and off of the heater, the thermocouple can give a negative temperature. The control system therefore would keep the heater continuously turned on to trying to increase the temperature, which however is fictitious. This may lead to overheating of the machine. Continuous control from an operator of the process is therefore necessary.

A possible solution is to limit the current with very precise data, so as to have a maximum temperature that can be reached by the heaters of around 180 ° C necessary for the correct sensor bakeout.

CONCLUSIONS

The starting point of the present thesis has been the study of the variety and diversity of the space and planetary environment conditions and the difficulty to reproduce those conditions by means of on-ground laboratory testing. In particular, the thermal-vacuum conditions and the outgassing process, which strongly influence the behaviour and the life cycle of materials and components used for space applications, have been investigated.

The PESCha (Planetary Environmental Simulation Chamber) facility, located in the premises of Thales Alenia Space in Torino, has been studied to map the performances of its various components (vacuum and thermal system, sensors to monitor the various conditions within the chamber, etc.), its capability to perform diversified tests in several fields of applications and the possibility to improve testing procedures and capabilities. A particular attention was given to the study of the outgassing phenomena and of the bake-out process. The working principles of a Thermoelectric Quartz Crystal Microbalances (TQCM) used to monitor the bake-out of space hardware have been analysed and a computer code was developed for the analysis and the interpolation of the acquired data and to show compliance with the outgassing requirements made applicable by ESA to flight equipment and materials. The computer code developed has allowed to simplify and speed up the data analysis and the requirement verification.

Another area of investigation was related to the implementation of a feedback system for the PESCha thermal control system which allows programmable and continuous operations of the chamber in the temperature range between -80 °C and +135 °C. A thermal model was developed to predict the chamber thermal behaviour and proper feedback thermal sensors were identified and procured. This thermal model will be validated once the feedback system is implemented and will be used to tune and operate the improved thermal control system.

The performance of a Residual Gas Analyser (RGA) was then analysed. This instrument is used to detect the chemical species present in the vacuum chamber during thermal vacuum experiments. It can be used to support the monitoring of the bake-out process performed with the TQCM, and therefore to speed up the process (which can last several days with significant cost), providing more accurate data. The performed RGA tests analysed the merits of the instrument, such as the capability to easily detect the mass spectrum of the species in the chamber, but also its deficiencies, such as the extreme sensitivity to water vapour affecting the sensibility to detect other volatile components. A dedicated bake-out system was therefore implemented on the RGA, consisting of a heater and of temperature sensors, to be able to clean the instrument and increase its sensitivity to all the outgassed components. The developed bake-out system has the advantage of being simple and easy to implement, since it was connected to the thermal control system of the heaters and the thermocouples used as standard instrumentation for experiments within the chamber. Future improvements to make the RGA bake-out more robust and reliable have also been studied and proposed for future implementation.

Appendix 1 – TQCM fitting code

```

close all
clear variables
%% In questa sezione apro il file, prendo soltanto i dati della tabella
e li inserisco in una matrice
i=1;
fine=1;
interpol=0;
ritardo_p=0;
while fine==1
    clear input
    input=input('Inserisci il nome del file da aprire (va inserito fra
apici)\n');
    fid=fopen(input);
    while 1
        tline = fgetl(fid);
        if tline==-1
            break
        end
        X=str2num(tline);
        if length(tline)>1&&tline(1)=='R'

ora=datetime([str2num(tline(52:55)),str2num(tline(46:47)),str2num(tline(
49:50)),str2num(tline(17:18)),str2num(tline(20:21)),str2num(tline(23:24)
]]);

        end
        if length(X)==18
            A(i,:)=X;
            i=i+1;
        end
    end
    fclose(fid);
    if ritardo_p==1
        ritardo=fix(minutes(ora-ora2-minutes(interpol)));
        fprintf('Il ritardo è di: %.2f Minuti\n',ritardo)
    end
    ora2=ora;
    if interpol~=0

A((interpol+ritardo):size(A,1)+ritardo,:)=A(interpol:size(A,1),:);
        A(interpol:(interpol+ritardo-
1),2)=(A((interpol+ritardo),2)-A((interpol-
1),2))/5.*[1:ritardo]+A((interpol-1),2));
        A(interpol:(interpol+ritardo-1),3)=-20*ones(ritardo,1);
    end
    %% Plotto i dati aperti, per avere una rapida visualizzazione
    figure
    plot((1:size(A,1))/60,A(1:size(A,1),2))
    hold on
    ylabel('Frequenza [Hz]')
    yyaxis right
    plot((1:size(A,1))/60,A(1:size(A,1),3))
    xlabel('Ore')
    ylabel('Temperatura [°]')

```

CHAPTER 4 – PESCha facility: Sensors implementation

```
grid
%% Questa sezione è utile per unire file diversi
z1=1;
h=0;
riga=1;
clear input
fineinput=0;
while fineinput==0
    input=input('Vuoi unire una sessione di lavoro(digita 1 per si,
0 per no)\n');
    if input>=0&&input<=1
        fineinput=1;
        if input==1
            interpol=i;
            ritardo_p=1;

            else
                fine=0;
            end
        else
            fprintf('Errore, reinserire il parametro\n')
        end
    end
end
%% In questa sezione vengono analizzate le zone di lavoro utile della
TQCM
for i=1:size(A,1)
    if A(i,3)<-18.5&&A(i,3)>-21
        z=0;
        if (z1-z)~=0
            h=h+1;
            tempo(h)=0;
        end
        Utili(riga,:)= [A(i,:),h];
        riga=riga+1;
        tempo(h)=tempo(h)+1;
    else
        z=1;
    end
    z1=z;
end

fprintf('Sono stati individuati %d campi di lavoro\n',h)
for i=1:length(tempo)
    fprintf('%d) durata: %.2f Ore\n',i,tempo(i)/60)
end

fineinput=0;
while fineinput==0
    clear input
    input=input('Quale vuoi utilizzare?\n');
    if input>=1&&input<=length(tempo)
        fineinput=1;
    else
        fprintf('Errore, reinserire il parametro\n')
    end
end
end
```

CHAPTER 4 – PESCha facility: Sensors implementation

```
%% In questa sezione impongo la sezione utile all'algorithmo la sessione
di lavoro utile
fine=0;
riga=1;
A=zeros(tempo(input),18);
for i=1:size(Utili,1)
    if Utili(i,19)==input
        A(riga,1:18)=Utili(i,1:18);
        riga=riga+1;
    end
end
A(:,1)=(0:tempo(input)-1)';
%% In questa sezione faccio l'interpolazione dei dati
A2=A;
A2somma=(A2(:,2)-A2(1,2))';
A3=ones(size(A2,1),1)*A2(1,2);
som=(0:size(A2,1)-1)/60;
fun=@(x) (sum((x(1).*(1-exp(-(som)./x(5))))+x(2).*(1-exp(-
(som)./x(6)))+x(3).*(1-exp(-(som)./x(7)))+x(4).*(1-exp(-(som)./x(8)))-
A2somma).^2));
clear input
input=input('Quanti set di numeri vuoi dare al solutore? \n');
for q=1:input %genero 2000 set di numeri randomi, il calcolo impiega un
po di tempo, circa 1.5 simulazioni al secondo
%    q
    x0=ceil(rand(8)*10000);
    x0(1,5:8)=ceil(sort(x0(1,5:8)/20)); % assumo che le tau son 20 volte
minori dei numeri generati sulle a
    x0(1,1:4)=sort(x0(1,1:4)); %assumo che le a e le tau ordinate
generino dei chi quadro minori
    fun(x0(1,:));
    if q==1
        minfin=fun(x0);
    end
    A4=[];
    b=[];
    Aeq=[];
    beq=[];
    lb=[0.1,0.1,0.1,0.1,0.1,0.1,0.1,0.1]; %parametro che limita
inferiormente il set possibile di dati
    ub=[]; %parametro che limita superiormente il set possibile di dati
    x = fmincon(fun,x0(1,:),A4,b,Aeq,beq,lb,ub); % Questa funzione
trova il minimo di una funzione in più variabili, in particolare bisogna
stare attenti a x0, ovvero il punto di inizio ricerca della funzione
    min=fun(x);
    if min<minfin
        minfin=min;% questo è il chi quadro minore, che viene
controllato ad ogni ciclo
        x0effettivo=x0(1,:);% salvo l'ultimo x0 che è stato usato per la
ricerca
        xe=x;
    end
end
end
%% Plot dei dati
t=(0:size(A2,1)-1)/60;
```

CHAPTER 4 – PESCha facility: Sensors implementation

```
fun2=@(t) xe(1).*(1-exp(-t./xe(5)))+xe(2).*(1-exp(-t./xe(6)))+xe(3).*(1-  
exp(-t./xe(7)))+xe(4).*(1-exp(-t./xe(8)));  
figure  
plot(t,fun2(t)) %plot della funzione interpolante  
hold on  
plot(t,(A2(:,2)-A3)','.') %plot dei dati effettivi  
hold on  
xlabel('Ore')  
ylabel('Frequenza [Hz]')  
grid  
  
fun3=@(t) (xe(1)./xe(5)).*(exp(-t./xe(5)))+(xe(2)./xe(6)).*(exp(-  
t./xe(6)))+(xe(3)./xe(7)).*(exp(-t./xe(7)))+(xe(4)./xe(8)).*(exp(-  
t./xe(8)));  
figure  
plot(t,fun3(t)) %plot della funzione interpolante derivata  
hold on  
xlabel('Ore')  
ylabel('Derivata Frequenza [Hz/Minuti]')  
grid  
  
fun4=@(t) -((xe(1)./(xe(5).^2)).*(exp(-  
t./xe(5)))+(xe(2)./(xe(6).^2)).*(exp(-  
t./xe(6)))+(xe(3)./(xe(7).^2)).*(exp(-  
t./xe(7)))+(xe(4)./(xe(8).^2)).*(exp(-t./xe(8))));  
figure  
plot(t,fun4(t)) %plot della funzione interpolante derivata seconda  
hold on  
xlabel('Ore')  
ylabel('Derivata seconda Frequenza [Hz/Minuti^2]')  
grid  
  
figure  
plot(t,abs(fun3(t)./fun4(t))) %plot della funzione interpolante derivata  
seconda  
hold on  
xlabel('Ore')  
ylabel('Rapporto delle derivate f1/f''')  
grid  
  
durata=0;  
for i=1:length(t)  
    if abs(fun4(t(i))./fun3(t(i)))<=0.01  
        durata=durata+1;  
    end  
end  
fprintf('La condizione 1/100 è stata raggiunta da:%.2f Ore\n',durata/60)  
if durata==i  
    fprintf('La durata è uguale allo step temporale, Possibile errore!!!  
(Controllare l andamento della funzione interpolante)\n')  
end  
  
figure  
if durata<i&&durata>0  
    plot(t(1:i-durata),abs(fun4(t(1:i-durata))./fun3(t(1:i-durata))))  
%plot della funzione interpolante derivata seconda  
    plot(t(i-durata:i),abs(fun4(t(i-durata:i))./fun3(t(i-durata:i))))
```

CHAPTER 4 – PESCha facility: Sensors implementation

```
end
hold on
if durata==0
    plot(t(1:i),abs(fun4(t(1:i))./fun3(t(1:i))))
end
plot(t,ones(size(t))*0.01)
xlabel('Ore')
ylabel('Rapporto delle derivate f"/f1')
grid

figure
plot(t,xe(1).*(1-exp(-t./xe(5))))
hold on
plot(t,xe(2).*(1-exp(-t./xe(6))))
plot(t,xe(3).*(1-exp(-t./xe(7))))
plot(t,xe(4).*(1-exp(-t./xe(8))))
xlabel('Ore')
ylabel('Frequenze')
legend('Funzione 1','Funzione 2','Funzione 3','Funzione
4','Location','northwest')
grid

A(:,4)=fun2(A(:,1)/60);
A(:,5)=fun3(A(:,1)/60);
A(:,6)=abs(fun4(A(:,1)/60)./fun3(A(:,1)/60));
%% Salvataggio dei dati
fineinput=0;
while fineinput==0
    clear input
    input=input('Vuoi salvare i dati in un file excel? (digita 1 per si,
0 per no)\n');
    if input==1
        clear input
        input=input('Nome del file (.xlsx) (va inserito fra apici)\n');

varnames={'Time_h','Frequency_Hz','Interpoleted_Frequency_Hz','Derived_f
requency_Hz/h','Second_Derived_frequency_Hz/h^2','Second_derivative/deri
vative_1/h','Temperature_C'};
        varnames2=[A(:,1),A(:,2)-
A3,fun2(t),A(:,3),A(:,4),A(:,5),A(:,6)];

varnames3={'a1','a2','a3','a4','tau1','tau2','tau3','tau4','Durata_super
amento_1/100_h'};
        varnames4=[x(1:8),durata/60];
        xlswrite(input,varnames,'Sheet1','A1')
        xlswrite(input,varnames2,'Sheet1','A2')
        xlswrite(input,varnames3,'Sheet1','H1')
        xlswrite(input,varnames4,'Sheet1','H2')
        xlswritefig(figure(1),input,'Sheet1','H3')
        xlswritefig(figure(7),input,'Sheet1','R3')
        xlswritefig(figure(2),input,'Sheet1','H25')
        xlswritefig(figure(3),input,'Sheet1','R25')
        xlswritefig(figure(4),input,'Sheet1','H47')
        xlswritefig(figure(5),input,'Sheet1','R47')
        xlswritefig(figure(6),input,'Sheet1','H69')
        fineinput=1;
    elseif input==0
```

```
        fineinput=1;
    else
        fprintf('Errore, reinserire il parametro\n')
    end
end
```

Acknowledgments

I thank Lilith Grassi and Roberto Destefanis for the opportunity given to me to write this thesis. They have always been available, both to provide me with all the information needed to understand the operation of the PESCha facility, and to facilitate the use of laboratories. I thank them because they made me feel immediately part of the activity, allowing me to be able to express myself at my best and to show my skills.

I also thank my colleagues from Thales Alenia Space, Pasquale, Angelo, Matteo, Simone, Martina, Francesca, Marco and Federica respectively who have made my time in the company pleasant.

I thank Professor Paolo Maggiore who made the creation of this thesis possible, always available both for clarifications and to provide practical support.

I thank my parents who have always supported me and have given me the opportunity to continue the journey started with the three-year degree. I also thank the rest of my family, always available and ready to help. A special mention goes to my uncle Engineer Marcello Marceddu, who unfortunately passed away at the beginning of the master's course, I know he would have been happy with this goal and that he would have liked to be present at the graduation to be able to see the result of years of advice and challenges.

Finally, I thank the rest of my family, made up of fellow university students, old friends and brothers from the 5th floor of the Einaudi College who have made these 5 years exciting and fun.